INTERACTION BETWEEN CATHODIC PROTECTION AND MICROBIALLY INFLUENCED CORROSION

A thesis submitted to The University of Manchester for the degree of

Master of Philosophy (MPhil)

In the Faculty of Engineering and Physical Sciences

2011

AZLAN BUJANG MASLI

SCHOOL OF MATERIALS

Corrosion and Protection Center

TABLE OF CONTENTS

LIST OF FIGURES

LIST OF TABLES

Final word count: 22,900.

ABSTRACT

The present work studied the interaction between cathodic protection and microbially influenced corrosion (MIC) on the surface of mild steel. Potential trending was observed when the currents were held constant, and current trending was observed when potentials were held constant. Scanning electron microscopy and energy dispersive x-ray spectroscopy were used to study surface deposits on the samples and further understand the result of the interaction. Sulfate reducing bacteria (SRB) were the main MIC factor studied in this work. The potentials of interest were the protection criteria of -850 mV vs copper-copper sulfate electrode (CSE) generally recommended to protect buried or immersed steel and the -950 mV (CSE) recommended for cathodic protection of steel exposed to risk of MIC.

The results obtained from the experiments suggest the following main findings:

- The activities of SRB underneath a biofilm caused ennoblement of potential if the current is held constant.
- It also caused increase in current required to cathodically polarize metal surface at a specified potential.
- Cathodic potentials did not have effect on attachment and viability of SRB on metal surfaces in the range of potential studied in this work.

The cathodic potential of -950 mV (CSE) recommended for cathodic protection under risk of MIC appeared to have effect of reducing the probability of deposition of iron sulfide, one of the main factors in corrosion acceleration for MIC. Furthermore, the formation of calcareous deposit helped reducing the current demand in cathodic protection under this potential, although SRB are still viable on the metal surface.

DECLARATION

I declare that no portion of the work referred to in the thesis has been submitted in support of an application for another degree or qualification of this or any other university or other institute of learning.

Azlan Bujang Masli.

COPYRIGHT STATEMENT

i. The author of this thesis (including any appendices and/or schedules to this thesis) owns certain copyright or related rights in it (the "Copyright") and s/he has given The University of Manchester certain rights to use such Copyright, including for administrative purposes.

ii. Copies of this thesis, either in full or in extracts and whether in hard or electronic copy, may be made only in accordance with the Copyright, Designs and Patents Act 1988 (as amended) and regulations issued under it or, where appropriate, in accordance with licensing agreements which the University has from time to time. This page must form part of any such copies made.

iii. The ownership of certain Copyright, patents, designs, trademarks and other intellectual property (the "Intellectual Property") and any reproductions of copyright works in the thesis, for example graphs and tables("Reproductions"), which may be described in this thesis, may not be owned by the author and may be owned by third parties. Such Intellectual Property and Reproductions cannot and must not be made available for use without the prior written permission of the owner(s) of the relevant Intellectual Property and/or Reproductions.

iv. Further information on the conditions under which disclosure, publication and commercialisation of this thesis, the Copyright and any Intellectual Property and/or Reproductions described in it may take place is available in the University IP Policy (see http://www.campus.manchester.ac.uk/medialibrary/policies/intellectualproperty.pdf), in any relevant Thesis restriction declarations deposited in the University Library, The University Library's regulations (see http://www.manchester.ac.uk/library/aboutus/regulations) and in The University's policy on presentation of Theses.

ACKNOWLEDGEMENT

Praise be to Allah, the Cherisher and Sustainer of the Worlds for Your blessings.

I would like to extend my appreciation and sincere thanks to my supervisor, Prof. Robert A. Cottis for his invaluable supervision, advice, guidance and honest feedbacks throughout my M. Phil research works. His wisdom was a bright searchlight guiding me through the darkness.

The following individuals have significantly contributed to the completion of the research work:

- Dr. J.F.D Stott for advice on microbially influenced corrosion and SRB analysis
- Dr. Sarah Leeds for lending her multipotentiostat
- Prof. Jonathan Lloyd and Christopher Boothman for SRB analysis and advice
- Stephen Blatch for his patience on my never ending requests for equipment
- Dr. Zhu Liu for her advice
- Numerous others not mentioned here

To the personnel mentioned above, I could never repay you in this life and I could only offer my sincere appreciation for all your contributions.

Special thanks to my sponsor, Petroliam Nasional Berhad (PETRONAS) for believing and investing in staff development.

A special appreciation for my mother, Hjh Sitam Busrah. Her prayers for me were the divine intervention for me to complete my studies.

Finally, my appreciation to my friends in the laboratory D29: Perla, Peng Wang, Saud and Carinho. You all cheered me up whenever I felt down, and your comments on my works have been very helpful. Thank you.

Dedicated to my wife (Nur Hidayah Nazahiyah Erham) and my children (Harith Fakhruddin Azlan and Najah Munirah Azlan). Your love, moral support and patience have been my fuel of strength in completing my academic journey.

1 INTRODUCTION

Microbially influenced corrosion (MIC) continues to be a major concerns among many industries that operate equipment exposed to contaminated soil and seawater. Its large and unpredictable corrosion rates makes it one of the most devastating corrosion types. Many high profile equipment failures in the oil and gas industries have been attributed to MIC. Not only has it affected expensive investment in critical equipment, but its effects are far reaching to the reputation of companies themselves. Two methods have been identified to handle MIC based on industrial experience, which are “keeping the system clean” and chemical treatments.

Keeping a system clean has been identified as one of the most effective methods to curb MIC. This method keeps MIC microorganisms off the metals surfaces and forming biofilm. However, this method is tedious and, in some circumstances, expensive to perform and maintain. For example, in the multiphase crude oil transport from offshore to storing facilities onshore via subsea pipelines, pigging activities are performed to keep the internal surface of the pipeline clean. However, for highly contaminated crude oil that contains seawater or sulphate reducing bacteria from the underground reservoir, pigging activities need to be performed very frequently and this leads to additional costs and resources such as manpower and pigging equipment, not to mention operational shutdowns that lead to lost revenue opportunities.

Chemical treatments are also identified as effective ways to limit MIC. For example, biocides are introduced into a system by means of periodical small amount injections. As with keeping the system clean, the more contaminated a system is, more amount of chemicals injections are needed. This would also lead to cost problems since the cost of chemicals are very high in the market. But these measures are meant to protect the internal surfaces of equipment exposed to MIC. The external surfaces of equipment exposed to MIC have only protective coating as a method to protect from corrosion. To assist corrosion prevention by coating, the industries look to cost effective ways, such as cathodic protection.

General application of cathodic protection is to protect external surfaces of structure/equipment from corrosive environment. It provides a safe cathodic potential

on the metal surface to slow or halt oxidative corrosion reactions. The potential needed to protect steel in corrosive environment has been well established, as well as the potential needed to protect it in risk of MIC. This is crucial especially for metals or equipment exposed to microbially active seawater. Past studies have indicated that cathodic protection indeed has an effect on MIC, but these effects vary in results. For example, while it was reported that high pH values at metal surfaces due to cathodic potential of have biocidal effect on microorganisms' viability, it has also been reported that even a potential of -1070 mV ($Cu/CuSO_4$) is not sufficient in preventing growth of SRB [1]. From practical experience, the industry has recommended a potential of – 950 mV for cathodic protection under anaerobic conditions, but no studies have been conducted to understand the gradual effects of various cathodic protection potentials on MIC microorganisms especially SRBs.

The present study intends to demonstrate the effect of cathodic potentials on SRB by applying constant cathodic potentials on mild steel exposed to seawater. The potentials chosen range from underprotection values to overprotection values and the effects on SRB viability on steel surfaces are studied using several analysis methods such as SRB presence test, Most Probable Number (MPN) analysis, scanning electron microscopy (SEM) and energy dispersive X-ray spectroscopy (EDX).

2 LITERATURE REVIEW

2.1 Fundamentals of Corrosion

There are three main reasons for concern about and the study of corrosion which are safety, economics, and conservation. Early failure of bridges or structures due to corrosion can result in human injury or even loss of life. Failure of operating equipment can have the same disastrous results. Corrosion is defined as the degradation of a material's properties or mass over time due to environmental effects. It is the normal inclination of a material's compositional elements to return to their most thermodynamically stable state. For most metallic materials, this means the formation of oxides or sulfides, or other basic metallic compounds generally considered to be ores. Luckily, the rate of these processes is low enough to enable the making of useful building materials. Only inert environments and vacuum can be considered free of corrosion for most metallic materials. Under usual circumstances, iron and steel corrode in the presence of both oxygen and water. If either of these materials is not present, corrosion usually will not take place. High corrosions rate may take place in water, in which the rate is increased by the acidity or velocity of the water, by the movement of the metal, by an increase in the temperature or aeration, by the presence of microorganisms, or by other less common factors. On the other hand, corrosion is generally stopped by films (or protective layers) consisting of corrosion products or adsorbed oxygen; high alkalinity of the water also reduces the rate of corrosion on steel surfaces. The amount of corrosion is controlled by either water or oxygen, which are necessary for the process to take place. For example, steel will not corrode in dry air and corrosion is insignificant when the relative humidity of the air is below 30% at normal or reduced temperatures [2]. Protection from corrosion by dehumidification is based on this fact. All structural metals corrode to some degree in natural environments. These corrosion processes follow the basic laws of thermodynamics. Corrosion is an electrochemical process and as such, under controlled conditions, it can be measured, repeated, and predicted. Since it is governed by reactions on an atomic level, corrosion processes can act on isolated regions, uniform surface areas, or result in subsurface microscopic damage. These forms of corrosion are complicated with further subdivisions. Just consider adding basic environmental variables such as pH, temperature, and stress, and the predictability of corrosion begins to be more difficult.

2.2 Passive film on iron

Iron in iron oxides can assume a valence of two or three. The iron is protected from the corrosion environment by a thin oxide film 1 to 4 nm in thickness with a composition of Fe_2O_3/Fe_3O_4. This is the same type of film formed by the reaction of clean iron with oxygen or dry air. The Fe_2O_3 layer is what gives passivity, while the Fe_3O_4 provides the base for the formation of a higher oxidizing state. Iron is harder to passivate than nickel, because with iron it is impossible to go directly to the passivation species Fe_2O_3. The Fe_2O_3 layer will not form until the Fe_3O_4 phase has existed on the surface for a reasonable period of time. During this time, Fe_3O_4 layer continues to form [3].

2.3 Forms of corrosion

There are many forms of corrosion. These include:

1. Uniform corrosion
2. Intergranular corrosion
3. Galvanic corrosion
4. Crevice corrosion
5. Pitting
6. Erosion corrosion
7. Stress corrosion cracking
8. Selective leaching

In microbially influenced corrosion, much attention is given to pitting corrosion, since this is the most common form of corrosion observed on MIC failures. Pitting corrosion is in itself a corrosion mechanism, but it is also a form of corrosion often associated with other forms of corrosion mechanisms, for example MIC. It is characterized by a highly localized loss of metal. In the severe case, it appears as a deep, tiny hole in a generally unaffected surface. The initiation of a pit is associated with the breakdown of the protective film on the metal surface. The depth of the pit eventually leads to a through perforation or a massive undercut in the thickness of the metal part. Often, the pit opening is covered with corrosion product, making it hard to detect during visual inspection activities. This, along with a tiny loss in weight or absence of apparent reduction in the overall wall thickness, could not provide a good perception of the

degree of the damage. Pitting may result in the perforation of a water pipe, making it useless even though a very small percentage of the total metal has been lost due to rusting. Pitting can also cause dangerous structural failure from localized weakening effects even though there is still a large amount of material remaining. Pits may also contribute in brittle failure, fatigue failure, environment-assisted cracking like stress corrosion cracking (SCC), and corrosion fatigue, by providing areas of stress concentration. The main factor that causes and accelerates pitting is electrical contact between dissimilar metals, or between concentration cells (areas of the same metal where oxygen or conductive salt concentrations in water differ). These couples cause a difference of potential that results in an electric current flowing through the water or across moist steel, from the metallic anode to a nearby cathode. The cathode may be brass or copper, mill scale, or any other portion of the metal surface that is cathodic to the more active metal areas. However, when the anodic area is relatively large compared with the cathodic area, the damage is spread out and is usually negligible. When the anode area is relatively small, the metal loss is concentrated and may be serious. Pitting may also develop on bare clean metal surfaces because of irregularities in the physical or chemical structure of the metal. Localized dissimilar soil conditions at the surface of steel can also create conditions that promote pitting.

The presence of microbial cells on a metal surface together with their metabolic activities, have influences on electrochemical processes. The colonies that become sessile on the metal surface, grow and form physical anomalies on the metal surface and forming local cathodes and anodes, giving rise to increased risk of pitting corrosion [4]. Thus, MIC is considered a devastating type of corrosion process, and the detailed understanding on effects of MIC on materials is essential to plan for a proper corrosion control for this type of corrosion process.

2.4 Microbially influenced Corrosion (MIC)

MIC could be destructive to almost all engineering materials [5]. The way that MIC affects corrosion has been argued by scientists. For example, it was thought that acid production by bacteria is how it affects corrosion, but experience with aerobic bacteria suggested that acid production was not a main cause of corrosion, while some other works reported that presence of bacteria was not a significant aspect ([6],[7]). Even the definition for MIC varies although it can be considered more or less similar, as follows:

- "MIC is an electrochemical process whereby micro-organisms may be able to initiate, facilitate or accelerate corrosion reactions through the interaction of the three components that make up this system: metal, solution and micro-organisms" [8].
- MIC refers to the influence of micro-organisms on the kinetics of corrosion processes of metals, caused by micro-organisms adhering to the interfaces, termed sessile bacteria [9].

It can be concluded from the above definition that:

- MIC is an electrochemical process
- Microorganisms are able to influence the degree, severity and the corrosion process itself.

MIC can take place in almost all locations such as soil, fresh water, and seawater. Industries such as oil and gas, power generation, and marine industries are also main concerns for MIC [10]. In a case considered as extreme, MIC has caused a failure of crude oil pipeline within 2 years although the pipeline had a design life of 25 years [11]. Corrosion problems in underground pipelines have also been attributed to MIC. The organism notorious for causing MIC is the sulfate reducing bacteria (SRB), although other microorganisms such as iron/manganese oxidizers, methane producers, organic acid producers and sulfur/sulfide oxidizers may also cause MIC. SRB has been reported to contaminate crude oil, resulting in increased levels of sulfur of fuels [12].

2.4.1 Biofilm formation

When bacteria settle themselves onto metallic surfaces, they begin to form a thin film known as “biofilm” under which cells are fixed at a substratum, normally embedded in an organic polymer matrix generated by the bacteria. Biofilms are believed to be about 95% water [13]. Biofilms affect chemical concentrations near the surface of the metal because they restrict oxygen and nutrient transport to the metal surface. Biofilm with a thickness of 100 µm can stop transport of nutrient to the bottom of the biofilm, and thickness of just 12 µm can create an anaerobic local spot for SRB activity. Metabolism of the bacteria uses oxygen and produces metabolites. Thus, the net effect of biofilm formation is that it generally creates concentration gradients of chemical species across the thickness of the biofilm [14].

The time taken for a biofilm to develop varies largely, as it may take minutes to hours depending on the environment where the metal is exposed [15]. The bacteria become “sessile – fixed to a substratum”, from their “planktonic state – floating around”, when the bacteria is fixed to the metal surface through exopolysaccharidic substances (EPS) to reduce energy demand from an unneeded appendage [16]. This EPS substance is the one forming biofilm that provides the necessary protection for microorganisms. Bacteria sticking to the metal surface will cause a significantly higher corrosion rate, and planktonic bacteria do not cause significant corrosion effects. The development of EPS helps the bacteria survive in their environment systems and protect themselves from external environment that could endanger them and increase intake of more nutrient by increasing surface area through the EPS. After the biofilm is fully developed, pH and dissolved oxygen factors are largely affected and become very different from the bulk solution, resulting in “ennoblement”, which can be explained as the move of the corrosion potential in the direction of more positive potentials that causes increasing vulnerability to pitting corrosion. Ennoblement consists of a change in the cathodic reaction on the metal, as the result of the microbial activity inside biofilms at the metal/surrounding boundary. This justifies the effects that biofilm formation can have on altering the electrochemistry of the biofilm-metal system [17].

2.4.2 Environment under biofilms

As discussed above, biofilm formation on metal surfaces gives rise to an environment at the biofilm/metal interface that is significantly different from the bulk solution in terms of pH, dissolved oxygen and other organic/inorganic species. Microorganism activities can have electrochemical effects. These electrochemical effects explain how they influence the kinetics of reactions in corrosion processes or even change the corrosion mechanisms altogether [18].

Variations in oxygen concentration in bulk water due to the existence of microbes can affect corrosion [19]. Variations in oxygen concentrations under a biofilm is considered even more drastic than the bulk water due to the intense metabolism of microorganism under it. Metabolism activities of the microbes also result in local cathodes and anodes within the biofilm and the area around the biofilm, and also causing differential aeration as depicted in Figure 2-1 below [20]. Fully developed biofilms can prevent migration of oxygen to anodic spots and as well preventing chloride and other anions to cathodic spots. Metabolites of the bacteria are also contained within the biofilm. The difference in oxygen concentration inside and outside the biofilms on the same metal surface causes differential aeration cell and can increase corrosion rates.

The corrosion rate in MIC is very high and unpredictable, and thus MIC is considered highly damaging compared to other types of corrosion. However, not all microorganisms that are found in the natural environment cause MIC, and thus discussion on specific types that cause MIC can really narrow down our understanding on this type of corrosion.

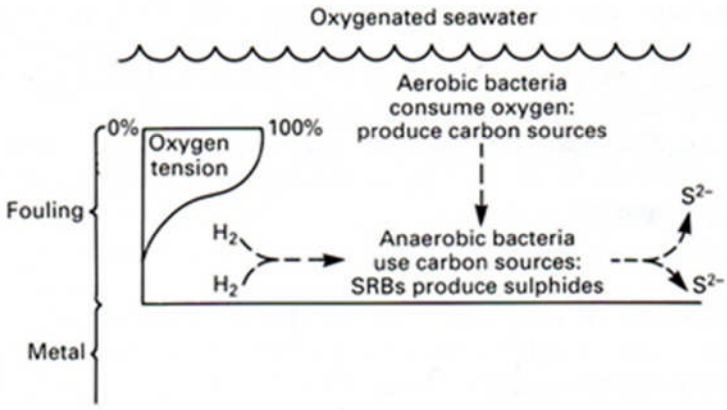

Figure 2-1: Oxygen Concentration gradient caused by a biofilm [20]

2.4.3 Microorganisms that cause MIC

It has been stated that the sulphate reducing bacteria (MIC) are the major cause of MIC [21]. But other researchers have found that MIC of stainless steel 304 in low-chloride (less than 100 ppm) waters occurs in three major corrosion processes which are reduction of pitting potential (caused by iron reducing bacteria), ennoblement (caused by manganese oxidizing bacteria) and pit stabilization (sulphate reducing bacteria) [22]. Thus, MIC could be caused by various bacteria in a closed system [23]. Figure 2-2 below shows the possible complex microorganism interactions and the chemical reactions happening under a biofilm. The interactions are possible among the following microorganisms, where they exchange metabolism products to be utilized by each other:

- Fermenters
- Methanogenic bacteria
- Nitrifying and denitrifying bacteria
- Manganese oxidizing bacteria
- Sulfur reducing and oxidizing bacteria
- Iron oxidizing and reducing bacteria

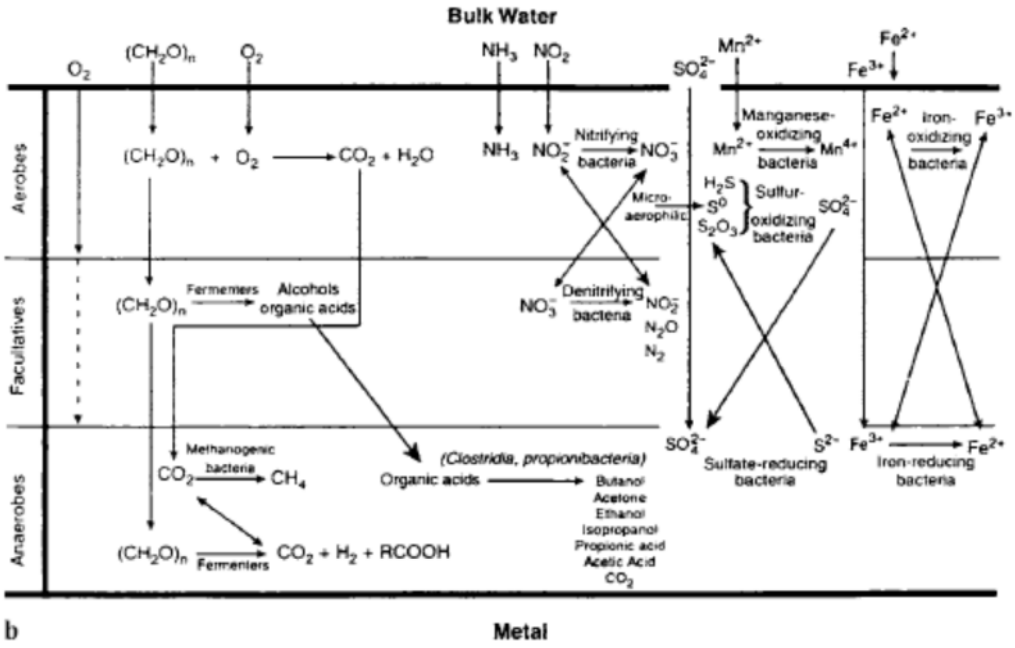

Figure 2-2: Various interactions of microorganisms under a biofilm [24]

2.4.4 Sulfate reducing bacteria (SRB)

These bacteria are the "usual suspect" every time an MIC failure occurs. Several strains of bacteria in the sulfate-reducing genera have been identified. They are defined as any microorganisms that can reduce sulfate to sulfide ([25], [26]). The physiology of this group of bacteria is distinctive compared to other anaerobic bacteria. Their physiology is almost similar to nitrate reducing bacteria, but all of them are strictly anaerobes and no examples of facultative aerobes have been identified. The most significant of SRB is the genera Desulfuvibrio, consisting of 5 species, of which 4 affect corrosion processes. These bacteria are obligate anaerobic, in which they will not grow in even very minute amount of oxygen. They are also heterotrophic, which means they require organic sources of carbon. To thrive, the bacteria will need exclusion of oxygen and a redox potential of around -100mV. They can survive in a wide range of pH (5-10) and temperature (5-50°C) [10]. Their mechanism of obtaining energy and sustaining growth is by oxidizing organic substrate and using sulfate as an electron acceptor, and thus producing sulfide [27]. SRB are classified into two categories, based on their ability to utilise lactate [28] . The category that cannot use lactate consume acetate and are very hard to culture in laboratory. Other microorganisms in the environment produce acetate, lactate and other short chain fatty acid to be used by SRB. Sulfide as a reduction byproduct of SRB often present as hydrogen sulfide or as black ferrous sulfide if iron is

available. If the environment does not contain sulfate, some SRB strains metabolise organic compounds such as pyruvate, producing carbon dioxide, hydrogen, and acetate. Although SRB can grow in a large range of temperature, their optimum growth temperature range is rather small, that is from 25°C to 35 °C. Their metabolites are often the basis for detecting their presence either in a laboratory or in the field.

2.5 MIC mechanism by SRB

Very often in MIC, corrosion of steel occurs under anaerobic conditions where SRB uses sulphate ions to produce hydrogen sulfide. Many MIC investigations are focusing on SRB as the main culprit.

2.5.1.1 Classical MIC mechanism by SRB

The classic theory trying to explain mechanism of MIC by SRB is called cathodic depolarization theory. Based on a mechanism proposed by Kuhr and Vlugt in 1934, the corresponding reactions are expressed as follows [18]:

Eq 2-1: $4Fe \rightarrow 4Fe^{2+} + 8e^{-}$ *(anodic reaction)*

Eq 2-2: $8H^{+} + 8e^{-} \rightarrow 8H_{ad}$ *(cathodic reaction)*

Eq 2-3: $8H_2O \rightarrow 8H^{+} + 8OH$ *(water dissociation)*

Eq 2-4: $SO_4^{2-} + 4H_2 \rightarrow S^{2-} + 4H_2O$ *(bacterial consumption)*

Eq 2-5: $Fe^{2+} + S^{2-} \rightarrow FeS$ *(corrosion product)*

Eq 2-6: $3Fe^{2+} + 6OH^{-} \rightarrow 3Fe(OH)_2$ *(corrosion products)*

Eq 2-7: $4Fe + 4H_2O + SO_4^{2-} \rightarrow 3Fe(OH)_2 + FeS + 2OH^{-}$ *(Overall reaction)*

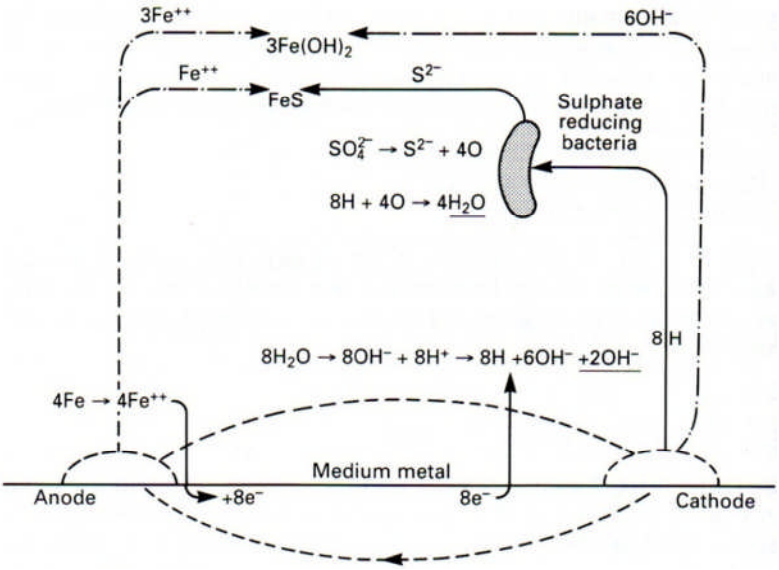

Figure 2-3: MIC mechanism by SRB [18]

Sulphate reduction causes cathodic depolarization. The kinetics of anodic reaction increases, and the net result is the generation of iron sulphide and the creation of an anodic site on the metal substrate.

The overall reaction Eq 2-7 gives description of the role of SRB in the overall corrosion reaction. Based on this, a few proposals on the MIC mechanism by SRB have been put forward such as:

- Importance of hydrogenase to the process
- Depolarizing effects of FeS
- SRB metabolite corrosiveness
- Iron sulfide and hydrogenase interactions
- Effects of H_2S

2.5.1.2 Alternates to the classical MIC mechanism

Metal sulfides are cathodic to the metal surface underneath, and they can also absorb molecular hydrogen [29]. New theories try to minimize the direct role of bacteria in the MIC mechanism. More emphasis has also been put on the effects of oxygen concentration differences and effects of local anodes and cathodes around the biofilm, but not totally ignoring the effects of bacterial metabolites. The role of the biofilm is also a useful way of explaining MIC.

MIC and biofilms have been researched for quite a long time, but still, the exact mechanisms of MIC and detailed structure of biofilms have not been fully understood. New theories proposed that regions near the metal (Figure 2-1) are more anaerobic compared to the region close to the bulk solution. An oxygen gradient is created from the outside of the biofilm towards the metal surface. Theories on biofilm structure attempt to put forth the roles of biofilm in accelerating corrosion. The structure depicted in the figure below pictures biofilm as a negatively charged and having an open structure, where pitting corrosion is active at the anodic site [30].

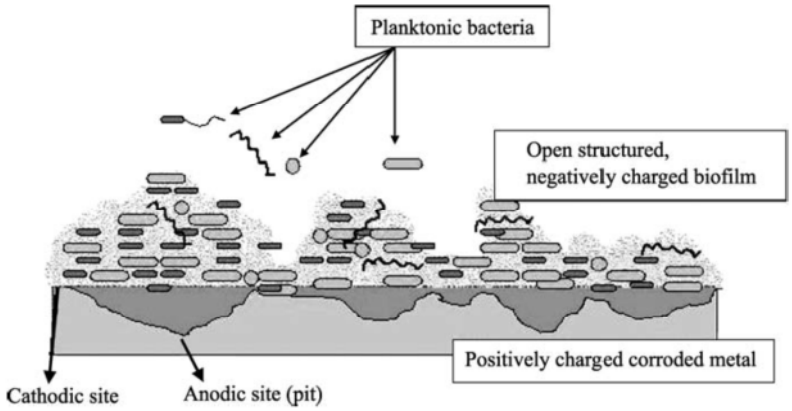

Figure 2-4: Biofilm as negatively charged structure [30]

Theories using biofilms structure and functions have been improved over time. Some researchers proposed that biofilms that do not even contain bacteria but containing exopolymers and functional groups, can produce an environment that has low local pH resulting in corrosion [31]. A more recent biofilm model depicts an open and varying thickness biofilm structure where it is likely to produce gradients of gases and chemical species under the biofilm. Figure below depicts the patchy biofilm model [32].

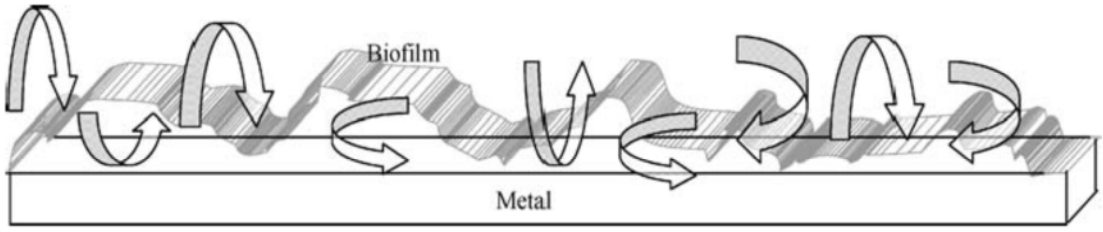

Figure 2-5: Patchy biofilm model showing transport of ions and chemical species [32]

In this model, migration and transport of ions and chemical species are possible, and thus gradients are formed. It also allows the creation of spots with varying concentration of ions and chemical species. This in turn results in differential aeration or

concentration cells, which also creates local anodic and cathodic spots. Anodic sites are where pitting occurs.

There are other microorganisms involved in MIC, but not having significance as much as SRB.

2.5.2 Iron/Manganese oxidizers

These microorganisms obtain energy by oxidizing Fe^{2+} to Fe^{3+} and are quite often observed in deposits that accompany MIC [33]. These microorganisms are observed in tubercles (hemispherical mass) in pits of the corroded steel surface. The iron oxidizers are shaped in an elongated form, often in long protein sheaths or filaments. The appearance of the cells are indistinctive, but the long filaments can easily be spotted under a microscope, and usually not confused with other bacteria under the same sample. The Gallionella bacterium, a type of iron oxidizer, has been a source of lots of cases stainless steel corrosion [34]. There are also some organisms that only amass iron or manganese. This accumulation of manganese or iron under a biofilm is thought to be the cause of corrosion of stainless steels and other ferrous materials in chlorine-treated aqueous systems. They are believed to be the cause of formation of manganese mounds sometimes observed on the ocean floor [35].

2.5.3 Methane producers

Methane producing bacteria are also known as methanogens. Methanogens consume hydrogen and are capable of performing cathodic depolarization [36]. However, they will consume acetate and become fermenters if the environment is low in nutrient. Methanogens lives in symbiosis with other bacteria and the symbiotic relationship with SRB and the others are reflected in Figure 2-2. Although there is not much corrosion cases by methanogens, they are as abundant as SRBs and are likely to cause problems as well as SRB. The case for facilitation of corrosion by methanogens still needs to be strengthened, but methanogens are as common in the environment as SRB and are just as likely to be a problem. Methanogens do not produce solid byproducts that really cause corrosion problems, which in this case is the reason they are not related to any of major corrosion cases.

2.5.4 *Organic Acid Producers*

These bacteria are not usually found in aerated environments such as open and circulating water systems [37]. However, gas transmission lines or closed anaerobic systems may have corrosion problems if organic acid producer infection occurs.

2.5.5 *Sulfur/Sulfide Oxidisers*

Sulfur/sulfide oxidizers are aerobic bacteria that thrive on the oxidation of sulfur/sulphide to sulfate. The suitable environments where they thrive are like inside sewer lines and they can cause fast degradation of concrete and the reinforcing steel [38]. These bacteria also survive on surfaces of concrete buildings and are responsible for the types of damages usually caused by acid rain. In most corrosion cases caused by sulfur/sulfide oxidizers, SRB are also found alongside. This is because both of these microorganisms are symbiotes that utilise energy in a sulfur cycle [39]. It can also be concluded that although these are two microorganisms with different survival requirements (aerobic for sulfur/sulfide oxidizers, and anaerobic for SRB), once they live in sysmbiosis in the sulfur cycle, they can survive, whatever is the environment they live in.

2.6 *Effects of MIC microorganisms on metals*

The processes of bacteria adhering to metal surfaces are affected by, among other factors, [40], [41]:

- Type of metal (for example, iron based or copper based)
- Alloy content of metals
- Surface conditions
- Microstructure of the metal

Bastidas et. al [42] reported MIC preferential attack on a premature weld failure of AISI 316 L stainless steel pipes welded with 308L electrodes, although the initial idea on the root cause was dissimilar weld metal. Attack was selective along the δ-ferrite precipitation. Spheroidal corpuscles were also found in pits on the metal surface, which

are habitually found in MIC related failure cases. Bacterial study by means of cultures of planktonic samples confirmed the presence of SRB in the seawater that was circulated in the circuit.

While capable of exhibiting preferential attack, Yuan and Pehkonen [43] demonstrated that different types of SRB have different effects on depth of pits. Two different biofilms were formed on coupon surfaces by two strains of SRB (Pseudomonas aeruginosa and Desulfubivrio desulfuricans). The increase in coverage, heterogeneity and thickness of the biofilms with time resulted in pitting corrosion of 304 SS underneath. The pits caused by D. desulfuricans was larger than that caused by Pseudomonas, which was attributed to the enhanced corrosion of the stainless steel by sulfide ions. Other corrosion products on carbon steel produced by SRB under the biofilm were reported by Liu [44] to even have protective properties. The corrosion products were formed in stages. The first to form is mackinawite ($Fe_{0.75}Ni_{0.25}S_{0.9}$) that has protective properties. This is then followed by the appearance of FeS and Fe_3S_4 that accelerate corrosion.

2.7 Corrosion control for MIC

A few cases of pipeline failure in temperate water temperatures have been caused by sulfate reducing bacteria. In the South China sea basin with a number of active oil and gas exploration and production activities, 5 major pipeline leak incidents have been reported from year 2004 to 2008, in which SRB were identified as the root cause of failures. Major incidents have such detrimental effects that the national oil and gas company of Malaysia, PETRONAS reported decrease in profit and cited pipeline replacement as one of the major causes of profit losses [45]. A pipeline failure at the Gulf of Suez that was reported to be due to microbial attack reported corrosion induced by microorganisms other than SRB. Although SRB are best known as MIC bacteria, other types of bacteria such as iron-fixing bacteria, methanogens and slime forming bacteria can also cause corrosion [46]. It can be concluded that MIC is indeed devastating and a proper corrosion control method is essential. Several categories of corrosion control for MIC include:

2.7.1 Barrier protection

This involves putting a barrier on the metal surface that isolates the corrosive environment from the metal surface. Anodic oxides, coatings, inhibitors and conversion coatings are a few examples of barrier protection.

2.7.2 Structural design

Improper structural design is the source of many corrosion problems, where the presence of crevices have the most devastating effect. Designs that could collect water and make it stagnant, is a good place for MIC to flourish and do exceptional damage. Thus, designing with these in mind could help mitigate MIC.

2.7.3 Thermodynamic and kinetic protection

Thermodynamic protection is based on making the free energy change into the positive direction, while kinetic protection involves manipulating the corrosion rate. Manipulating thermodynamics of corrosion processes could halt or slow down corrosion processes, while manipulating one half of either anodic or cathodic reaction of a corrosion process could slow down corrosion rate and other effects. Impressed current cathodic protection is an example of thermodynamic and kinetic protection [47].

2.8 Introduction to cathodic protection

Cathodic protection is an established corrosion control method for protection of underground and undersea metallic structures, such as oil and gas pipelines, cables, utility lines and structural foundations. Cathodic protection is generally useful in the protection of oil drilling platforms, dockyards, jetties, ships, submarines, condenser tubes in heat exchangers, bridges and decks, civil and military aircraft and ground transportation systems. The designing of cathodic protection systems is rather complex. However, it is based on simple electrochemical principles. Corrosion current flows between anodes and cathodes due to the existence of a potential difference between the two as demonstrated below.

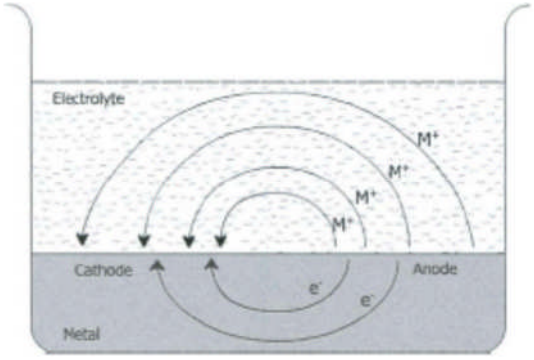

Figure 2-6: Flow of corrosion current due to potential difference [48]

As shown in the figure above, electrons released in an anodic reaction are consumed in the cathodic reaction. If we supply additional electrons to a metallic structure, more electrons would be available for a cathodic reaction which would cause the rate of cathodic reaction to increase and that of anodic reaction to decrease, which would finally minimize or eliminate corrosion. This is basically the purpose of cathodic protection. The additional electrons are supplied by direct electric current. If enough direct current is applied, the potential difference between the anode and cathode is eliminated and corrosion would finally stop. Figure 2-7 below demonstrates how cathodic protection works in terms of E-pH diagram. Cathodic protection brings down the potential of a metal that has a free corrosion potential at the active potential and pH to a lower potential that is defined as an "immune" area. This is also demonstrated in the E-log I diagram.

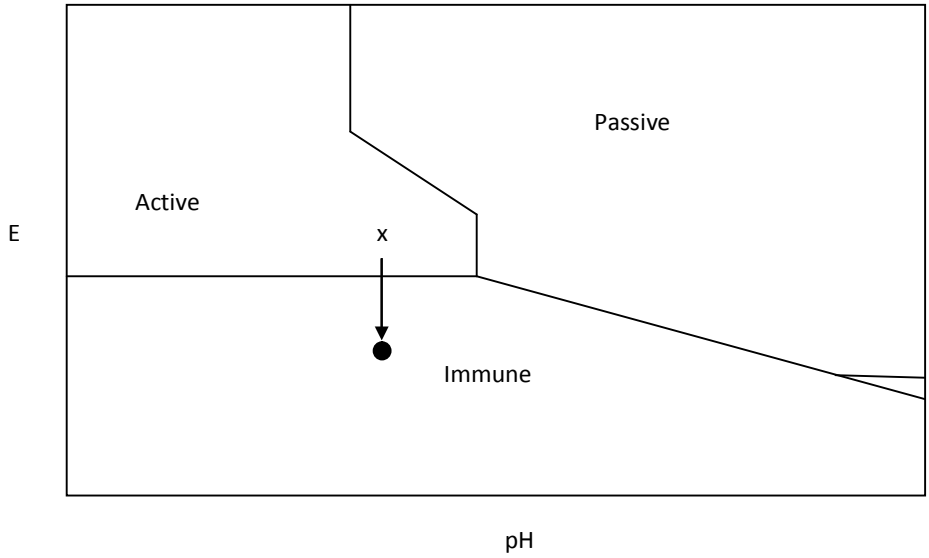

Figure 2-7: E-pH diagram demonstrating reduction of potential from active to immune region

2.8.1 *Electrochemistry of cathodic protection*

The main principle of cathodic protection is reducing the potential of the metal surface to a protective potential E where $E < E_{corr}$. In elaborating cathodic protection in terms of polarization diagram, the figure below could be used. Figure below attempts to explain cathodic protection by schematic polarization diagram showing corrosion point 'C' and protective point 'P' for iron (assuming that oxygen reduction occurs and no other oxidizing agents are present).

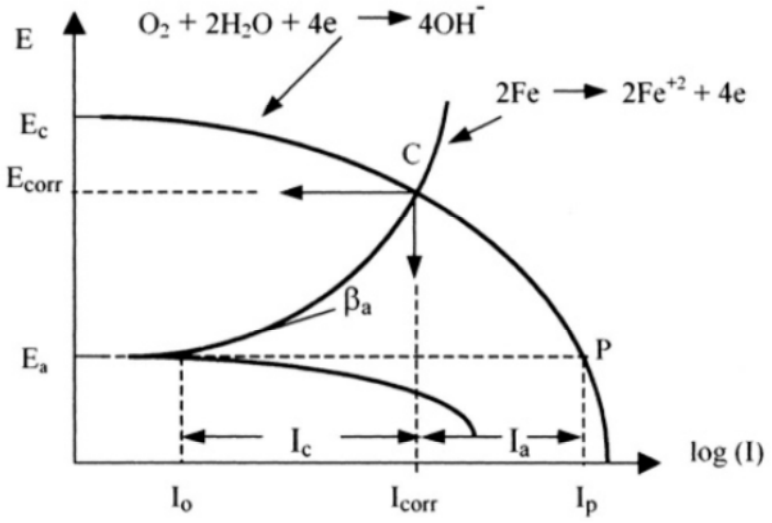

Figure 2-8: Polarization diagram showing corrosion point 'C' and protective point 'P'

From the figure above [49], if the applied potential E, and applied current I are more than E_a and I_a respectively, metal dissolution is possible along curve E_a-C. External supply of electron must be provided to the system to reduce metal dissolution if the applied potential and current are between E_a and E_{corr} and I_a and I_{corr} respectively. Ideal cathodic protection is achieved if applied potential is the open circuit potential of the metal ($E \leq E_a$) and the applied current is purely cathodic ($I \leq I_p$). If applied potential is less than E_a, the metal is also protected at a higher current, but hydrogen evolution is possible leading to coating defects or hydrogen embrittlement. The principle above is applied in the real world mainly by two methods. One method involves current supplied to protected metal using a sacrificial metal that is galvanically more active than the protected metal which is termed "sacrificial anode". The other method involves supply from an external DC current source termed "impressed current" method.

2.8.2 *Cathodic protection by Sacrificial anode*

In cathodic protection, the structure to be protected must be given a cathodic current flow so that it operates as a cathode. The requirement for an external DC current to achieve this can be eliminated by using an anode constructed of a metal that is more active in the galvanic series than the metal to be protected called a sacrificial anode. A galvanic cell is established with the current direction as required.

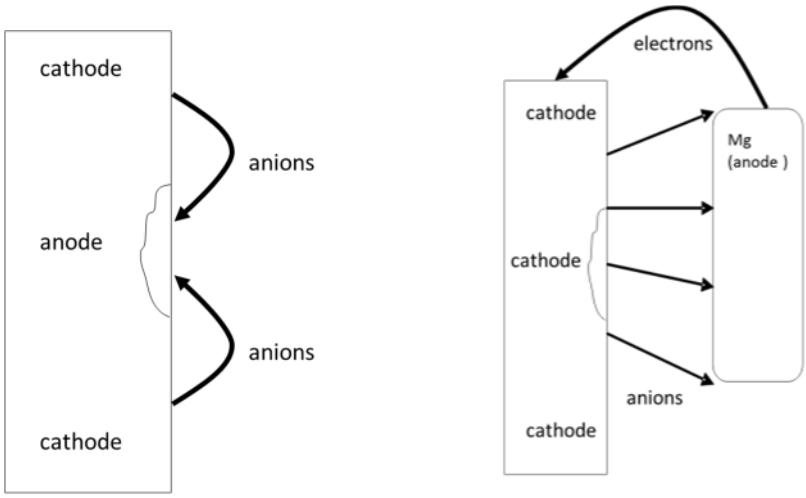

Figure 2-9: Metals without cathodic protection (left) and with cathodic protection (right)

One example of sacrificial anode material is magnesium or magnesium-based alloys.. Magnesium is more active than steel, has a greater tendency to ionize. The open-circuit potential difference between magnesium and steel is about 1 volt. This means that one anode can protect only a limited length of pipeline or over a defined surface area. This low voltage can have an advantage over higher impressed voltages in that the danger of overprotection to some portions of the structure is less and because the total current per anode is limited; the danger of stray-current damage to adjoining metal structures is reduced. Magnesium rods have also been used in steel hot water tanks to increase their service life. The greatest degree of protection is in more conductive electrolyte such as hard waters, compared to soft waters which have lower conductivity.

Zinc or aluminium have been used extensively in seawater applications. Sacrificial anodes for offshore structures in seawater are commonly made of special aluminium alloys because these anodes are low in cost and provide the highest current output per anode weight (as depicted Table 2-1). Zinc anodes are used on coated and buried

pipelines offshore, where the risk for passivation of aluminium anodes is higher due to a lower current density requirement. Zinc or aluminium sacrificial anodes used on ship hulls are usually combined with a paint system. The anodes are placed close to each other on the area around the propeller because the current could leak to the propeller, and the current demand is high due to turbulence around this area. Ballast tanks on tankers and bulk carriers also use zinc and aluminium anodes [50].

2.8.2.1 Sacrificial anode requirements

To provide cathodic protection, a current density of a few milliamps per square meter of metal area exposed is required. In order to determine the anodic requirement, it is necessary to know the energy content of the anode and its efficiency. With this information it is possible to determine the size of the anode required, its expected life, and the number of anodes required. The three most common metals used as sacrificial anodes are magnesium, zinc, and aluminium. The energy content and efficiency of these metals are shown in the table below [51].

Anode material	Theoretical Energy content, ampere-hour per kilogram of mass (Ah/kg)	Typical Anode Efficiency, %	Practical Energy content = Theoretical energy x Anode efficiency (Ah/kg)
Magnesium	2205	50	1102
Zinc	816	90	734
Aluminium	2965	60	1779

Table 2-1: Efficiencies of several common anode materials [51]

Each of the anodes have their own limitations. Zinc is more economical to use than magnesium, but because of the relatively small cell voltage it produces, it is primarily useful to protect ships in seawater or to prevent corrosion in systems that require only small currents. Although magnesium is more expensive and consumed faster than zinc or aluminimum, it provides the largest potential and current. Aluminium cannot be used in environments with pH more than 8, since alkaline conditions will make aluminium self-corrode rapidly.

2.8.3 Cathodic protection by impressed current

This system uses external source of electricity. High voltage from the external source is converted to low voltage DC current by means of a transformer-rectifier. This direct current is impressed between buried anodes and the structure to be protected. Use of inert anode is preferred, as these will last for the longest possible time. Typical anodes used are graphite, titanium, silicon and niobium plated with platinum. The applied current is limited by electrolyte resistivity and by the anodic and cathodic polarization. Impressed current system makes it possible to apply the potential level that is necessary to obtain the current density required by means of the rectifier, whatever the value of the potential is. Electric current flows in the soil from the buried anode to the underground structure to be protected. Therefore, the anode is connected to the positive terminal of the rectifier and the protected structure to the negative terminal. All cables from the rectifier to the anode and to the structure are electrically insulated. If not insulated, wires from the rectifier to the anode can act as an anode and deteriorate rapidly, while cables from the rectifier to the structure may pick up some of the electric current, which would then be lost for protection [52].

2.8.3.1 Current requirements using impressed current method

Metal to be protected and the environment it is exposed to determine the current density required for complete protection. The applied current density must always be larger than the current density equivalent to the measured corrosion rate under the same conditions. Therefore, as the corrosion rate increases, the impressed current density must be increased to provide protection. Three factors affect current requirements:

1. The nature of the electrolyte
2. Resistivity of the electrolyte
3. The degree of aeration.

The current requirement increases with increasing acidity of the electrolyte. For example, soils with high resistance have a lower cathodic current needed to provide protection. The required current to provide cathodic protection can vary from 5 to 220 mA/m^2 of bare surface. Application of impressed current technique in the real world

requires field testing to determine the necessary current density to provide cathodic protection in a specific area. The testing techniques are only some way to obtain approximations. After installation of the system, it is necessary to conduct a potential survey and make the necessary adjustments to provide the desired degree of protection [53].

2.8.3.2 Anode materials and backfill for impressed current system

The determination of anode materials and the backfill (or groundbed) material used in impressed current systems in different environments and applications play a major role, because these anodes are the method through which the protective current is delivered to the protected structure or metal. The type of anode is vital in influencing the reactions on the anode surface. For consumable metals such as scrap steel or cast iron, the main reaction is the anodic metal dissolution. Metal dissolution is negligible if the anode has passive surfaces and the main reactions are gas evolutions. For example, oxygen is evolved in the presence of water, and chlorine gas is evolved if the electrolyte contains chloride ions. The gas evolution reactions also happen on non-metallic conducting anodes surfaces such as graphite. On partially passive surfaces, both the metal dissolution and gas evolution reactions could happen. Corrosion product buildup is associated with the metal dissolution reaction.

A wide range of materials can be used for impressed current anodes. The balance between anode performance and costs play a big role in determining the right anode material to be used. The following Table 2-2 shows selected anode materials in general use under different environmental conditions [54].

Marine Environment	Concrete	Potable water	Buried in soil	High purity liquids
Platinised surfaces Iron and steel Mixed-metal oxides Graphite Zinc High-Si Cr cast iron	Platinised surfaces Mixed-metal oxides Polymeric	High-Si iron Iron and steel Graphite Aluminum	Graphite High-Si cast iron High-Si iron Mixed metal oxides Platinized surfaces Polymeric, iron and steel	Platinized surfaces

Table 2-2: Different anode materials for impressed current systems under different environments [54]

The properties of backfill that hold the impressed current anodes are also important. To increase the effective anode size and lower the resistance to soil, carbonaceous material such as coke breeze and graphite are used. This type of backfill also reduces consumption of the anode material because the anodic reaction is transferred from the anode to the backfill. Three factors are considered to ensure low resistivity of the backfill material

1. Composition
2. Particle size
3. Degree of compaction

The particle size and degree of compaction also influence how anode-generated gases escape. Since it is quite problematic to properly establish the above backfill properties properly in the ground, ready-made anodes and backfill inside metal containers that are factory-prepared according to the best of the above factors are used. These metal containers will be eventually consumed under operational conditions. A set of parallel cylindrical anode rods placed vertically deep underground are commonly used in the industry (termed vertical deep anode). These provide minimised anode bed resistance and induced stray currents, smaller right-of-way surface area, and improved current

distribution. However, vertical deep anodes also incur higher capital expenditure per unit of current output, are difficult to repair in case of any anode damage, and may block gas generated at the anode from escaping [51].

2.8.4 Protection criteria

The appropriate levels of cathodic protection current that are applied have been practically determined by industrial experience or by experiments. Current which is too low, will lead to insufficient corrosion protection, and too much current (overprotection) can cause coatings to disbond and hydrogen embrittlement. Furthermore, corroding structures do not have uniform corrosion potentials or protection requirements over their entire surface. Practical protection criteria need to take such variations into account. The following are the protection criteria that have been proposed for buried steel structures [47]:

- Potential of structure $\leq$ - 850 mV w.r.t. saturated $Cu/CuSO_4$ reference electrode (under aerobic conditions).

This was first proposed in 1928 [55] and has been widely applied since then for buried and immersed steel structures. Two descriptions on this criteria are stated in NACE RP0169 as follows [56]:

1. "A negative (cathodic) potential of at least 850 mV with the cathodic protection applied. This potential is measured with respect to a saturated copper-copper sulphate reference electrode contacting the electrolyte. Voltage drops other than those across the structure to electrolyte must be considered for valid interpretation of this voltage measurement."
2. "A negative polarised potential of at least 850 mV relative to a saturated copper-copper sulphate reference electrode".

The first description is the 'ON potential' with consideration of voltage drop from the reading, while the second description is non-specific. Voltage drop (or IR drop) is defined as the potential that develops between the structure and the reference electrode due to the resistance from electrolyte, coating and metallic path travelled by the current.

The ON potential is simply the potential measured when the protection current is applied. It is also called the half-cell potential criterion, and is the best known and widely used in industry. It was stated by Mears and Brown [57] that complete cathodic protection can be achieved if the surface of the corroding metal is polarised to the open circuit potential of the anode. However, it cannot be assumed to be this way because the standard equilibrium potential (E_0) of Fe/Fe^{2+} is 0.440 V (vs SHE). Assuming the interfacial Fe^{2+} concentration when corrosion stops is around 10^{-6} g ions/l, then using Nernst equation, the equilibrium potential (E_a) is [58]:

$$Eq\ 2\text{-}8: E_a = E_0 + \frac{0.059}{2} log a_{Fe^{2+}}$$

Where $a_{Fe^{2+}}$ is the activity or the thermodynamic concentration of the ferrous cation mentioned above. From Eq 2-8, E_a= -0.617 mV (SHE) or -0.93 V vs CSE, which is somewhat more negative but not much difference with NACE recommended level of -850 mV vs CSE. The satisfactory performance under the less stringent potential requirement may be related to the formation of protective ferrous hydroxide on the surface. Potential protection criteria are based on the potential of the structure at very close region in the soil interface with the protected metal. It is difficult to measure the potential of a metal surface against this metal-soil interface. Thus it is usually done by placing the reference electrode at a distance away from the structure. This method has to include in some correction factor due to IR drop.

However, when taking surface potential readings, the IR drop error will tend make measurement inaccurate. With IR drop, the pipeline potential appears to be more negative than the true pipe-to-soil potential. Thus it is necessary that corrections are made for the IR drop for assessments of buried structures. This is where the OFF potential reading is applicable. OFF potential is the potential measured right after interrupting the current source [59], where this is mainly concerning impressed current cathodic protection systems. This temporary interruption of current supposedly produces a reading free from IR drop effects. The basis for this methodology is illustrated in Figure 2-10. A so-called “waveform analysis” has to be done to establish a suitable time interval after the current is interrupted for reading the OFF potential. This time interval are typically 200-500 ms. As shown in Figure 2-10, transient potential

spikes tend to occur in the transition from the ON to the OFF potential, which should be avoided in establishing the OFF potential. If the reading is taken immediately right after interrupting the source, the reading is actually much more positive [60].

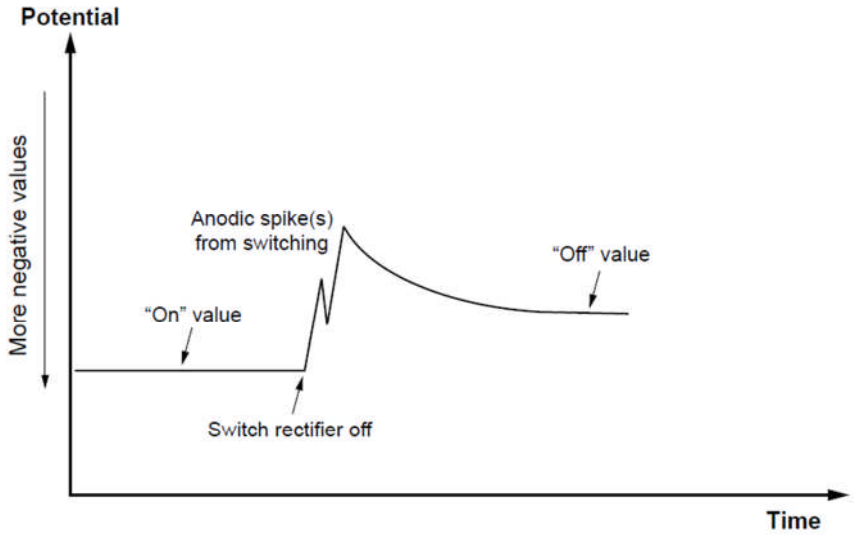

Figure 2-10: Measurement of instant-OFF potential by interrupting the current supply [60]

- Positive potential shift of ≥ 100 mV when the current is interrupted.

This criterion is described in NACE RP0169-2002 as:

"A minimum of 100 mV of cathodic polarisation between the structure surface and a stable reference electrode contacting the electrolyte. The formation of decay of polarisation can be measured to satisfy this criterion."

This criterion specifies a minimum 100 mV difference between the free corrosion potential (depolarised potential) and the OFF potential [61]. However, this measurement is made by interrupting the current source to measure potential decay instead of polarising the metal 100 mV more negative than the free corrosion potential because not many operators really measure the free corrosion potential of their equipment [59]. This criterion poses a problem because of the undefined time limit to determine the depolarised potential since this potential varies with coating conditions, environment and polarisation level [61]. Since this criterion uses less current density than the ON potential criterion, it is more suitable for structure that have poor or aging coating, where the ON potential criterion is not economical.

- Potential of structure ≤ -950 mV w.r.t. saturated $Cu/CuSO_4$ reference electrode (under anaerobic conditions where microbial corrosion may be a factor)

This criterion is based on field experience and also thermodynamically determined using the Fe-S-H_2O ternary systems equilibrium diagram proposed by Horvath and Novak [62].

- Negative potential shift of ≥ 300 mV when current is applied (rarely used and may cause problems)

This criterion has been the alternative for quite some time, but was removed because of problems associated with IR drop uncertainties when applied [63].

As specified by BS EN 13174:2001, the current density needed to protect bare steels in seawater should be more than 80 mA/m^2 in initial and repolarisation stage, and more than 50 mA/m^2 in maintenance stage [64]. However, DNV-RP-B401 specifies the current densities needed in more details including factors such as depth and climatic region based on surface temperature of seawater as shown in Table 2-3 below.

Depth (m)	Tropical (>20°C)		Sub-Tropical (12-20°C)		Temperate(7-11 °C)		Arctic(>20°C)	
0-30	150	70	170	80	200	100	250	120
>30-100	120	60	140	70	170	80	200	100
>100-300	140	70	160	80	190	90	220	110
>30-100	180	90	200	100	220	110	220	110

Depth (m)	Tropical (>20°C)	Sub-Tropical (12-20°C)	Temperate(7-11 °C)	Arctic(>20°C)
	Final	Final	Final	Final
0-30	100	110	130	170
>30-100	80	90	110	130
>100-300	90	110	140	170
>30-100	130	150	170	170

Table 2-3: Current densities (mA/m^2) required for cathodic protection of bare metal exposed to seawater [65]

In turn, several factors affect the current density requirements such as velocity of water movement, salinity, pH, temperature and water depth that affects the dissolved oxygen contents.

Different material-environment combinations will require different protection criteria. Other metals used in buried conditions, such as copper, aluminum, and lead, have different criteria than steel. Table 2-4 below provides a listing of cathodic protection criteria for different materials and environments. It should be noted that excessively negative potentials can be damaging to materials such as lead and aluminum and their alloys, due to the formation of alkaline species at the cathode [66].

Metals	CP criteria	References
Buried steel and cast iron (not including concrete reinforcements)	-850 mV ($Cu/CuSO_4$) – aerobic environment -950 mV anaerobic environment. Minimum negative 300 mV shift under application of CP Minimum positive 100 mV shift when depolarising (after CP current switched off)	NACE RP0169-83, BS CP 1021:1973 BS CP 1021:1973 NACE RP0169-83 NACE RP0169-83
Steel (offshore pipelines)	-850 mV ($Cu/CuSO_4$) Minimum negative 300 mV shift under application of CP Minimum positive 100 mV shift when depolarising (after CP current switched off)	NACE RP 0675-75
Aluminium	Minimum negative potential shift of 150 mV under application of CP Positive 100-mV shift when depolarizing (after CP current switched off) Positive limit of -950 mV ($Cu/CuSO_4$) Negative limit of -1200 mV ($Cu/CuSO_4$) Negative limit of -1200 mV ($Cu/CuSO_4$)	NACE RP 0169-83 NACE RP 0169-83 BS CP 1021:1973 NACE RP 0169-83
Copper	Positive 100-mV shift when depolarizing (after CP current switched off)	NACE RP 0169-83
Lead	-650 mV ($Cu/CuSO_4$)	BS CP 1021:1973
Dissimilar metals	Protection potential of most reactive (anodic) material should be reached	NACE RP 0169-83

Table 2-4: Cathodic protection criteria for different metals [66]

2.9 Industrial application of Cathodic protection

Offshore pipelines transporting crude are typically protected with a combination of sacrificial anodes and coating, often with a concrete weight coat. The anodes are from zinc shaped as bracelets around the pipe. A typical distance between anodes is 10 joints. Aluminium is not used for the anodes because of a tendency to passivate and become ineffective in seabottom mud, although some new alloys may be acceptable. The cathodic potential is designed such that the potential should be more negative than -800mV (SCE) along the protected pipeline [51]. A few researches and studies demonstrated that MIC has effect on cathodic protection [67], [68], [69].

2.10 Effect of Microorganisms on cathodic potential

It is necessary to modify the cathodic potential applied in the presence of microorganisms [70]. Impressed current cathodic protection forces the following reactions:

Eq 2-9: $O_2 + 2H_2O + 4e^- \rightarrow 4OH^-$

Eq 2-10: $2H_2O + 2e^- \rightarrow H_2 + 2OH^-$

This causes an increase in alkalinity, and thus shifting the equilibrium to the following reactions, where hydroxyl ions causes the precipitation of magnesium hydroxide if the surface pH achieves a critical value of 9.3 [71]:

Eq 2-11: $Mg^{2+} + 2OH^- \rightarrow Mg(OH)_2$

Eq 2-12: $HCO_3^- + OH^- \rightleftharpoons H_2O + CO_3^{2-}$

Eq 2-13: $Ca^{2+} + CO_3^{2-} \rightleftharpoons CaCO_3$

Reactions and Eq 2-11 and Eq 2-13 are known as precipitation of calcareous deposits. Calcareous deposit is thought to be the main factor that affects the economics of cathodic protection. Microbiologically produced acetic acid can dissolve a porous calcareous film and induce an increase in corrosion current density demand.

2.10.1 Effect of MIC on corrosion protection electrochemistry and vice versa

MIC and cathodic protection have effects on each other. Understanding how MIC microorganisms affect cathodic potential helps planning for corrosion control measures to be taken for protection of steel against MIC by cathodic protection. Moos and Gumpel [67] studied the microbiological influence on the electrochemical potential of stainless steel by studying its open circuit potential in variable conditions of the bulk fluid such as change in availability of nutrients, addition of biocide and varying oxygen concentration. They found that the addition of biocides resulted in marked decrease of the free corrosion potential, while variations in nutrients and oxygen availability did not have much influence. The direct effect of cathodic protection on viability of biofilms was studied by Miyanaga [72]. By applying cathodic potential on artificial biofilm containing *Pseudomonas aeruginosa*, he concluded that increased cathodic polarization (more negative potential) causes electrostatic repulsion in between the steel and the bacteria. pH under the biofilm was reported as very alkaline with more than 99% of the area underneath having pH more than 9. Guezennec [68] tried to understand the same subject on the direct effects of cathodic protection on MIC under synthetic and natural seawater. He found that both biofilm and bacterial metabolism can interfere with cathodic protection. Iron sulfides produced by the microorganism contributes to current demand of the cathodic protection system and if hydrogen is generated during cathodic protection, this cathodically produced hydrogen can encourage growth of hydrogenase active microorganism such as sulfate reducing bacteria. Using soil as electrolyte, Kajiyama et. al [69] found that cathodic protection have substantial effects in halting MIC by decreasing the number of living iron bacteria as a result of environmental changes on the protected surface, including an increase in pH and decrease in redox potential (E_h).

Cathodic potential applied to metals have direct or indirect effects on the viability of sessile microorganisms causing MIC. Applying cathodic potential to metal surfaces has a direct effect on the chemistry of the metal surface and the surrounding areas. Applied potential at metal surface also have effects on the bacteria attached to the surface, since this potential brings about some chemical and electrochemical reactions that might have direct or indirect effect on the bacteria. For example, the consumption of oxygen at the polarized surface might have effect on reproduction of aerobic bacteria [73]. It is also

possible to physically or chemically alter metal surfaces to lessen bacterial settlement on the surface [74]. For example, electropolished surfaces are much less susceptible to biofilms buildup compared to surfaces that had other methods of preparation such as sandblasting, grinding and polishing [75]. Electrostatic repulsion from cathodic polarization is also a factor preventing bacterial attachment to the metal surface, since bacteria are considered negatively charged. Thus they will not be able to attach themselves to the negatively charged metal surfaces due to this ([76], [77]). However, the simple electrostatic repulsion theory was also disputed by a study finding that bacterial cells are able to affix to negatively charged metal surface by utilizing divalent cations such as Ca^{2+} and Mg^{2+} as a link [40].

In order to determine the appropriate potential for cathodic protection under risk of MIC, Horvath and Novak worked on thermodynamics and suggested the protection criterion of -0.95V ($Cu/CuSO_4$) to protect steel against MIC [62]. For anaerobic conditions under large fouling deposit on low carbon steel, with the presence of acid producing bacteria or SRB, a cathodic potential of $-900mV$ (vs. SCE) with polarization shift of approximately 200mV is required for a cathodic protection [78]. Although these findings suggest that a potential of more negative than -900 mV (vs $Cu/CuSO_4$) has detrimental effects on microorganisms, it has also been found that cathodic polarization of $-1070mV$ (vs $Cu/CuSO_4$) applied to pure iron surface could not stop the growth of sulphate reducing bacteria [79], and another study reveals increase in bacterial count with more negative potential [80]. This is because hydrogen can be generated at cathode, which is also important in generating an environment that supports anaerobic bacteria rather than aerobic bacteria [73]. While studies on tin oxide and titanium cathodes reveal the same result as iron based metals [81], studies on other metals with polarized surfaces reveal varying results compared to iron based metals. For example, a study on bacterial attachment to copper has shown an increase in bacterial population with cathodic polarization [82]. Although the results of these studies suggest strong initial effects of CP electrochemistry on bacteria settlement and reproduction, in the longer term, a cathodically polarized steel surface protected by direct current is favorable to the settlement of larger fouling organism, but pulsed current cathodic polarization instead of using direct current has been proven to impede biofouling on steel in seawater [83]. Not only does cathodic polarization have effects on bacteria, the opposite case has also been observed. For example, effects of bacterial activity on

cathodic protection. The activities under a biofilm increase the kinetics of the oxygen reduction reaction. Thus, it increases the open circuit potential and shifts the cathodic polarization curve towards higher potential (positive direction) and more currents [84]. Thus, the main consequence is an increase in current density necessary to polarise metal to the appropriate protection potential [85].

2.10.2 Change in pH at metal surface during cathodic polarization and its effect on bacterial activity

Cathodic polarization has direct effect on the pH near the polarized metal surface. It alters the chemistry at the metal surface by producing a high localized pH due to generation of hydroxyl ions [68]. This might also affect the area adjacent to the environment with the pH increase. The polarised surface is a negatively charged region, and the negatively charged hydroxyl ions diffusion layer thickness is reportedly ranging from 50 micrometer in stirred conditions to around 500 micrometer in stagnant conditions [86]. The pH value is also affected by conditions of the bulk solution as well as the level of cathodic polarisation. A more negative potential results in higher current densities at the metal surface and thus more production of hydroxyl ions [87]. In one study, pH as high as 11.5 was reported [73]. The pH at the surface affects all aspects of bacterial activity, from their settlement, growth to viability on the metal surface. Hydroxyl ion formation is directly related to electron availability, as measured by current demand. Thus higher current should produce higher pH, greater oxygen consumption and increase in hydrogen generation [81]. High pH values can harm or destroy bacteria due to lysis of lipids and proteins in the cell membrane by alkali. Chemical reactions related with pH increase have further restraining effects on bacterial attachment [88].

It can be concluded that there is compelling evidence that cathodic protection does have effects on the microorganisms that cause MIC (and thus interpreted as having effect on MIC). These microorganisms, conversely, have an influence on important factors in cathodic protection, such as current and the cathodic potential. The experimental works presented in this thesis are designed to investigate the gradual effects of cathodic potentials on MIC and of particular interest, how the MIC is affected (and affects) the cathodic protection criteria (ON potential) discussed in Section 2.8.4.

3 EXPERIMENTAL WORKS

The experimental works consists of two parts, Stage 1 and Stage 2:

1. The first part (Stage 1) are preliminary experiments which are further divided into two:
    a. Controlling cathodic potential of mild steel in salt water using a power supply and variable resistor (Test cell 1)
    b. Potential sweep - determination of current density needed to polarise mild steel in seawater. (Test cell 2)

    The results of the first part are used to determine parameters needed to perform the second part of the experimental works.

2. The second part (Stage 2) is the actual experiment using parameters and findings from the first part, that studies the effect of cathodic protection on SRB, which is divided into two parts:
    a. Galvanostatic – Current is held constant during cathodic polarization using method described in Stage 1 Test Cell 1.
    b. Potentiostatic – Potential is held constant during cathodic polarization of mild steel samples in seawater using a polypotentiostat.

3.1 Preparation of metal coupons for Stage 1

The base metal used in the experimental work is mild steel. To prepare the main sample, a mild steel rod (19 mm diameter) is cut to small pieces of 1 cm length. The small coupon has a cross section of 2.835 cm^2 in surface area. Copper wire is spot welded to the back of the sample to provide electrical connection. The wire is then protected in a small plastic tube, and mounted together. The metal sample is lightly coated with a mixture of araldite resin and hardener to form a thin film of the resin onto the metal surfaces, and left to cure for 24 hours. This step is necessary to reduce stress effect on the metal surface and to enhance contact between resin and metal surface when it is fully mounted into the resin. This enhanced contact will help prevent unnecessary crevice corrosion on the metal-resin interfaces that can potentially create interfering currents that affect accurate reading of polarization behaviours. The coupon is then placed into a cylindrical plastic mould. A mixture of araldite resin and hardener (10:1 weight ratio) is poured into the mould. It is left to cure for another 24 hours.

After curing, the mounted coupon is finished to P120, P240 and finally P400 metallographic grinding paper. A sample of the finished mounted metal coupon is shown in the figures below.

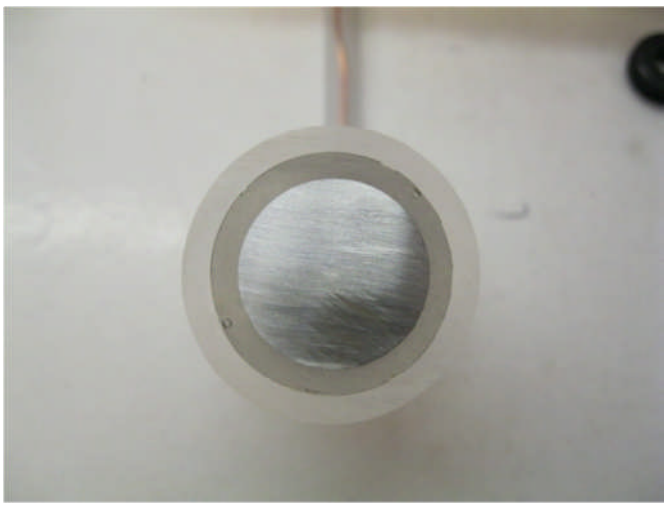

Figure 3-1: Front view of the mounted coupon

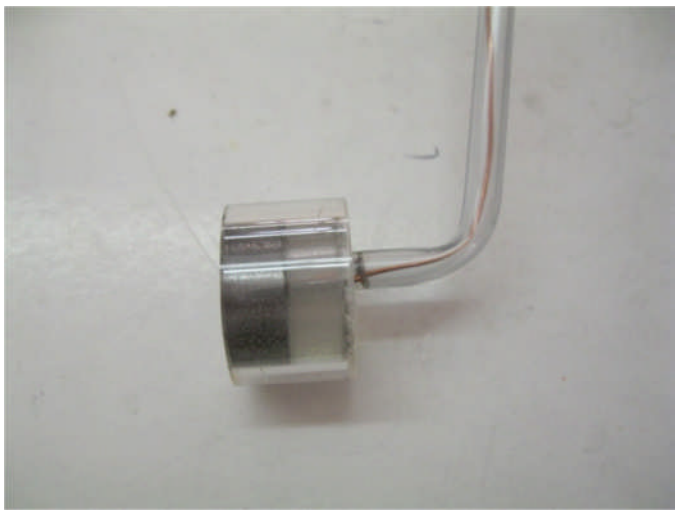

Figure 3-2: Side view of the mounted coupon showing copper wire connection

To ensure electrical continuity, the finished metal coupon is tested using a multimeter.

3.2 Controlling cathodic potential of mild steel in salt water using a power supply and variable resistor – Stage 1 Test cell 1

3.2.1 Objective

To set up polarization of mild steel in salt water using power supply and resistors connection and determine the cathodic potential stability through time.

3.2.2 Specimen preparation

The main sample was prepared as described in Section 3.1.

3.2.3 Test solution

Test solution used in this test cell was salt water. Salt water is prepared by diluting 35 g sodium chloride in 1 liter of deionised water. The resulting solution has salinity value of 3.5%, the average salinity of seawater.

3.2.4 Experimental set up

A power supply was set to 12V and connected to a fixed resistor and linear variable resistor. The positive terminal was connected to the resistors and subsequently to a graphite counter electrode inside the salt solution. The working electrode is then connected to the negative terminal. A Luggin capillary was placed near the surface of the working electrode, which was then connected to a reservoir to hold the saturated calomel reference electrode in contact with the test solution. The connection is shown in the figure below.

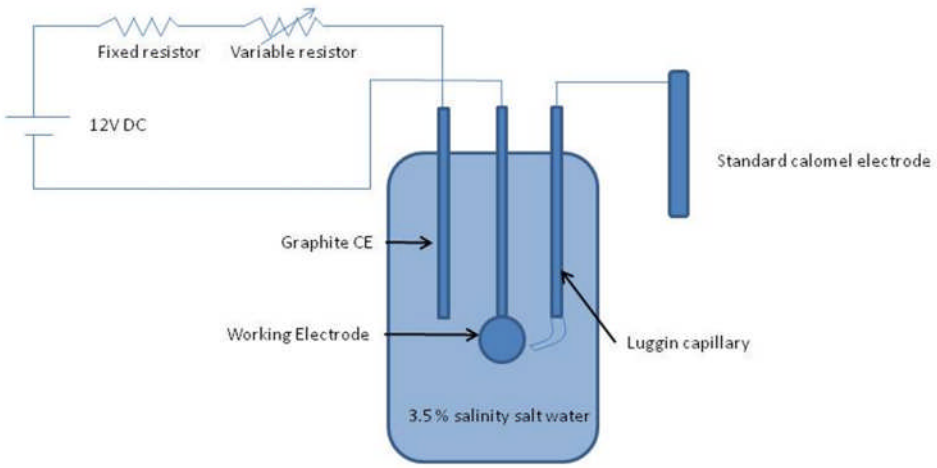

Figure 3-3: Test cell setup (Stage 1 Test Cell 1)

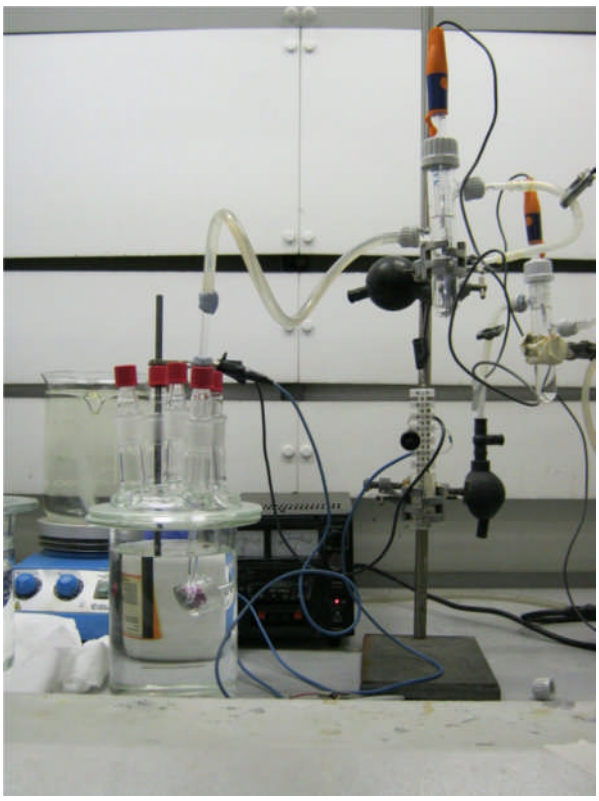

Figure 3-4: Experiment equipment setup

3.2.5 Experimental procedure

The duration of this experiment was 5 days. The variable resistor was used to periodically adjust the potential of metal specimen. The new resistance value was also held for a sufficiently long time to determine its stability.

3.2.6 Results

The following table summarises the potential readings with this setup:

Date	Time (hrs)	Variable resistor value (kΩ)	Potential V (vs SCE)	Average absolute deviation (mV)
21.01.11	2100	39.2	-0.839	3.56
	2200		-0.829	
22.01.11	1000		-0.835	
	1700	31.3	-0.850	2
23.01.11	0900		-0.855	

Date	Time (hrs)	Variable resistor value (kΩ)	Potential V (vs SCE)	Average absolute deviation (mV)
24.01.11	1800		-0.851	
25.01.11	1500	23.5	-0.880	2.67
	1900		-0.873	
26.01.11	1100		-0.878	
	1745	15.6	-0.889	

Table 3-1: Result of potential readings for Stage 1 Test Cell 1

3.2.7 Conclusion

It can be observed from the table that the readings are quite stable when held for a sufficiently long time. Although it is not absolutely stable, the deviations are considered quite small since the potential deviation from the mean potential is by an average of 2.7 mV. It is concluded that the variable resistor can be used to control cathodic potential of mild steel and hold the potential stable. This configuration is further tested using multiple working electrodes in seawater in Stage 2.

3.3 Polarisation behavior of mild steel in seawater – Stage 1 Test cell 2

3.3.1 Introduction to potentiostat

A potentiostat is an electronic instrument required to control and run three-electrode cell experiments. It maintains potential of the working electrode at a predetermined level with respect to a reference electrode by controlling current at an auxiliary electrode [89]. A simple electric circuit below represents the potentiostat controlling a 3-electrode system.

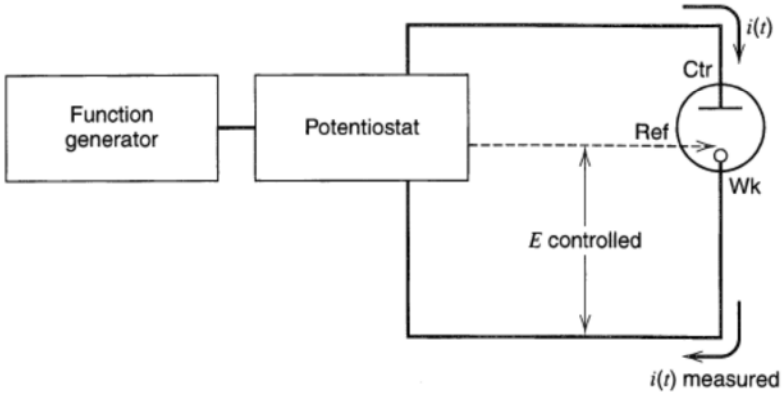

Figure 3-5: Potentiostat in a 3-electrode experiment [89]

Potentiostat can be viewed alternatively as an active element that can exert through the working electrode the amount of current required to achieve the potential defined by the function generator. The current is unique because current and potential are correlated. From the electrochemistry standpoint, it enables the supply of electrons needed to sustain the electrochemical processes at the rates consistent with the potential. The response from the potentiostat, which is the current, is actually observable in three-electrode experiments.

ACM Instruments Gill AC potentiostat connected to a computer were used in this experimental work to perform a potential sweep experiment.

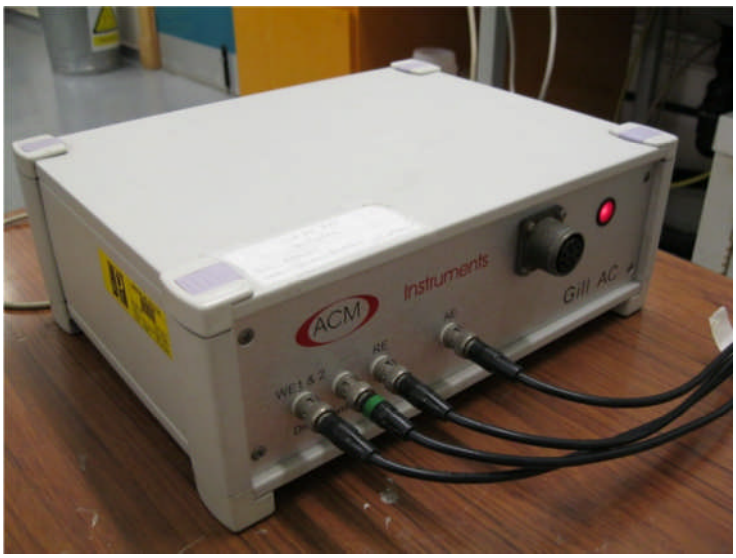

Figure 3-6: ACM Gill AC potentiostat

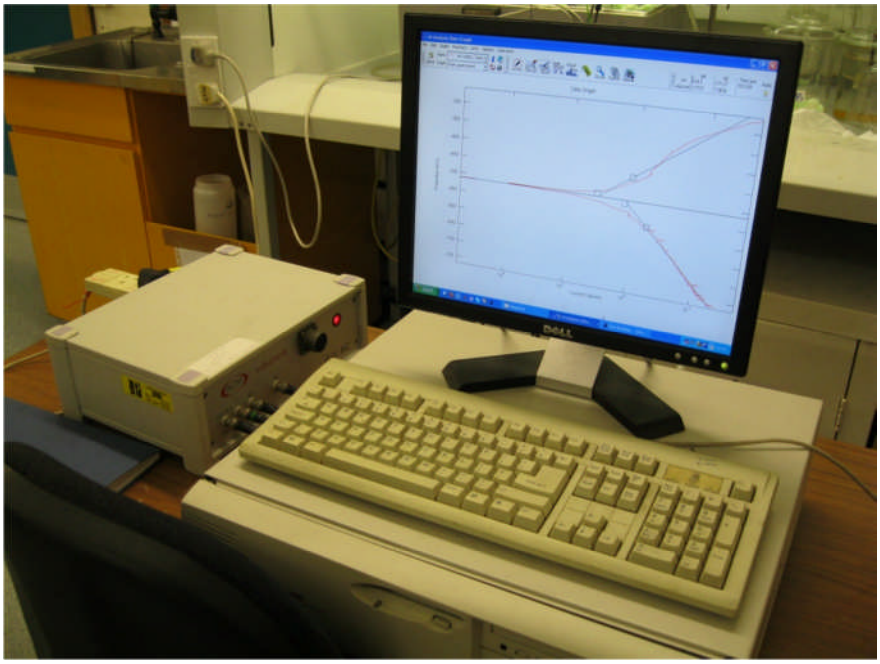

Figure 3-7: Data acquisition system

In order to determine the correct amount of resistance to be connected to the working electrodes and have the right amount of current that polarizes the working electrodes to the correct potential, it is necessary to observe polarization behavior of the sample (mild steel) in the intended medium (seawater). The potential sweep experiment was conducted using the above equipment.

3.3.2 Checking DC performance of ACM potentiostat

It is important to make sure that the potentiostat is in good working condition and accurate in giving potential and current readings. Thus, a simple linear polarization resistance (LPR) measurement using an ACM dummy cell is performed.

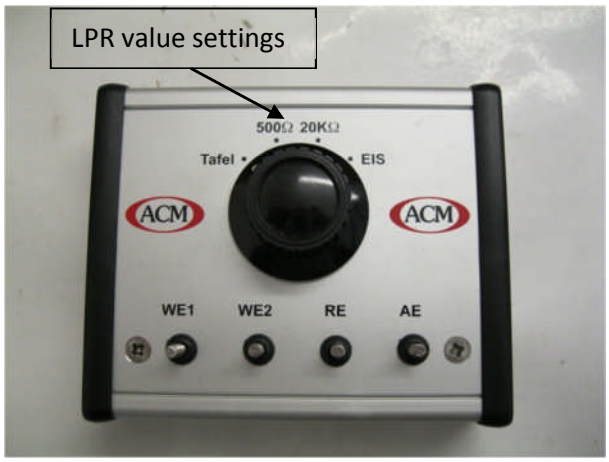

Figure 3-8: ACM dummy cell

The LPR measurement is done with the following parameters:

Start potential: -10mV

End potential: 10mV

Sweep rate: 10mV/min

Area of working electrode: 1 cm^2

Test duration: 2 minutes

Dummy cell is set to exhibit LPR behavior of 500 ohm. The following graph was obtained from the measurement.

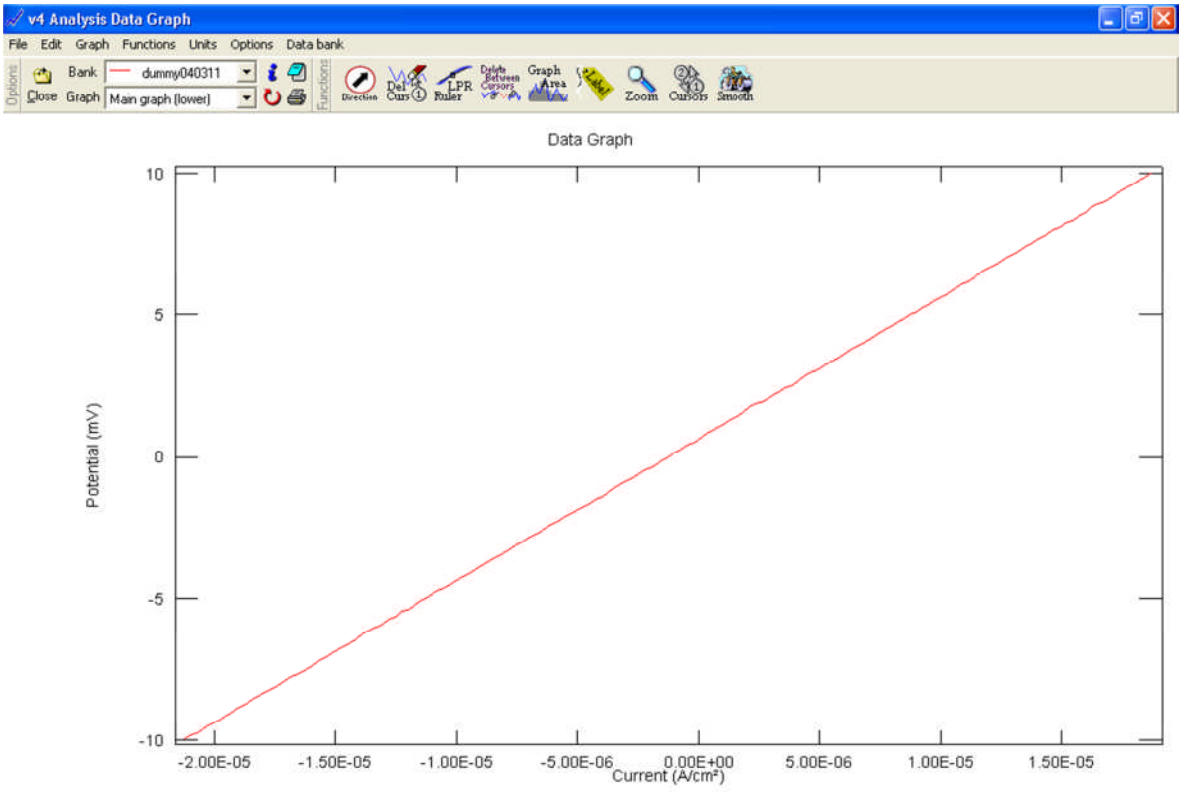

Figure 3-9: LPR graph obtained for potentiostat check

From the graph above, it can be determined that the linear polarization resistance value measured is the slope of the graph that is approximately

Eq 3-1: $\frac{17.5mV}{35\mu A} = 500\Omega$

The ACM Gill AC potentiostat is properly calibrated and ready for use.

3.3.3 Potential sweep experiment

3.3.3.1 Objective

To determine polarization behavior of mild steel in seawater. The values obtained from this experiment were then used to estimate the required current density to polarize mild steel to various cathodic potentials.

3.3.3.2 Specimen preparation

The main mild steel sample was prepared according to procedure described in Section 3.1.

3.3.3.3 Test solution

The medium used in this experiment was natural seawater.

3.3.3.4 Experimental setup

The potential sweep experiment to determine the resistance needed for the cathodic potential experiment was done with two compartments of separate anode and cathode. The anode and cathode compartment were connected using a salt bridge. The figure below shows the experimental setup. The corresponding connections AE, WE and RE go to Gill AC potentiostat.

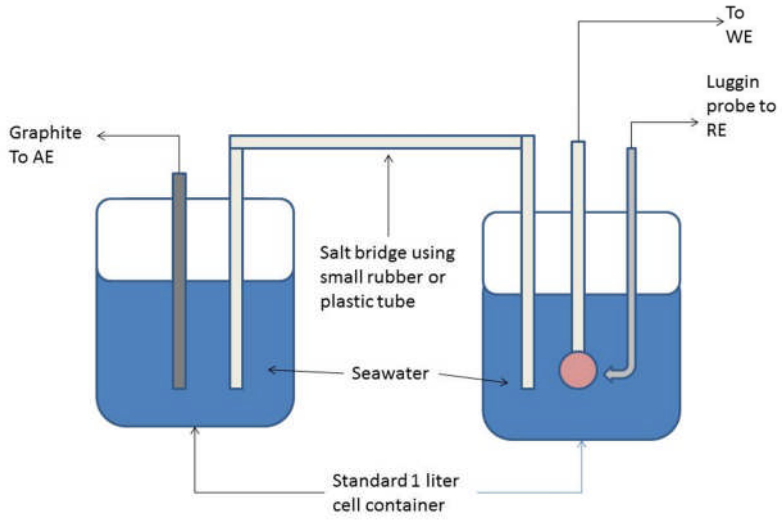

Figure 3-10: Stage 1 Test cell 2 equipment setup

3.3.3.5 Experimental procedure

The experiment was performed using the following parameters:

Start potential: -300 mV

End potential: -1100 mV

Sweep rate: 5 mV/min

Duration of experiment: 160 mins

3.3.3.6 Results

After the potential sweep experiment is completed, the following graph was obtained (Figure 3-11), that represents polarization behavior of mild steel in seawater.

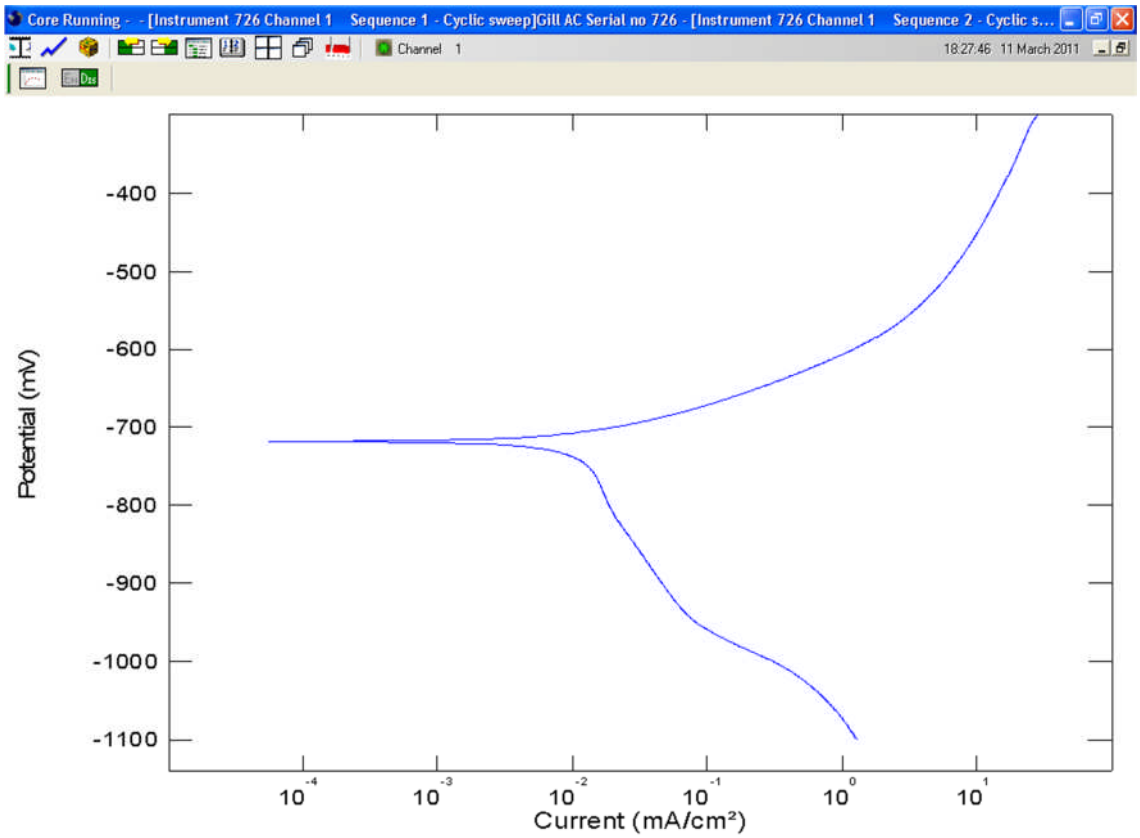

Figure 3-11: Polarization behaviour of mild steel in seawater

3.3.3.7 Discussion and Conclusion

The following reactions occur at cathode and anode:

Eq 3-2: Anode: $2Cl^- - 2e^- \rightarrow Cl_2$

Eq 3-3: Cathode: $O_2 + 4H_2O + 4e^- \rightarrow 4OH^-$

The free corrosion potential measured in this experiment for mild steel was around –730 mV (SCE).

Since the reference electrode used in the experiment was saturated calomel electrode, the corresponding values in copper-copper sulfate needs to be determined. The following table summarises typical values of practical reference electrodes in comparison to normal hydrogen electrode (NHE):

Common name	Electrode	V vs NHE
Saturated Calomel Electrode (SCE)	Hg/Hg_2Cl_2/sat. KCl	+0.241
Calomel	Hg/Hg_2Cl_2/1M KCl	+0.280
Mercurous sulphate	Hg/Hg_2SO_4/sat. K_2SO_4	+0.640
	Hg/Hg_2SO_4/0.5M H_2SO_4	+0.680
Mercurous oxide	Hg/HgO/1M NaOH	+0.098
Silver chloride	Ag/AgCl/sat. KCl	+0.197
Copper sulphate	Cu/sat. $CuSO_4$	+0.316
Zinc/Seawater	Zn/Seawater	-0.800

Table 3-2: Common practical reference electrodes vs normal hydrogen electrode (NHE)

From the table above, SCE is more negative from copper sulphate electrode by 75 mV. Thus, potential from SCE can be converted to the equivalent CSE potential values by subtracting 75 mV. From the experiment, the following current densities were obtained.

Potential reading in experiment (vs SCE)	Corresponding Potential (vs CSE)	Current density ($\mu A/cm^2$)
-725	-800	4.83
-775	-850	16.27
-825	-900	22.88
-875	-950	36.58
-925	-1000	59.48

Table 3-3: Conversion of SCE potentials to CSE potentials

The potentials above represent a range of underprotection values (-800 mV CSE) to some overprotection values (-1000 mV CSE) for steel exposed to seawater [90]. The potentials of interest are the typical values for protecting steel in seawater at -850 mV (CSE) and the recommended potential for anaerobic conditions -950 mV (CSE) [56]. In order not to confuse in between CSE (copper sulfate electrode) and SCE (saturated calomel electrode), all potential measurements in this work are referred to CSE values although the actual potential measurements are taken against a SCE.

3.4 *Exposure of mild steel wires to microbially influenced corrosion – Galvanostatic experiment*

3.4.1 Seawater as a source of MIC

Natural seawater is used in this experiment as the medium to provide a corrosion environment with MIC microorganisms. On average, molar compositions of seawater are as follows [91]:

Component	**Concentration (mol/kg)**
H_2O	53.6
Cl^-	0.546
Na^+	0.469
Mg^{2+}	0.0528
SO_4^{2-}	0.0282
Ca^{2+}	0.0103
K^+	0.0102
Inorganic Carbon	0.00206
Br^-	0.000844
Boron	0.000416
Sr^{2+}	0.000091
F^-	0.000068

Table 3-4: Molar compositions of seawater [91]

Seawater also contains a variety of living microorganisms (these are excluding planktons). As listed in Section 2.4.3, the non-exhaustive list these bacteria are:

- Fermenters
- Methanogenic bacteria
- Nitrifying and denitrifying bacteria
- Manganese oxidizing bacteria
- Sulfur reducing and oxidizing bacteria
- Iron oxidizing and reducing bacteria

Seawater could be a source of MIC, in aerated or deaerated conditions. The microflora listed above live in symbiosis and can possibly survive each other in all conditions. The experimental work is interested with SRB since SRB are the most notorious microorganism associated with MIC, and the presence or viability of SRB can be verified with a simple most probable number test using a growth media [12].

Seawater for this experimental works was obtained from the seaside of Blackpool (United Kingdom) two days before the experimental work was scheduled to start. Seawater was poured into two sterilized 10 liter plastic container (with screw seal) through a sterilized metal sieve. The sterilization on these items was done by passing them through boiled water 12 hours before the trip to Blackpool. These containers were used to carry the seawater from the seaside to the working laboratory for a distance of 50 miles. The plastic container was covered with aluminum foil during transportation that took around 1.5 hours. After the seawater reached the laboratory, it was stored in the dark for 24 hours to let suspended solid and sand settle down.

3.4.2 Objective

The experiment is designed to hold current and observe the potential trending. A simple SRB presence test was also performed on all samples to the see effects of the different current densities applied according to Table 3-3. Three steel wires were used as working electrodes in separate anode and cathode compartments. These wire samples were connected to a simple potential control circuit and power supply for polarizing the exposed wire surface. The equipment setup was almost similar to a cathodic protection of steel in seawater with impressed current.

3.4.3 *Specimen preparation*

The test specimens used in this experiment were mild steel wires. These wires come in 1 mm diameter. Wires are used in this experiment because they are suitable and small in size for a simple SRB presence test. In order to provide a specific reaction area in the corrosion cell, the wire is sheathed with an electrically non-conductive polymer with 600V rating. After the polymer is laminated throughout the steel wire, it is heated with a heat gun to make it malleable. This 'heat shrink sleeving' makes the polymer shrink snugly fit around the wire, preventing any liquid seepage under it. A 10 mm exposed end of the wire provides a surface area of 32.2 mm^2 of metal. The exposed end of the wire was then polished with P400 polishing paper to remove oxide film on its surface.

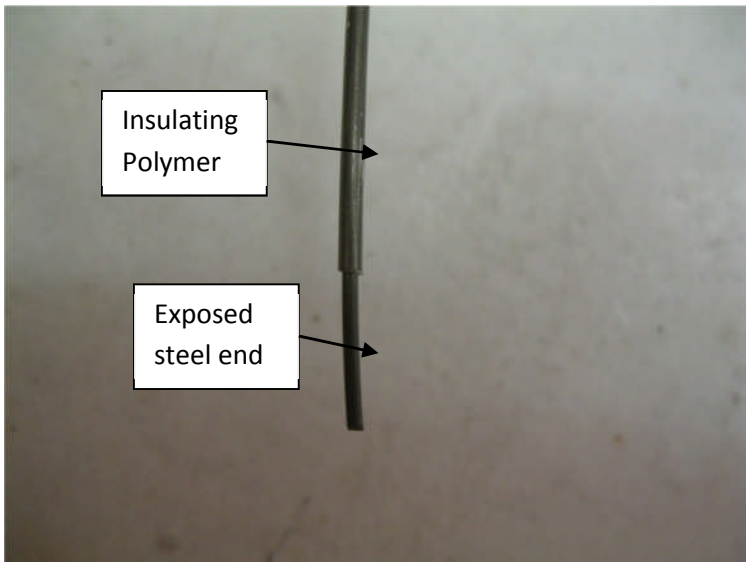

Figure 3-12: Mild steel wire and insulative polymer

3.4.4 *Test Solution*

The test solution used in this experiment is natural seawater. The handling procedure of the test solution is described in Section 3.4.1.

3.4.5 *Experimental setup*

An 18-turn potentiometer circuit connected to a 10V power supply is used to control potential on the metal surface in this experiment. 18-turn potentiometer has a high resolution adjustment in its resistance range and high power rating (0.75W), making it suitable to be used. The potentiometer is soldered on a circuit board, and is connected to 2 copper wires through the circuit board which are connected to the steel wires through a screw connector. Three individual steel wires are used for each sample tested in this experiment. These three wires provide triplicate samples for a simple SRB presence test

with a growth medium. The steel wires are placed at equal distances around the opening of the salt bridge in the cathode compartment.

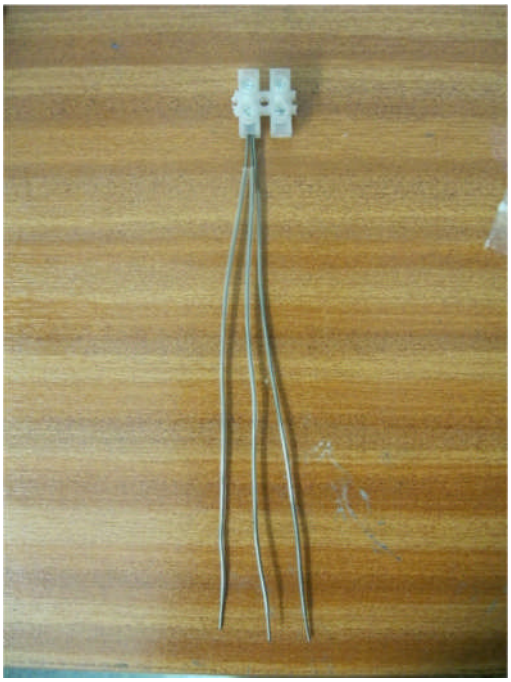

Figure 3-13: One sample consisting of 3 steel wires

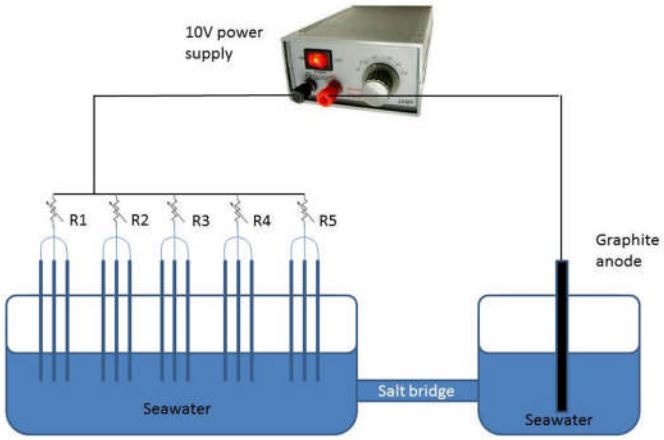

Figure 3-14: Schematic diagram of experimental setup Stage 2 Cell 1

Five samples (each with three wires) were tested with the potentials as described in Table 3-3. In order to provide the right current density estimated in experiment described in Section 3.3.3.7, the multiturn potentiometers were set to the resistance values are calculated for each potential.

The following Table 3-5 summarises all the set resistances needed for all samples.

Potential reading in experiment (vs SCE)	**Corresponding Potential (vs $Cu/CuSO_4$)**	**Current density ($\mu A/cm^2$)**	**Potentiometer**	**Potentiometer resistance (kΩ)**
-725	-800	4.83	R1	2197
-775	-850	16.27	R2	637
-825	-900	22.88	R3	464
-875	-950	36.58	R4	290
-925	-1000	59.48	R5	178

Table 3-5: Potentiometer settings

The multiturn potentiometer was set to the desired values by connection to a multimeter and turning the adjusting knob until the desired resistance value is achieved.

The graphite counter electrode was separated from the cathode compartment by having two separate containers connected with a salt bridge. The purpose of having separate anode and cathode compartment is to prevent local reaction at anode, which is generation of chlorine gas and hypochlorous acid, to affect the viability of natural microorganisms in seawater, and to prevent the local reaction to interfere with cathodic reactions at cathode. The anode compartment is bubbled with air to remove as much as possible traces of chlorine gas generated at the counter electrode. The salt bridge connecting anode and cathode compartment is stuffed with glass wool to stop or slow down migration of harmful hypochlorous acid formed by reaction between chlorine and hydroxyl ions to the cathode compartment. The cathode compartment is naturally aerated, and covered with aluminium foil for isolation from light sources since UV light could actually harm SRB species [92].

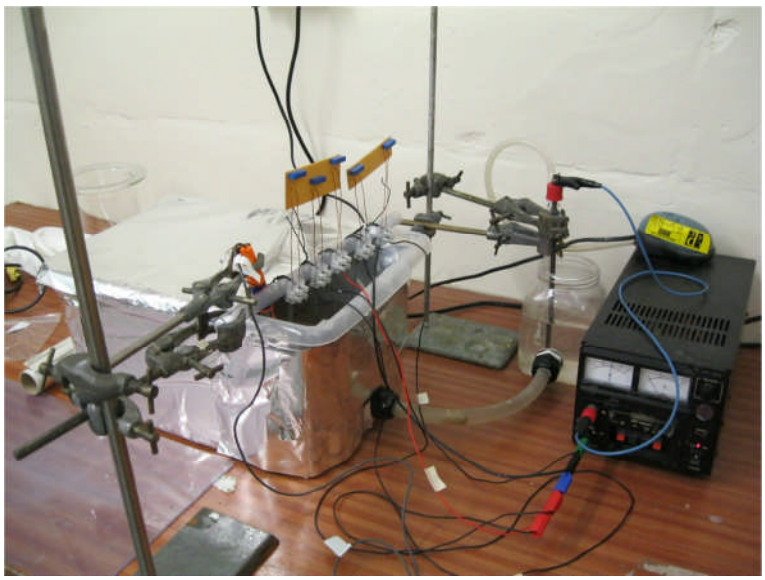

Figure 3-15: Experimental equipment setup (Stage 2 Cell 1)

The following are the reactions at anode and cathode, as implied in Section 3.3.3.7 :

Eq 3-2: At anode: $4Cl^- - 4e^- \rightarrow 2Cl^2$

Eq 3-3: At cathode: $O_2 + 4H_2O + 4e^- \rightarrow 4OH^-$

Further reaction at anode forms hypochlorous acid:

Eq 3-4: $Cl_2 + OH^- \rightarrow HOCl + Cl^-$

3.4.6 Experimental procedure

3.4.6.1 Cathodic polarization

After connecting the complete circuit, the power supply was turned on and immediately potential reading of the working electrode was taken using a multimeter, against a saturated calomel reference electrode. Three potential readings were taken every day for 7 days.

3.4.6.2 SRB presence analysis

At the end of the experiment, the exposed part of the wires are cut with a sterilized wire cutter, straight into a small sterile plastic container. The cut wire is then used for a simple SRB presence test. The SRB presence test is done by exposing the cut wires to the SRB growth media Postgate B. The components of the growth medium was prepared according to Table 3-6, with addition of 20 g/l NaCl and 3 g/l $MgCl_2$ [93]:

Ingredient	Amount
KH_2PO_4	0.5g
$CaSO_4$	1.0g
NH_4Cl	1.0g
$MgSO_4.7H_2O$	2.0g
Sodium Lactate	3.5g (4.49ml of 60% Syrup)
Yeast extract	1.0g
$FeSO_4.7H_2O$	0.5g
Ascorbate	0.1g
Thioglycollate	0.1g
Tap water	1000ml

Table 3-6: Postgate B ingredient

The pH of the final solution was adjusted to 7-7.5 by carefully dropping 1M NaOH. The ingredients made up 1L of Postgate B solution and were transferred to fifteen 10mL vials. These vials were then autoclaved for 1 hour.

Figure 3-16: Sterile container for transfer of wire samples

The sample wires (15 in total) were transferred into the vials from the sterile plastic container in an anaerobic chamber. The vials were kept for one week at 25°C before the result of SRB growth could be observed.

3.4.7 Results

3.4.7.1 Potential trending during 7-day exposure to seawater

- 4.83 µA/cm^2

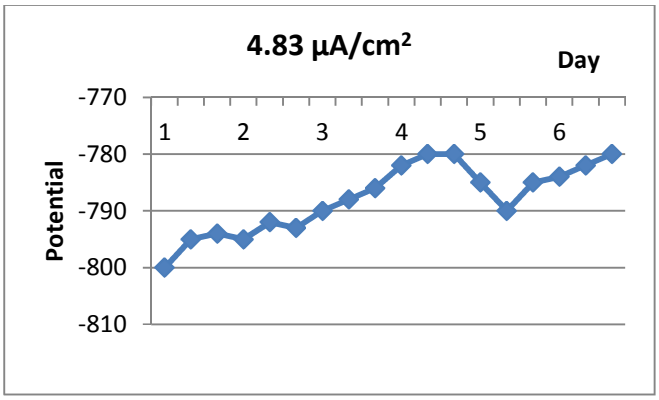

Figure 3-17: Potential trending for sample at 4.8 µA/cm^2

The potential is found to be unstable unlike the experiment using plain salt water described in Section 3.2. The potential readings are found to be more positive with time. In this case, the potential goes as far as 20 mV towards the positive region.

- 16.27 µA/cm^2

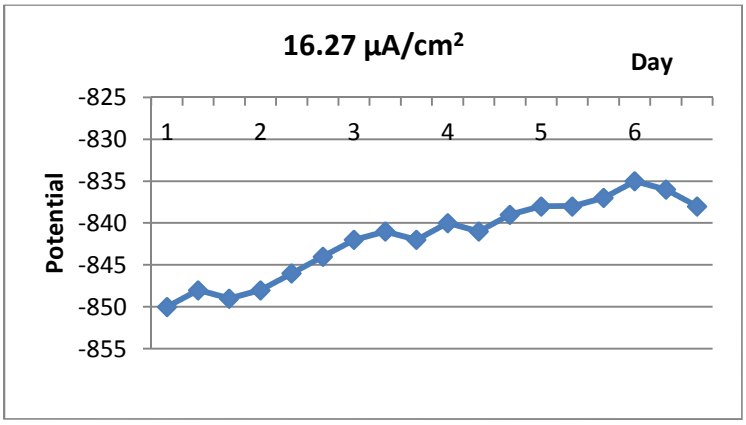

Figure 3-18: Potential trending for sample at 16.3 µA/cm^2

The potential reading is found to be not stable, going to the same trend as observed for the -800 mV samples. The potential reading goes towards the positive region with time, and goes up as much as 15 mV.

- 22.88 µA/cm^2

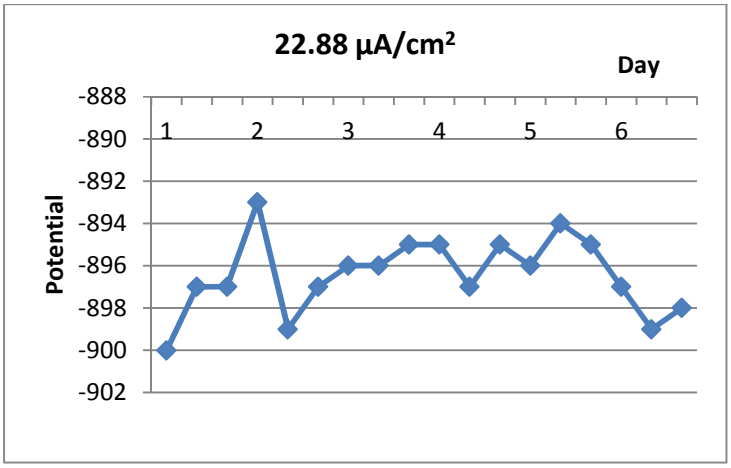

Figure 3-19: Potential trending for sample at 22.9 µA/cm^2

The potential reading for this sample is also not too stable, but the trending is not as per previous 2 samples at -800 and -850 mV. The trending goes up and down in the negative and positive directions, for the whole duration of exposure in within the potential range - 900 mV to - 894 mV.

- 36.58 µA/cm^2

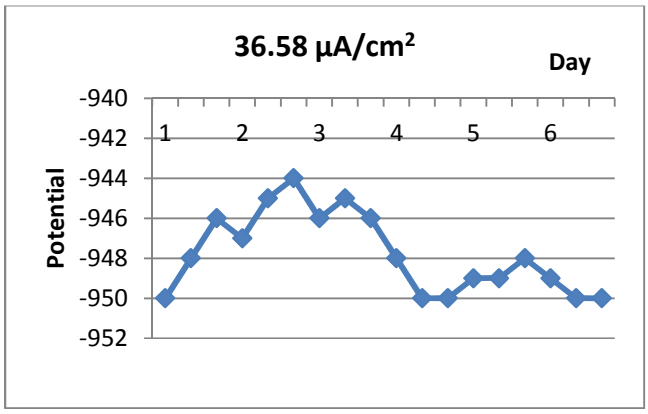

Figure 3-20: Potential trending for sample at 36.6 µA/cm^2

Fluctuation to both positive and negative directions is still observed. The potential trending goes towards the positive direction for the first 3 days, but then returning to the set potential in the last 4 days of the experiment and is considered quite stable during the last three days of the experiment. Thin but visible calcareous deposit is formed on the specimens.

- 59.48 µA/cm^2

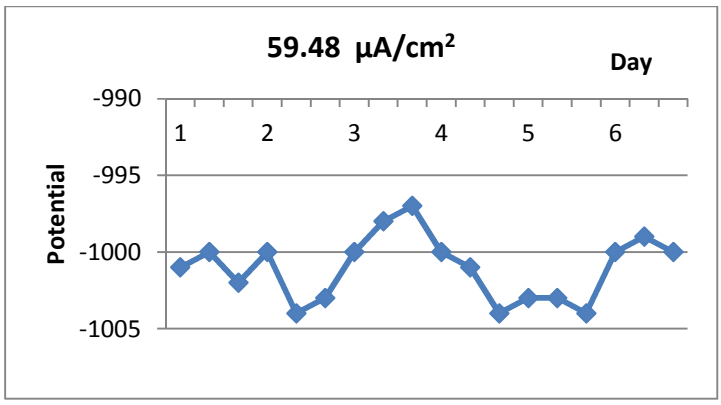

Figure 3-21: Potential trending for sample at 59.5 µA/cm^2

Potential instability is evident during the whole exposure duration and visible calcareous deposit is formed on the specimen.

3.4.7.2 SRB presence test

The results of the SRB presence test can be observed after one week incubation of the steel wires in 10 mL bottles containing Postgate B growth media at 25^{o}C. Black

precipitate forming in the bottles indicates some growth and activity of SRB. The following figure demonstrates the black precipitate forming in bottles containing the steel wires. The tests were done in triplicate. The figure below shows SRB activity to be evident in samples polarized at – 800 to –900 mV, but absent at –950 and –1000 mV. The amount of black deposit were observed to peak at – 900 mV.

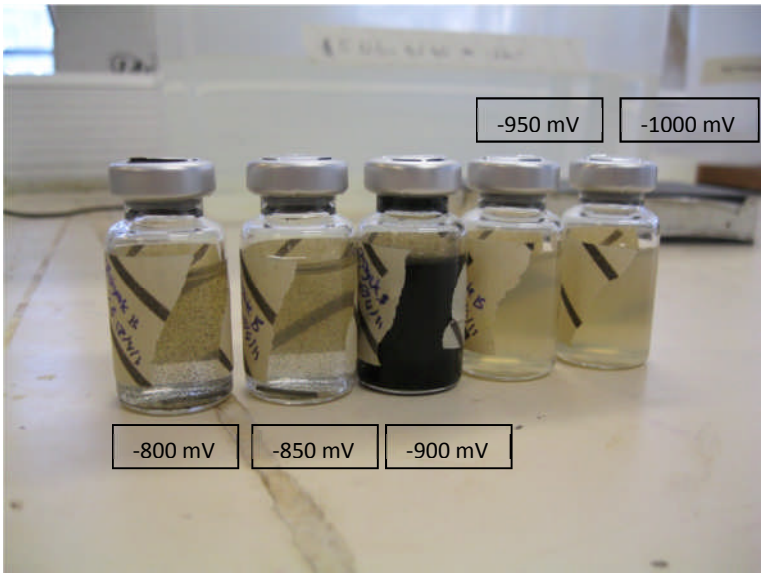

Figure 3-22: Results of SRB presence analysis

3.4.7.3 Calcareous deposit formation

Samples polarized at – 950 mV and - 1000 mV showed some formation of thin calcareous deposits as shown in figures below, but not visible in samples more positive than these potentials.

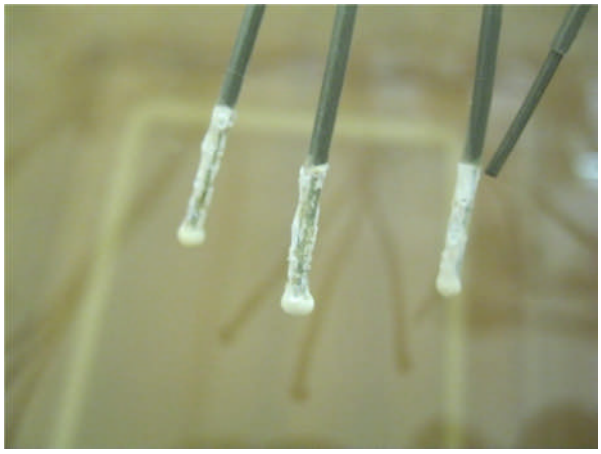

Figure 3-23: Thin calcareous deposit observed on samples at 36.6 $\mu A/cm^2$

The potential trending for samples polarized at -950 and -1000 mV shows an increase in the first 3 days, then rapidly decreasing and stabilizing for 4 days. The formation of calcareous deposit on the surface of the samples causes a decrease in current demand [73]. However, since the experimental setup was not a proper potentiostat that can actually control current to maintain a fixed potential, the potential increases towards the positive region as the scale builds up. After day 3 of the experiment, the calcareous deposit has covered the whole cathode surface and current demand stabilized.

3.5 Potentiostatic - Exposure of mild steel to seawater using multichannel potentiostat

3.5.1 Objective

This experiment was performed to polarize steel wire samples at very constant potentials in seawater. The potentials chosen in this experiment were based on findings described in Section 3.4. To achieve the constant potentials for a long time, a multipotentiostat was used. The multipotentiostat was supposed to be able to control stable potentials on multiple working electrodes. It should also have a proper connection for measurement of specimen potential against a reference electrode and the total current passing through.

3.5.2 Specimen preparation

The specimens used in the experiment were mild steel wires. These samples were prepared according to procedure described in Section 3.4.3. The wires were also enclosed in a plastic tube for better handling. There were 4 steel wires used per potential. Three of the wire samples were to be used for MPN analysis and the fourth was used for observation under SEM.

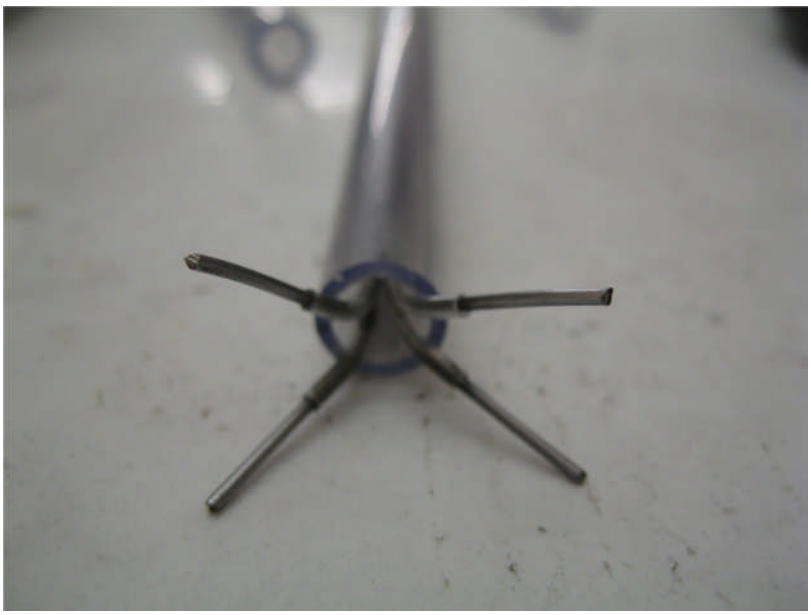

Figure 3-24: Sample used for Stage 2 Cell 2

3.5.3 Test solution

The test solution used was natural seawater. The seawater used in this experiment was boosted with yeast extract to maintain the growth and sustainability of the microorganisms in it for the duration of the experiment. A concentration of 200 mg/l yeast extract was used.

3.5.4 Experimental setup

3.5.4.1 Cathodic polarization using multipotentiostat

The multipotentiostat used in this experiment has 6 separate potentiostats in one box, designed by Prof. R.A Cottis and constructed by his PhD student Sarah S. Leeds [94]. These potentiostats uses a common ±12V power supply to power all the potentiostats and control potentials of 6 samples independently using a common counter electrode, rather than the more normal configuration, which uses a common working electrode. The following Figure 3-25 shows the potentiostat box and its corresponding components and controls.

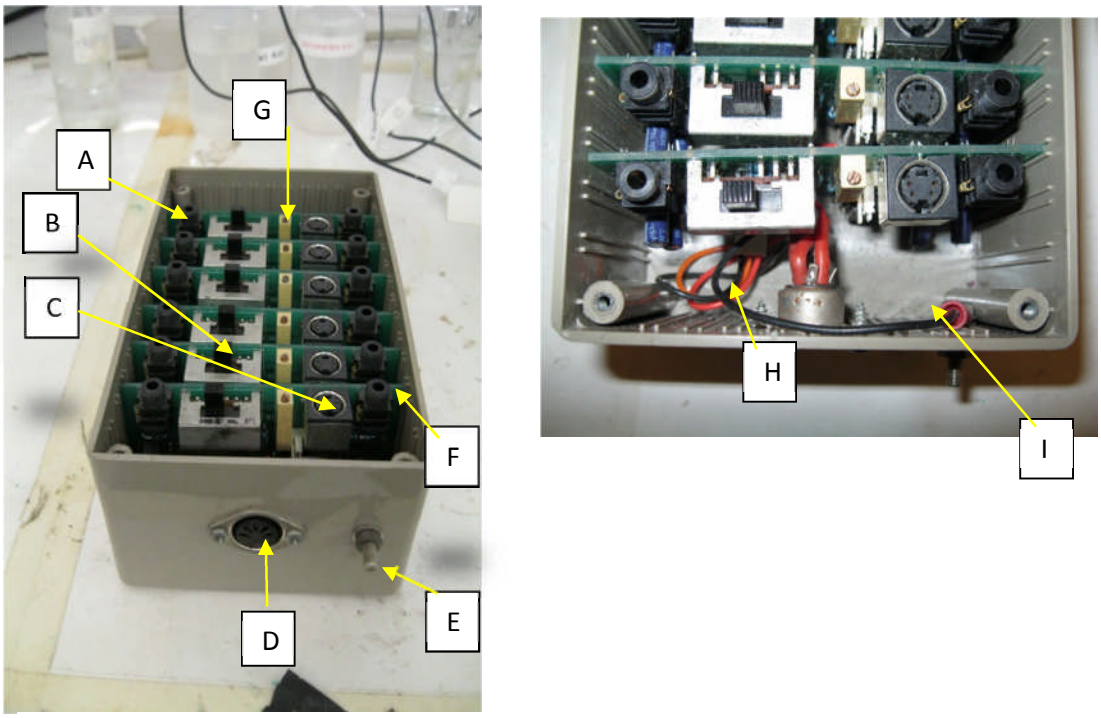

Figure 3-25: Showing 6 potentiostats in a plastic casing and the corresponding connections and controls

The following Table 3-7 shows the legend for each of the above labels.

Legend	Function
A	Connection for reading voltage of potentiostat
B	Resistor selector for 100Ω, 10k Ω or 1M Ω
C	Connection to electrochemical cell
D	±12V power supply
E	Grounding pin
F	Connection for current reading
G	Connection to adjust potentiostat
H	Power supply wire for 6 potentiostats
I	Grounding wire

Table 3-7: Description of multipotentiostat's connections and controls

Mini-Din PCB mount socket was used to connect the electrochemical cell to the potentiostat. The following shows the wire leads used in the potentiostat.

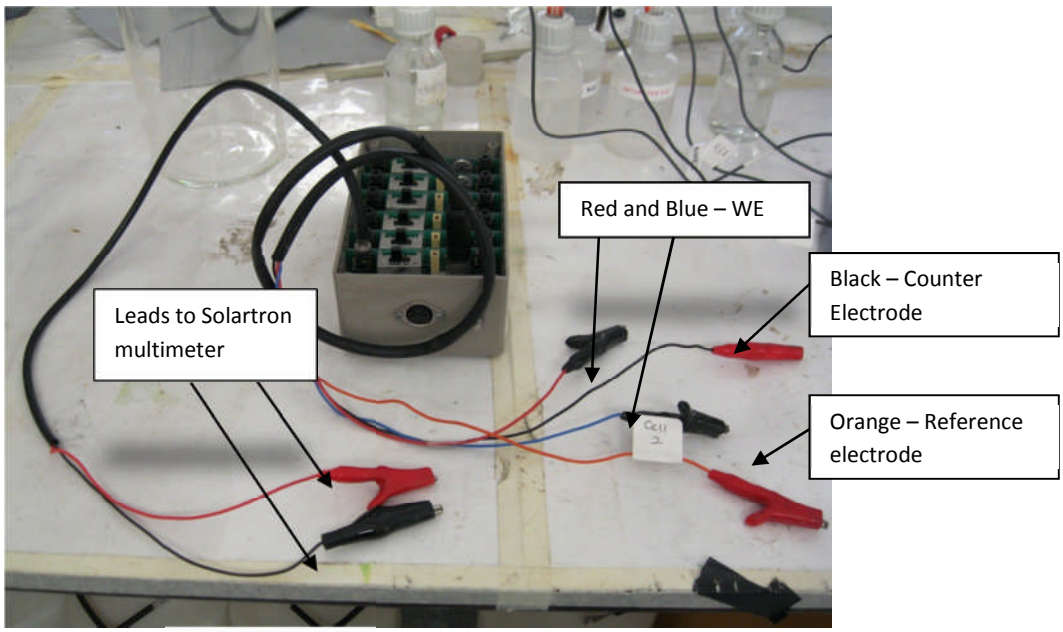

Figure 3-26: Showing connections to electrochemical cell and voltage/current reading leads

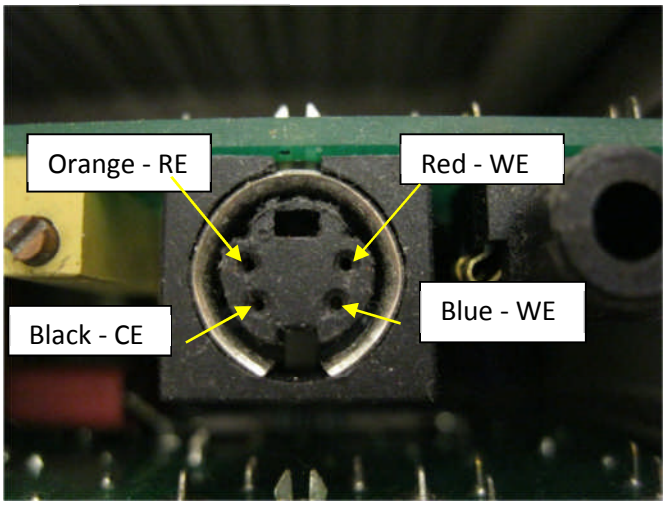

Figure 3-27: Wiring of Mini-Din PCB mount on the potentiostat board

3.5.4.2 Functional testing of multipotentiostats

Prior to any proper experimental works, a test was performed on the multipotentiostat to test its functionality using a dummy cell. The dummy cell consists of a graphite counter electrode, two steel wire samples and two SCE reference electrodes immersed in natural seawater. The objective of the testing is to determine whether the potentiostat box can

actually hold the potentials of steel wire samples independently, and as well to see the stability of the potential control. Two of the potentiostats were connected to the dummy cell, and it was adjusted to hold the potential of the two samples (by adjusting G from Figure 3-25) at -800 and -850 mV for 3 days. Readings taken from this functional testing proved that the potentiostat was able to provide a stable potential over the testing duration.

3.5.4.3 Cathodic polarization electrochemical cell setup

The electrochemical experiment cell consist of 4 samples cathodically polarized at the following potentials (vs CSE) in a cathode compartment containing 20 litres seawater :

Cell 1: – 800 mV

Cell 2: – 850 mV

Cell 3: – 900 mV

Cell 4: – 950 mV

Each potentiostat was connected to separate reference electrodes placed close to each sample. The graphite auxiliary electrode was placed in a separate anode compartment (aerated with Rena 50 air pump) and separated by a salt bridge containing glass wool to prevent unwanted ions from the anode compartment from reaching the cathode compartment. Each of the samples in the cathode compartment was placed at the same distance (7 cm) from the salt bridge opening. The cathode compartment was then covered with aluminum foil to prevent UV light from penetrating.

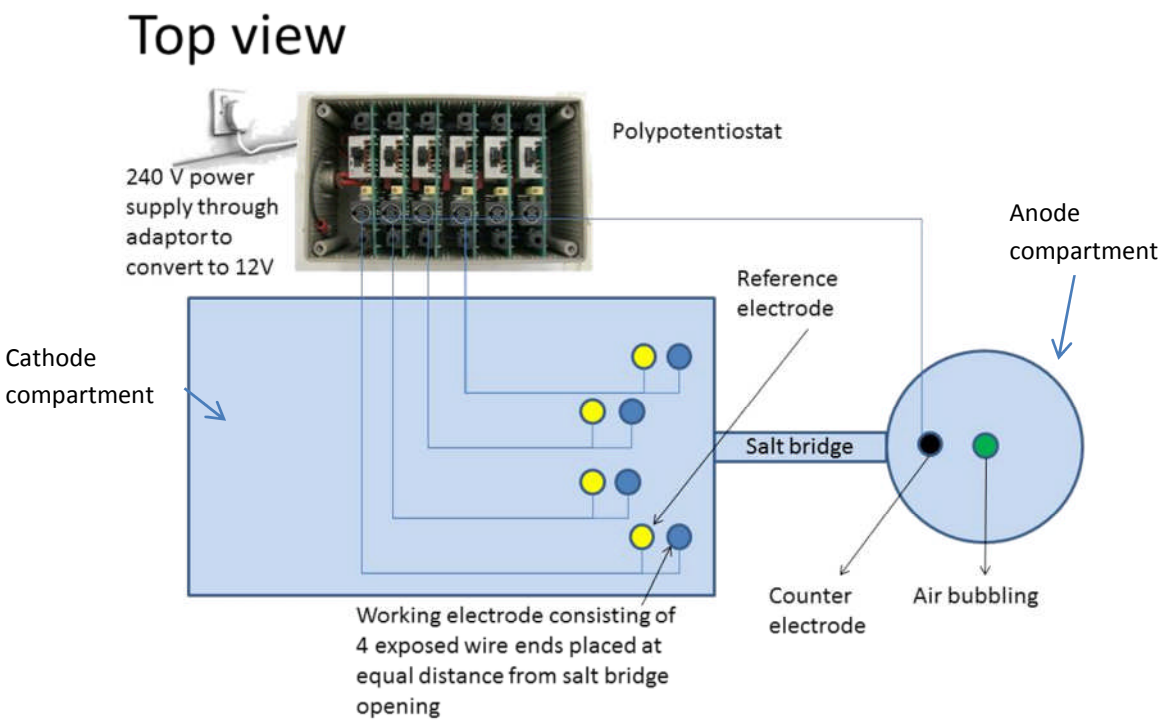

Figure 3-28: Experimental setup – Stage 2 Cell 2

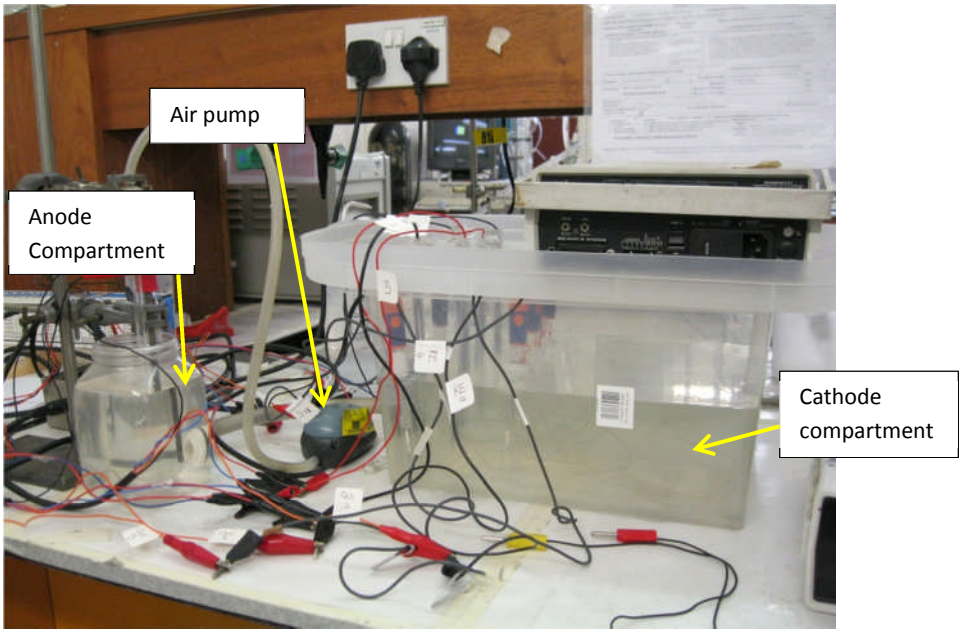

Figure 3-29: Equipment setup – Stage 2 Cell 2

3.5.5 Experimental procedure

3.5.5.1 Exposure of steel specimens to seawater

The readings of potential and current were taken using a Solartron 7150 Plus multimeter. This multimeter is suitable to be used because this experiment involves very small current due to small surface area, and monitoring minute potential changes, that may be in the range of tens of microvolts (negligible). The Solartron 7150 Plus

multimeter is capable of measuring a very small amount of current from 1 µA to 2 A in 1 µA resolution. The changes in potential can be measured in up to 10 microvolt resolution. The potential for each sample is then set by turning the multiturn potentiometer (G in Figure 3-25) to set all the samples at the potentials described in Section 3.5.4.3. The following are the initial potential and current readings:

Sample number	Potential (mV)	Current (mA)
Cell 1	-800.43	0.016
Cell 2	-850.43	0.033
Cell 3	-900.12	0.050
Cell 4	-950.26	0.076

Table 3-8: Initial potential and current readings

One reading of potential and current was taken on each sample per day. The duration for exposure of the specimens was 42 days (6 weeks).

3.5.5.2 Most Probable number (MPN) procedure

MPN or most probable number analysis is the most common way to assess microbial populations in industrial samples. The growth test uses commercially available growth media for the groups of organisms that are most commonly related with industrial problems. Serial dilutions of suspended samples are grown on solid agar or liquid media. Based on the growth observed for each dilution, estimates of the most probable number (MPN) of viable cells present in a sample can be obtained. The figure below demonstrates the MPN method [95].

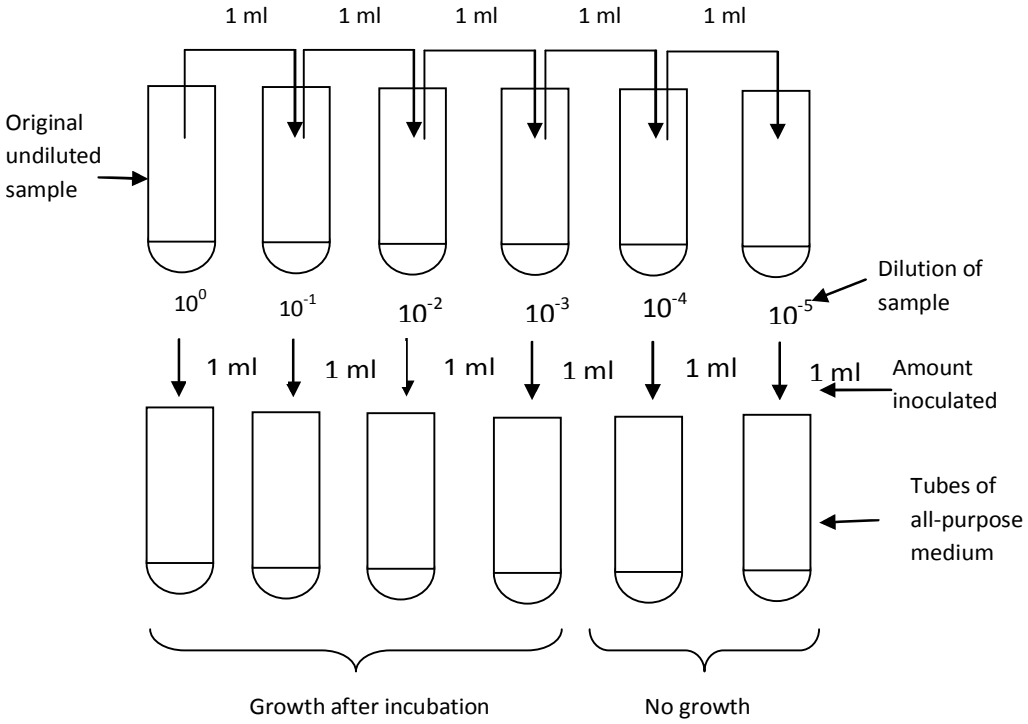

Figure 3-30: Illustration on most probable number method with 5-time dilution

The MPN analysis for this experiment was done using 6-time dilutions, which means that this procedure was able to estimate up to 10^6 viable SRB colony forming units (cfu) per mL of suspension. Enhanced Postgate B medium was used in this experiment, and placed in 10mL vials. This media was added with oxygen scavenger to enable exposure to open air for around 10 minutes maximum. This was critical because transferring the metal specimens into the media bottles requires a short exposure to open air and thus risking small amount of oxygen ingress into the growth media.

3.5.5.3 Preparation of bacterial suspension for MPN procedure

After the exposure ended on the 42nd day, the potentiostats were turned off. A spatula was sterilised by immersing in alcohol and burning the alcohol on flame. This spatula was then used to scrape the slime forming on the steel samples into the media vials. The exposed end of the wires was then cut straight into the 10 mL vials containing the Postgate B media. These steps were done in target 60 seconds for each sample to minimise exposure of the samples to oxygen in the air. The vials containing the cut steel wire were sealed and then ultrasonicated for 2 minutes to break the biofilm formed on

the steel surfaces, and as well to spread evenly the density of the microflora in the suspension.

Serial dilution was performed using a sterile syringe, as demonstrated in Figure 3-30. After the dilution was complete for all 12 steel wires (84 vials), the vials were sealed with an aluminium cap to prevent ingress of oxygen. The bottles were then incubated at constant temperature of 30^{o}C for 14 days.

3.5.5.4 Scanning electron microscope (SEM) and energy dispersive X-ray spectroscopy (EDX) analysis

One of the cut steel wires from each sample was observed under the SEM. The samples were gently washed under deionised water to remove loose debris. The samples were then put on a SEM sample placeholder with carbon sticker. EDX analysis was used to obtain information about the composition of the corrosion products.

3.5.6 Results

3.5.6.1 Potential and current trending

Since the multipotentiostat used was stable and free of interference (as tested in Section 0) and could hold the potentials at constant value throughout the experiment, only the trending for currents were obtained. The following figures show the current trending for all the potentials.

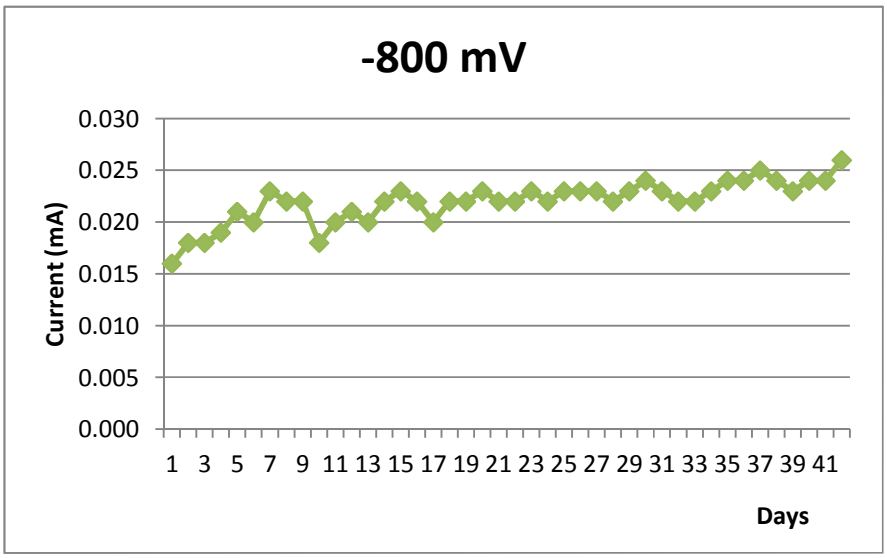

Figure 3-31: Current trending for sample polarized at -800 mV

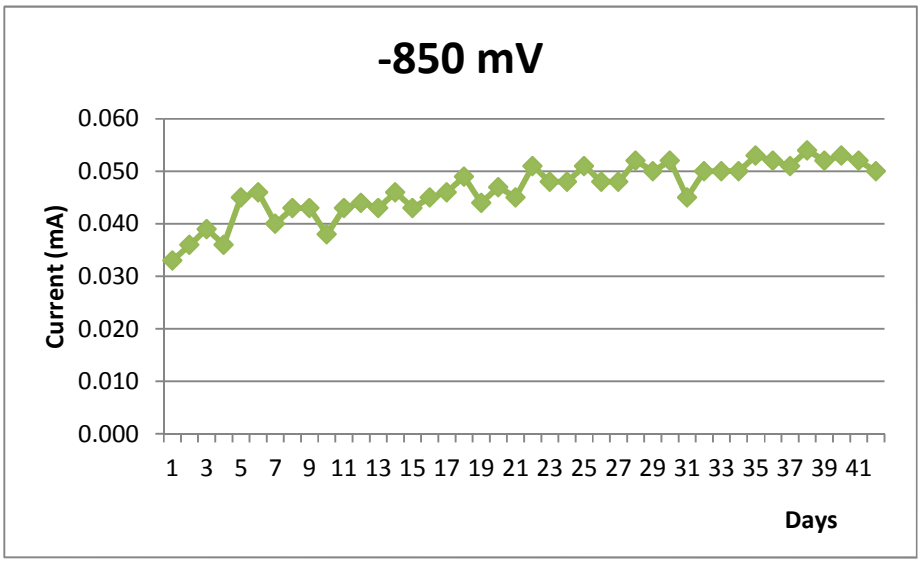

Figure 3-32: Current trending for sample polarized at -850 mV

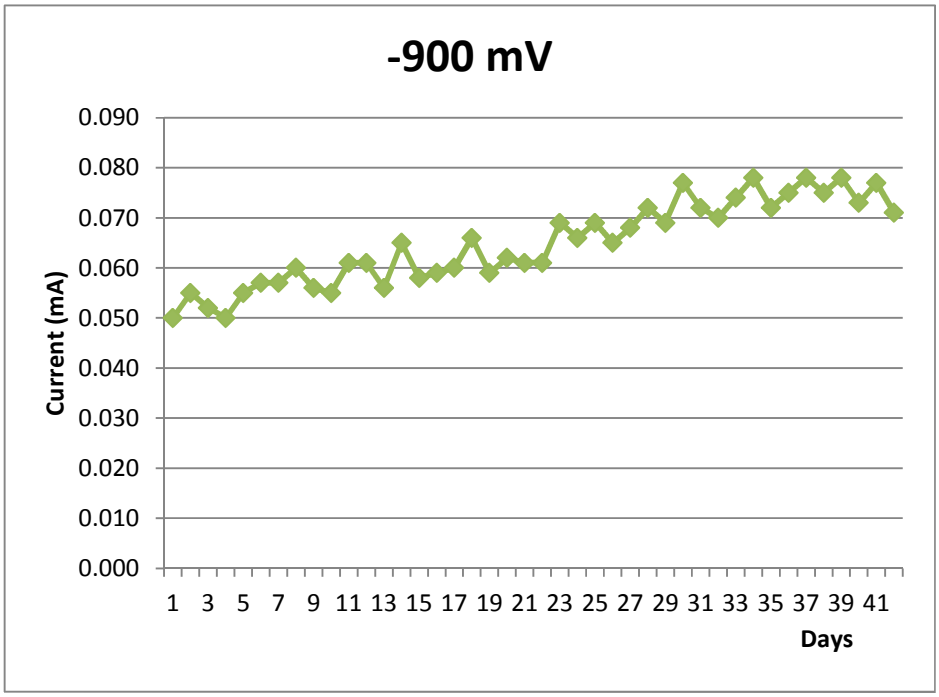

Figure 3-33: Current trending for sample polarized at -900 mV

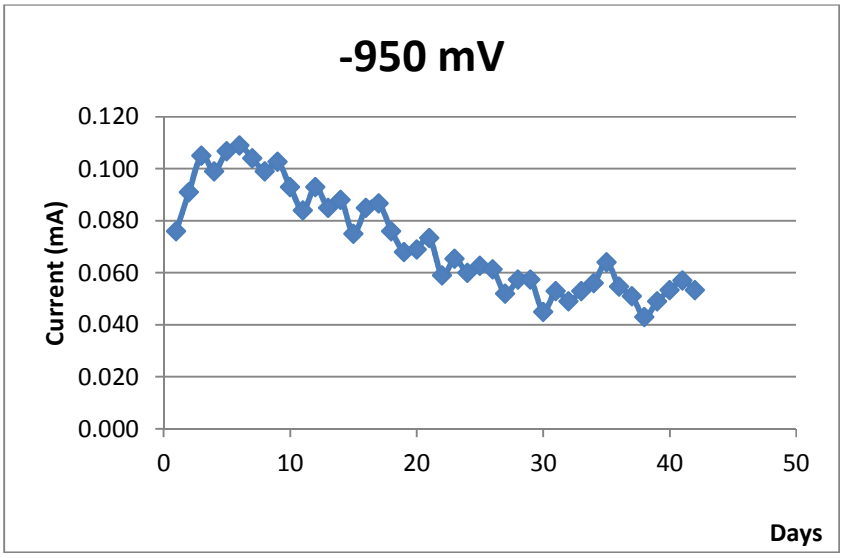

Figure 3-34: Current trending for sample polarized at -950 mV

As observed from the figures above, the samples held at -800 mV to -900 mV showed increase in current to maintain the potentials. The current increase observed was rather gradual throughout the experiment. However, the current trending for sample polarized at -950 mV showed increase in current for the first 10 days (up to 109 µA) and then gradually decreasing towards the end of the polarization duration (final value of 53 µA). Visible thin calcareous deposit was also observed on this sample.

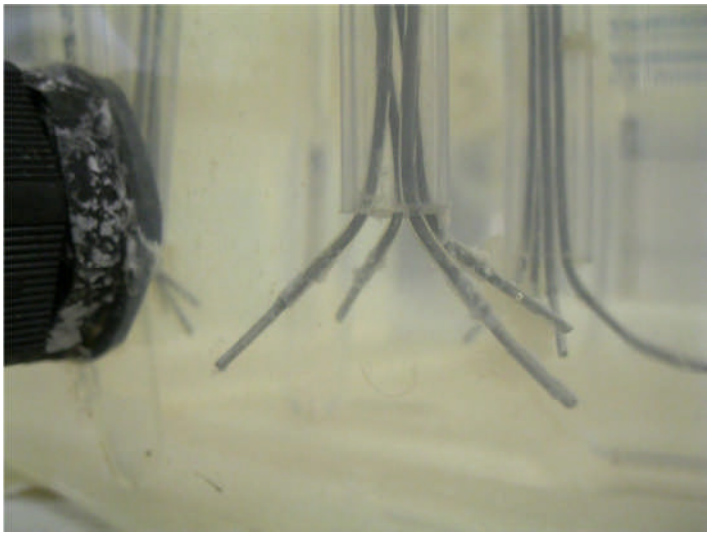

Figure 3-35: Thin calcareous deposit on sample polarized at -950 mV

3.5.6.2 MPN count for SRB

After the procedure for MPN as described in Section 3.5.5.2, the number of positive SRB growth in each dilution series were counted. The procedure to determine the SRB count (colony forming unit, cfu/ml) was based on a method described by a NACE standard [96]. Colony forming unit (cfu) is a measure of viable bacteria or fungal numbers that are able to form a colony. The most probable number count is different from a microscopic count where microscopic count includes all viable and non-viable cells, whereas MPN only counts viable cells [97]. Based on this method, a range of three successive dilutions containing both positive and negative vials were chosen from each dilution series. The following table shows the result of the dilutions.

Sample Potential (mV)	Sample replicates	Vials						
		1	2	3	4	5	6	7
-800	1	x	x	x	x			
	2	x	x	x	x	x		
	3	x	x	x				
-850	1	x	x	x	x			
	2	x	x	x	x			
	3	x	x	x	x	x		
-900	1	x	x	x				
	2	x	x	x	x			
	3	x	x	x	x	x		
-950	1	x	x	x	x			
	2	x	x	x	x	x		
	3	x	x	x				

Table 3-9: MPN count result based on NACE TMO194-94 [96]

For the table above, 'x' marks the vials with positive SRB growths, and empty boxes marks negative growths. The boxes bordered with thick lines indicate the range of the first three dilutions with positive and negative vials taken into account for the colony forming units (cfu) estimation. So from the table above, vial 3 was taken as the first dilution, vial 4 taken as second dilution and vial 5 taken as the third dilution.

The following demonstration shows the MPN calculation for sample polarized at -850 mV, the result as shown in the second row of Table 3-9.

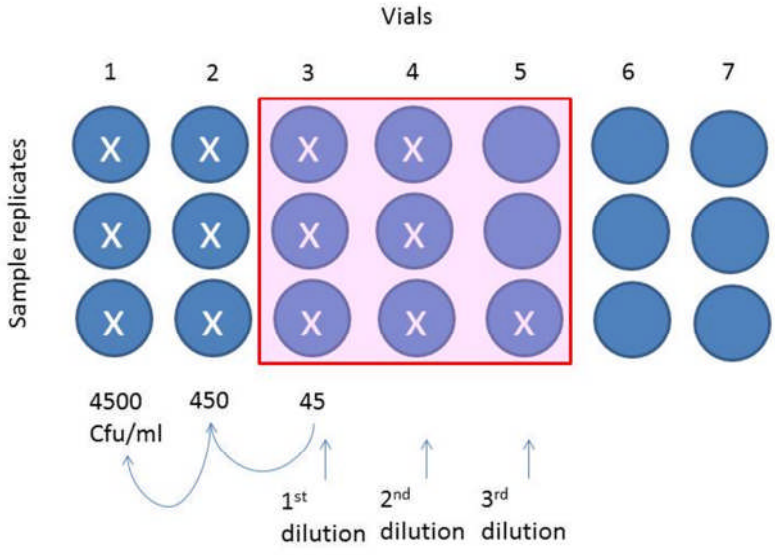

Figure 3-36: MPN calculation for sample polarized at -850 mV

The first three dilutions taken are vials 3, 4 and 5. From the figure above, the reading was taken as 3-3-1. From the table provided in NACE TMO194-94 [96], a value of cfu/ml of the first dilution (in this case, vial 3) is given and in this case, is 45 cfu/ml. Then, the number is further factored to 10 times for vial 2 and another 10 times for vial 1. This gives the original number of cfu/ml for vial 1 (the original vial containing the wire with biofilm cut after the experiment) as 4500 cfu/ml. However, since the result for this count is to be reported in terms of cfu per unit area of metal sample:

MPN count for 1^{st} vial: 4500 cfu/ml

Total volume of the vial is 10 ml, total count = 4500 cfu/ml x 10 ml = 45,000 cfu

MPN of SRB cfu/area of steel = 45,000 cfu / 0.32 mm^2 ≈ 141,000 cfu/mm^2.

3.5.6.3 SEM and EDX observation

The following figures show the observation of the samples under SEM, and the corresponding EDX spectra.

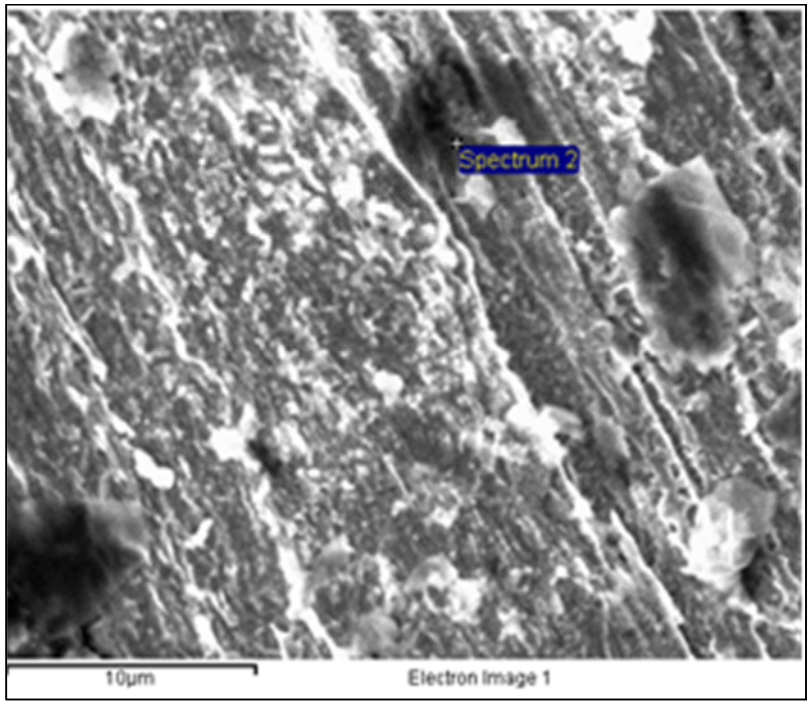

Figure 3-37: SEM image for sample polarized at -800 mV

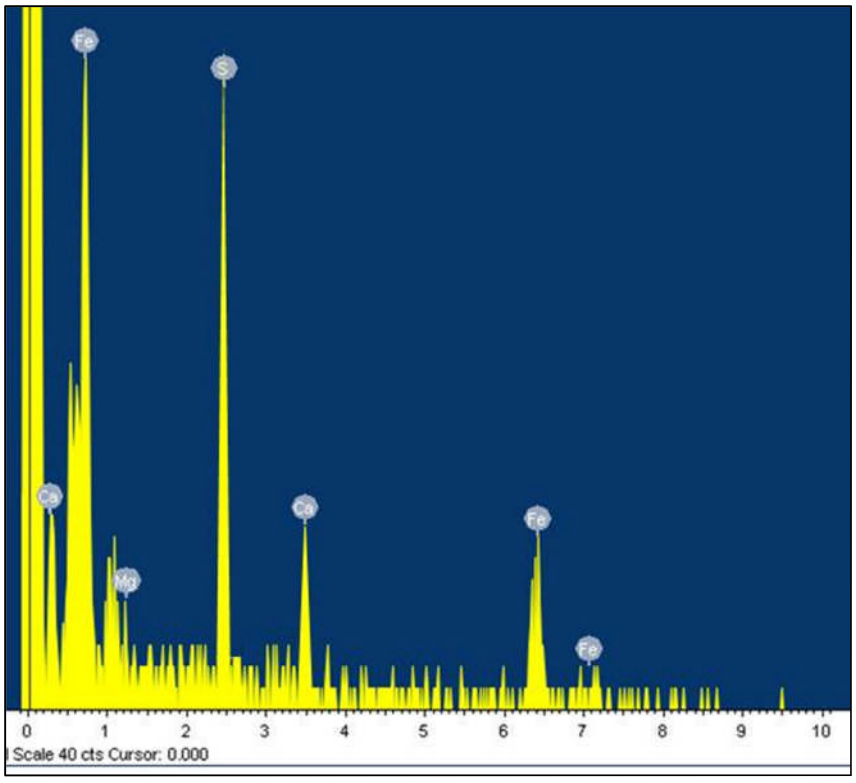

Figure 3-38: EDX spectra for sample polarized at -800 mV

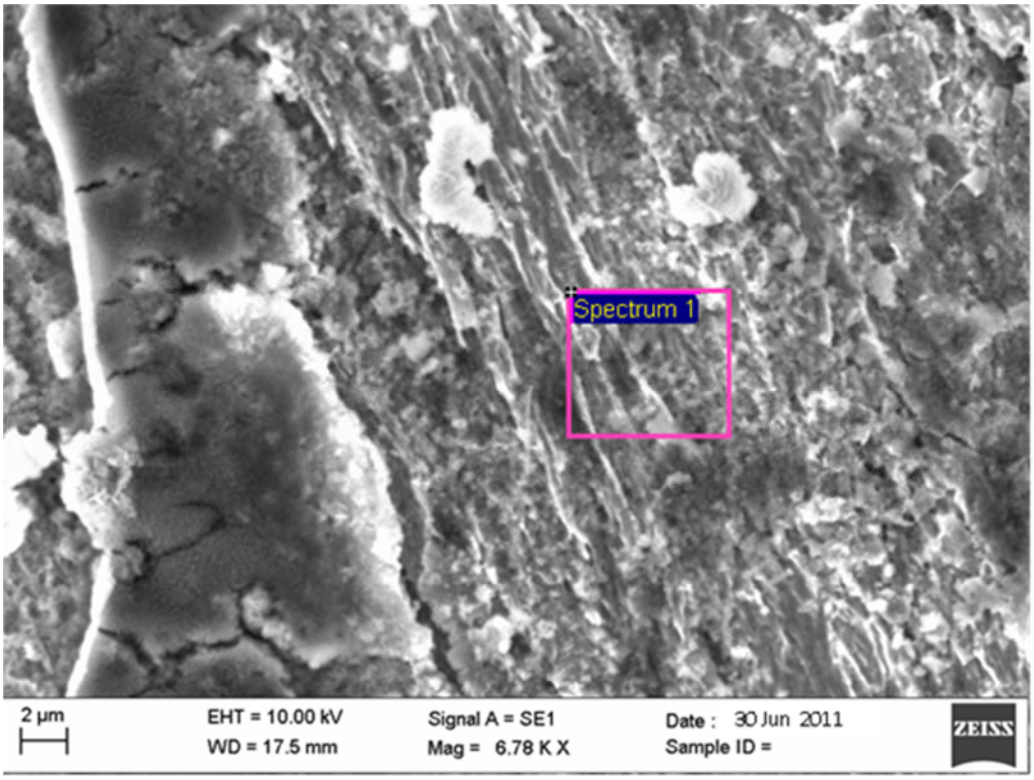

Figure 3-39: SEM image for sample polarized at -850 mV

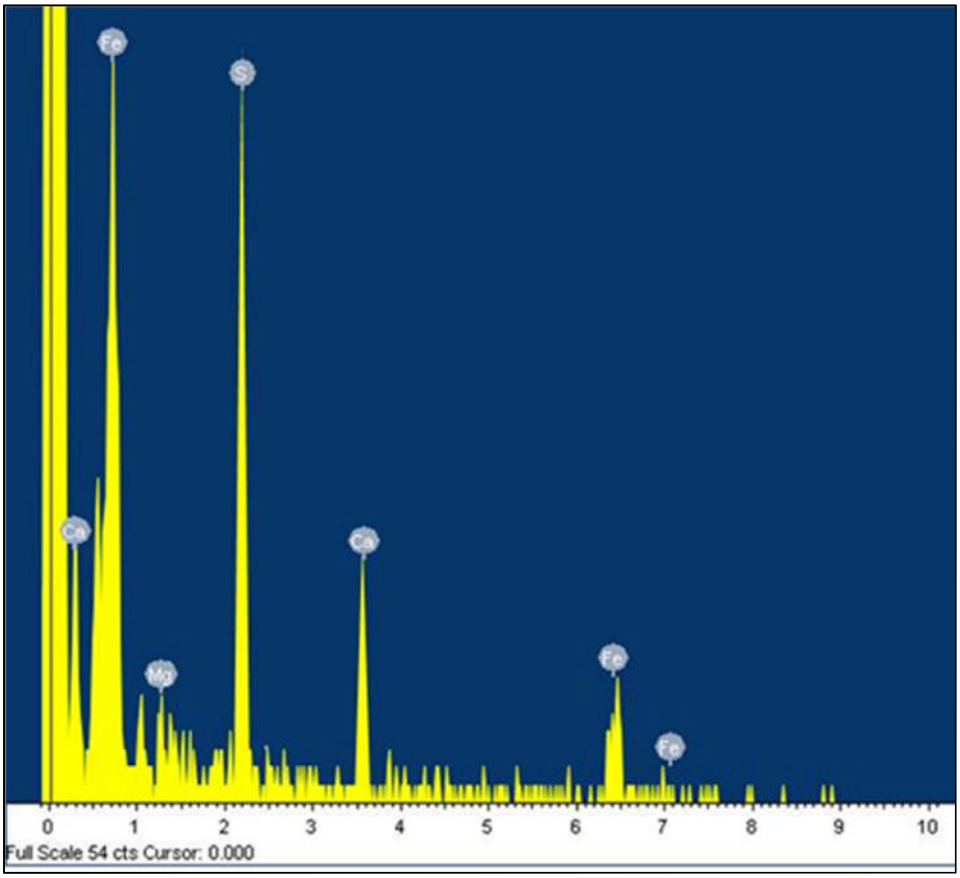

Figure 3-40: EDX spectra for sample polarized at -850 mV

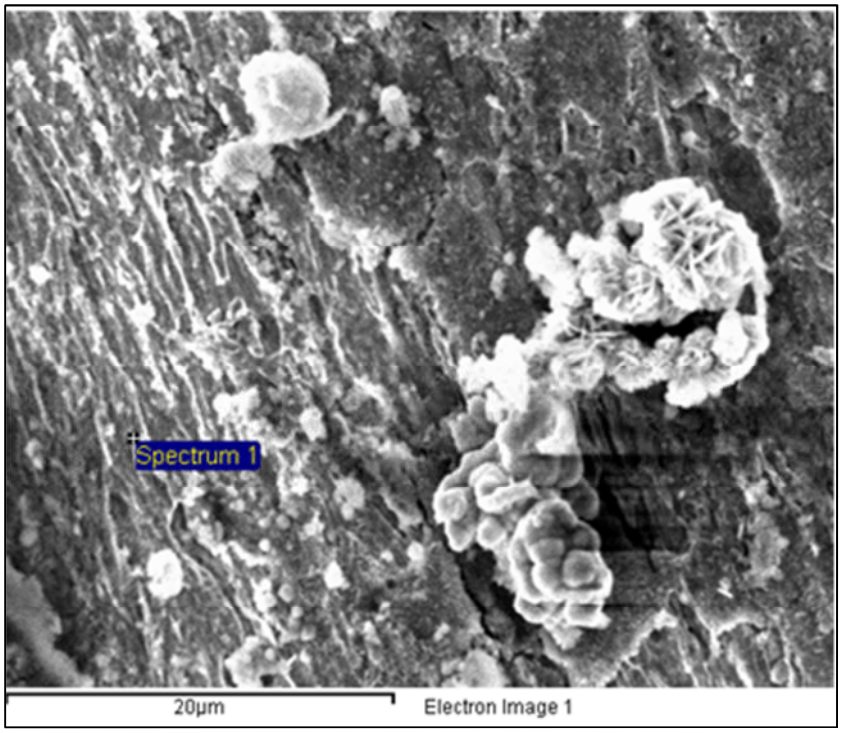

Figure 3-41: SEM image for sample polarized at -900 mV

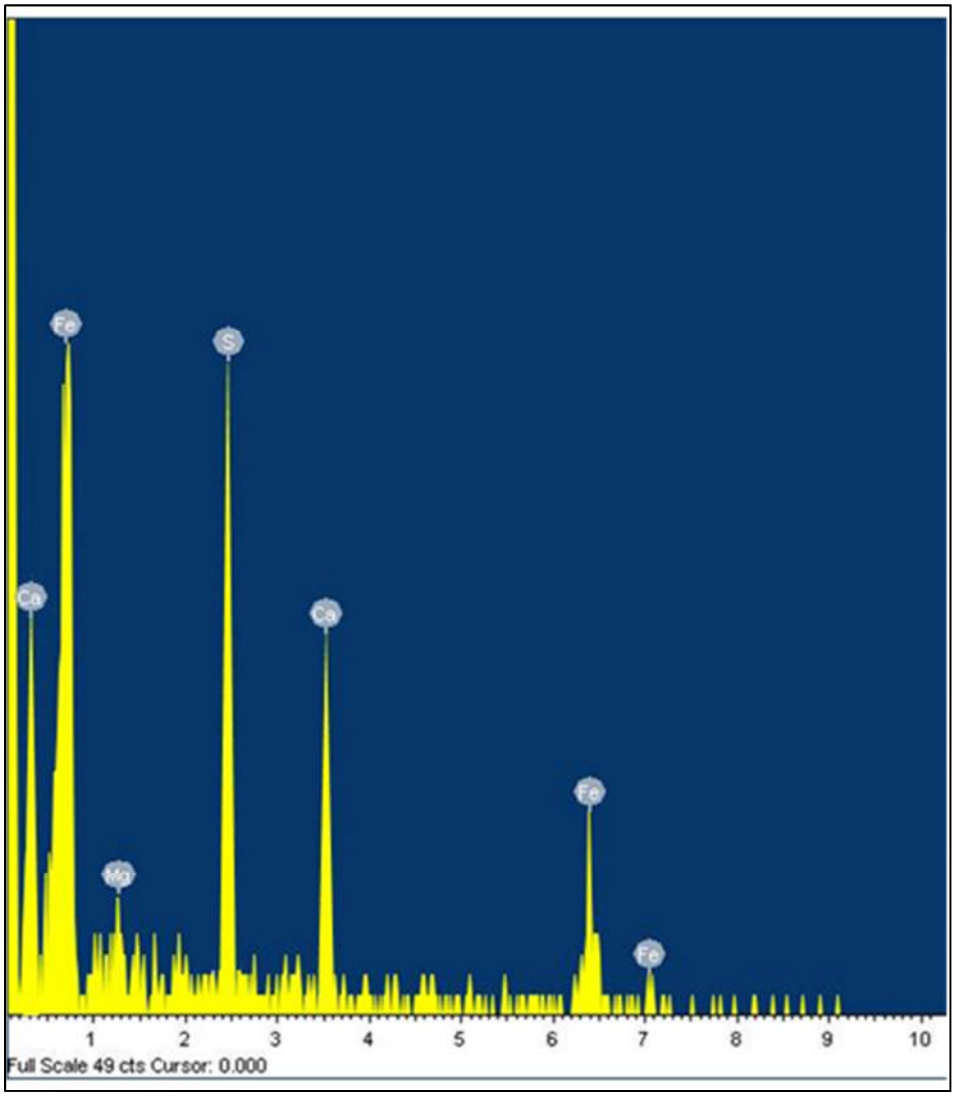

Figure 3-42: EDX spectra for sample polarized at -900 mV

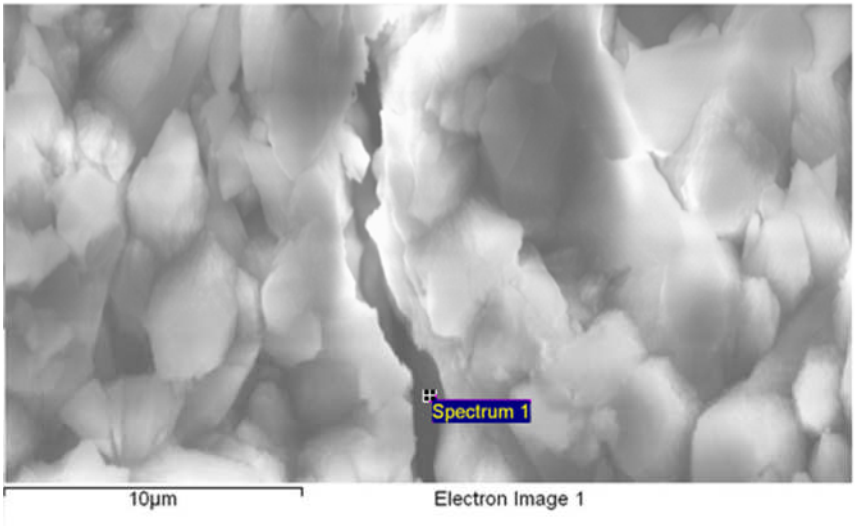

Figure 3-43: SEM image for sample polarized at -950 mV showing calcareous deposit

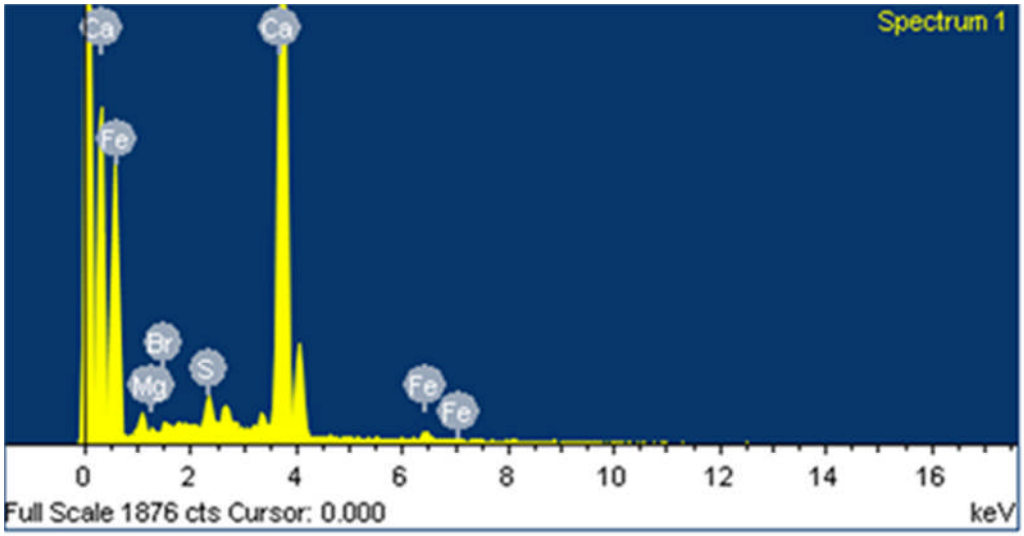

Figure 3-44: EDX spectra for sample polarized at -950 mV on calcareous deposit

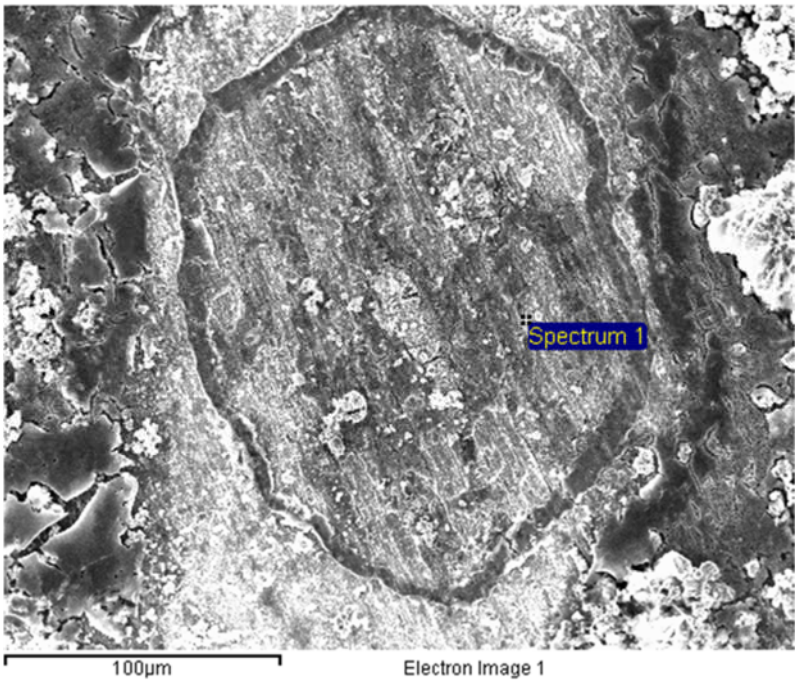

Figure 3-45: SEM image for sample polarized at -950 mV on part with no calcareous deposit

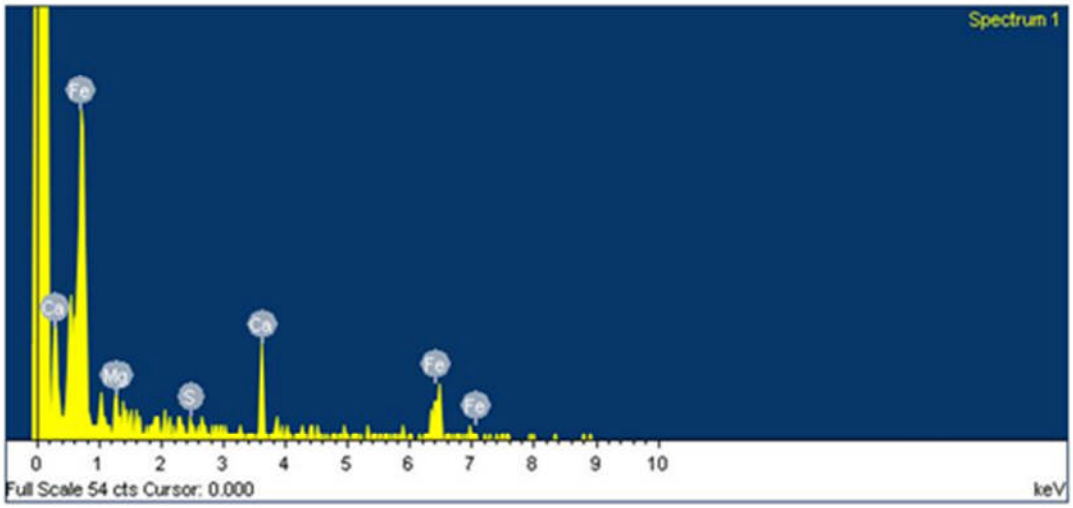

Figure 3-46: Corresponding EDX spectra for the area without calcareous deposit at -950 mV

4 DISCUSSION

4.1 Galvanostatic experiment – Potential trending

This experiment was different from the one described in Section 3.2 using plain salt water. The potential trending measured in the experiment described in Section 3.2 proved to be quite stable along the experiment's duration, but this was not the case for the experiment described in Section 3.4.

The presence of SRB and other microflora in the test solution, together with Mg^{2+} and Ca^{2+} (for calcareous deposit formation) are the marked differences between this experiment and the experiment described in Section 3.2. Thus, it is thought that biofilm formation and the deposition of calcareous deposit could have influenced the potentials. As observed from Figure 3-17 and Figure 3-18, the potential moved towards more positive values during the experiment duration. The potentials went towards more negative values as shown in Figure 3-20 and Figure 3-21 where visible thick calcareous deposit formed.

The observation where the potentials went towards noble direction was also consistent with the works of a few researchers ([84], [98]). Dexter and Lin [84] exposed two types of biofilm formed on the surface of steel exposed to seawater and applied static current density of 20 μA/cm^2. One biofilms was formed naturally, and another one was formed by *Vibrio Harveyi*. The naturally biofilmed sample, which had mixed aerobic and anaerobic bacteria such as SRB, showed potential becoming more positive.

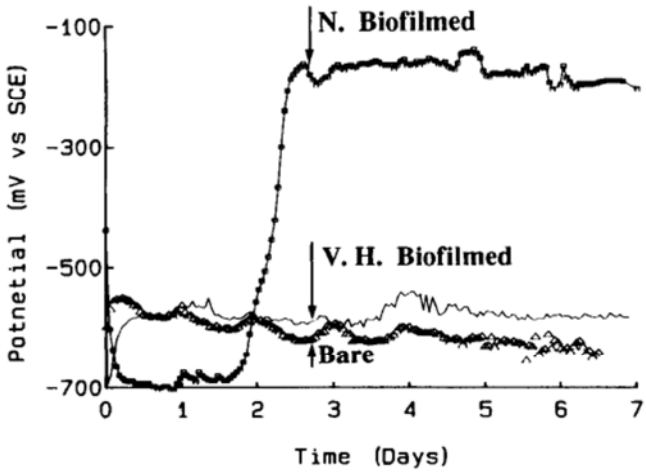

Figure 4-1: Naturally biofilmed sample showing ennoblement of potential at 20 μA/cm^2 in filtered seawater [84]

Potential ennoblement shown in Figure 4-1 above amount to as much as 500 mV (naturally biofilmed), as compared to Figure 3-18, the ennoblement only amounted to only 15 mV and 6 mV from Figure 3-19. The works of Dexter and Lin were done in a continuously flowing system where the nutrients available for the microorganisms were continuously renewed. The experimental work described in Section 3.4 was performed in a stagnant condition without addition of any nutrient to boost the growth of the microflora in the seawater medium. This may explain the more active potential ennoblement in Figure 4-1 compared to Figure 3-18, and also the absence of SRB for samples polarized with current density of 37 µA/cm^2 and 60 µA/cm^2. The following Figure 4-2 shows the potential trending at current density of 50 µA/cm^2 from the work of Dexter and Lin [84].

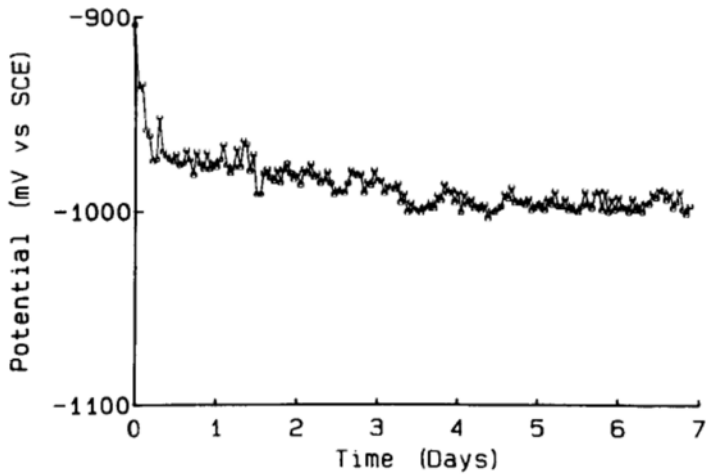

Figure 4-2: Potential vs. time for sample polarized at 50 µA/cm^2 in filtered seawater [84]

This current density allowed the formation of calcareous deposit as reported in their work [84], as well as in this experimental work. Figure 4-2 above shows quite stable potential trending towards more negative values. This potential trending is also observed in this experimental work as shown in Figure 3-20 and Figure 3-21, where the samples formed calcareous deposit.

Booth and Tiller [98] exposed mild steel in medium containing two types of SRB (hydrogenase containing *Desulfuvibrio desulfuricans* able to utilize hydrogen for sulfate

reduction and non-hydrogenase *Desulvibrio orientis*). Potential mesurements were taken from a range of current densities from 0-100 μA/cm^2. The results of the galvanostatic experiments are shown in Figure 4-3 and Figure 4-4.

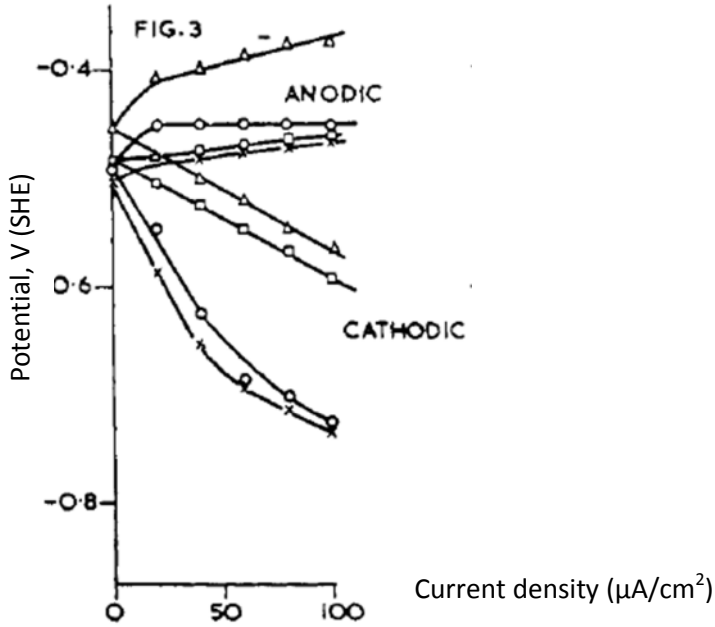

Figure 4-3: Anodic and cathodic polarization curves for mild steel in hydrogenase containing D. desulfuricans (o – initially; x – after 1 day incubation; □ – after 3 days; Δ - after 6 days) [98]

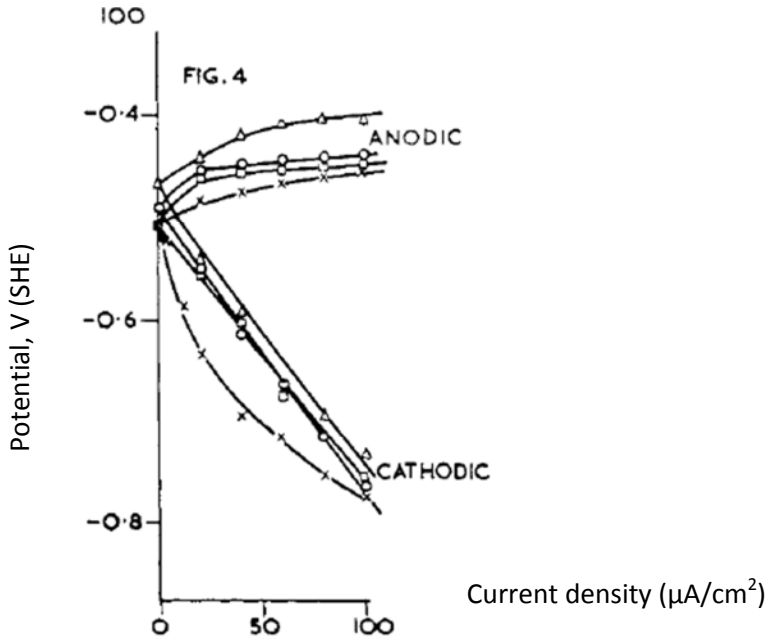

Figure 4-4: Anodic and cathodic polarization curves for mild steel in hydrogenase containing D. orientis (o – initially; x – after 1 day incubation; □ – after 3 days; Δ - after 6 days) [98]

Both set of cultures produced result showing potential ennoblement during the experiment duration. However, at a given current density, the potential ennoblement is more noticeable for D. desulfuricans (hydrogenase containing SRB) as depicted in Figure 4-3.

One possible cathodic reaction during cathodic protection is the hydrogen evolution at the more negative potentials

Eq 2-10: $2H_2O + 2e^- \rightarrow H_2 + 2OH^-$

The hydrogenase-containing SRB located down at the bottom of the biofilm formed at the metal surface could be stripping the hydrogen generated for growth. The consumption of the hydrogen may have the ability to cause loss of polarization needed in cathodic protection [84]. This loss of polarization was observed in this experiment as the potential going towards the noble direction.

Both anodic and cathodic processes affect corrosion rates. For example, if hydrogen produced on the cathode is not removed either by evolution of a gas or some reaction utilizing oxygen, the cathodic reaction slows down. As opposed to cathodic polarization where potential becomes more negative because of current flow effect at or near cathode. Removal of cathodic hydrogen depolarizes the total cell, resulting in increase in corrosion rate as shown in Eq 2-4. As discussed in Section 2.5.1.1, this mechanism is frequently referred to as a mechanism of MIC. Hydrogenase active microorganisms are able to use the hydrogenase enzyme to use hydrogen produced at cathode, as well as to produce depolarizing compounds.

4.2 Current increase for samples polarized at -800 mV to -900 mV

Increasing current (and thus current density) observed for the samples under cathodic polarization exposed to MIC were also observed from several previous works ([70],[68],[84],[85],[98]).

The works of Booth and Tiller described in Section 4.1 the also showed increase in current density at fixed potential. As for the purpose of comparison, the following figure shows current density reading at -850 mV (CSE) extrapolated from Figure 4-3. The potential -850 mV (CSE) was marked at -0.534V from Figure 4-3 using Microsoft

Powerpoint 2010 cursor-ruler measurement and object grouping features. The corresponding current was then interpolated and represented in Figure 4-5 below.

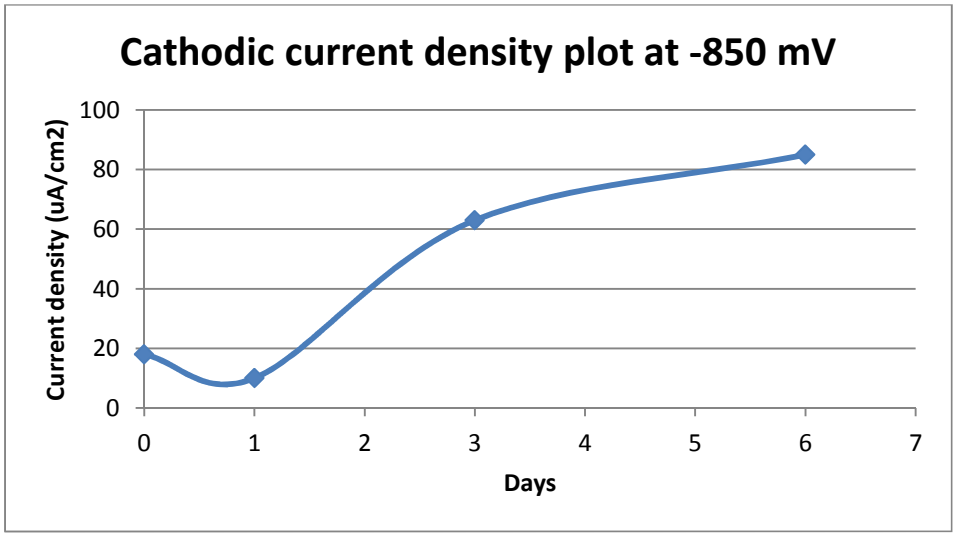

Figure 4-5: Current density plot (interpolation) from the works of Booth and Tiller [98]

The current density trending observed from Figure 4-5 goes down on the first day, presumably when the SRB adjusts to the interfacial conditions established by the cathodic current [84]. Then, the current density increases dramatically (amounting to 75 µA/cm^2), much more than the increase observed in Figure 3-32 where the current density increase observed was only about 15 µA/cm^2. The SRB culture used in the works by Booth and Tiller were continuously renewed to ensure active growth and this may explain the larger increase in current density.

Cathodic polarization forces the reduction of oxygen to produce hydroxyl ions

Eq 2-9: $O_2 + 2H_2O + 4e^- \rightarrow 4OH^-$

At more negative potentials, the evolution of hydrogen becomes possible

Eq 2-10: $2H_2O + 2e^- \rightarrow H_2 + 2OH^-$

As hypothesized in Section 4.1, anaerobic bacteria such as SRB are utilizing the generated molecular hydrogen through hydrogenase for their respiration.

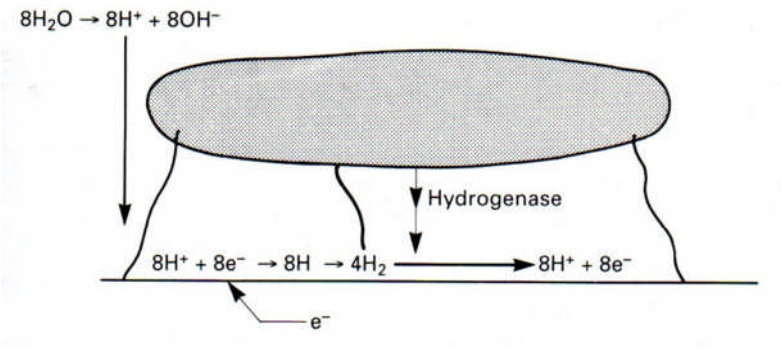

Figure 4-6: Hydrogenase producing microorganism such as SRB causing increase in current demand [99]

However, this reaction may only depict part of the phenomena occurring at cathode. Iron sulfide can also be formed by reaction of sulfide ions and ferrous ions after reduction of sulfate by SRB:

Eq 2-5: $Fe^{2+} + S^{2-} \rightarrow FeS$ (corrosion product)

This was the case as observed from the EDX spectra from Figure 3-38, Figure 3-40 and Figure 3-42 where the three samples showed evidence of presence of FeS. Iron sulfides are more cathodic to steel ([100],[101]). Iron sulfide forming on metal surfaces in turn causes increase in cathode area causing increase in current demand to polarize the samples at a fixed cathodic potential. Additionally, H_2 consumption via hydrogenase-containing SRB could also contribute to this.

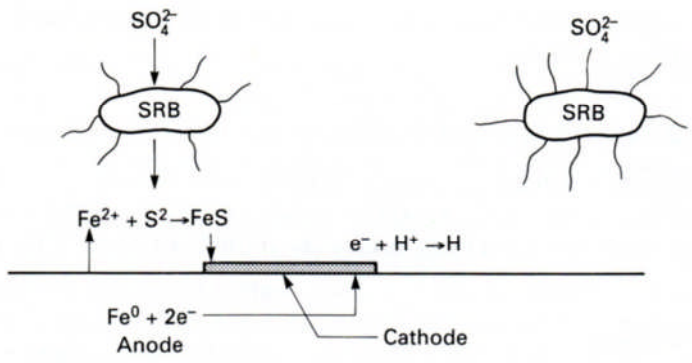

Figure 4-7: Increase of cathode area on metal surface by deposition of FeS as a result of SRB respiration [102]

However, the corrosion rate of mild steel is not only controlled directly by SRB activity, but also indirectly through the nature of iron sulfides formed as part of the respiration activities. Cathodic reactions were stimulated by SRB by removal of molecular hydrogen (direct) and formation of iron sulfides (indirect). Dissolved oxygen was also stated as a way by which SRB stimulate cathodic reaction [103].

4.3 Current decrease for sample at -950 mV and absence of FeS on metal surface

The sample polarized at -950 mV showed visible calcareous deposit as seen in Figure 3-35. The EDX spectrum was also taken from a crack in the calcareous deposit (Figure 3-43) and from an area without calcareous deposit (Figure 3-45). Neither spectrum showed evidence of iron sulfide, as observed from the corresponding EDX spectra Figure 3-44 and Figure 3-46.

The initial increase in current demand observed in Figure 3-34 was thought to be attributed to the initial process of microbial settlement on the metal surfaces. Due to the large current and negative potential, the metal surface becomes more alkaline due to a more aggressive formation of hydroxyl ions, leading to formation of calcareous deposit and decreased current demand. The effect of calcareous deposit in decreasing current demand for cathodic protection is well noted [104].

A factor thought to impede iron sulfide precipitation is the cathodic potential itself. A thermodynamic diagram of iron-iron sulfide-water was generated online from argentumsolutions.com to depict the thermodynamic stability regions of a few sulfide compounds. This diagram was generated using Fe as base metal, and interacting ion is HS^- at pH 7.02 to 16 to denote alkaline conditions under cathodic protection. Using the cursor-ruler measurement and object grouping feature from Microsoft Powerpoint 2010, a mark on the potential -950 mV (-634 mV SHE) is made on the chart as depicted in the following figure.

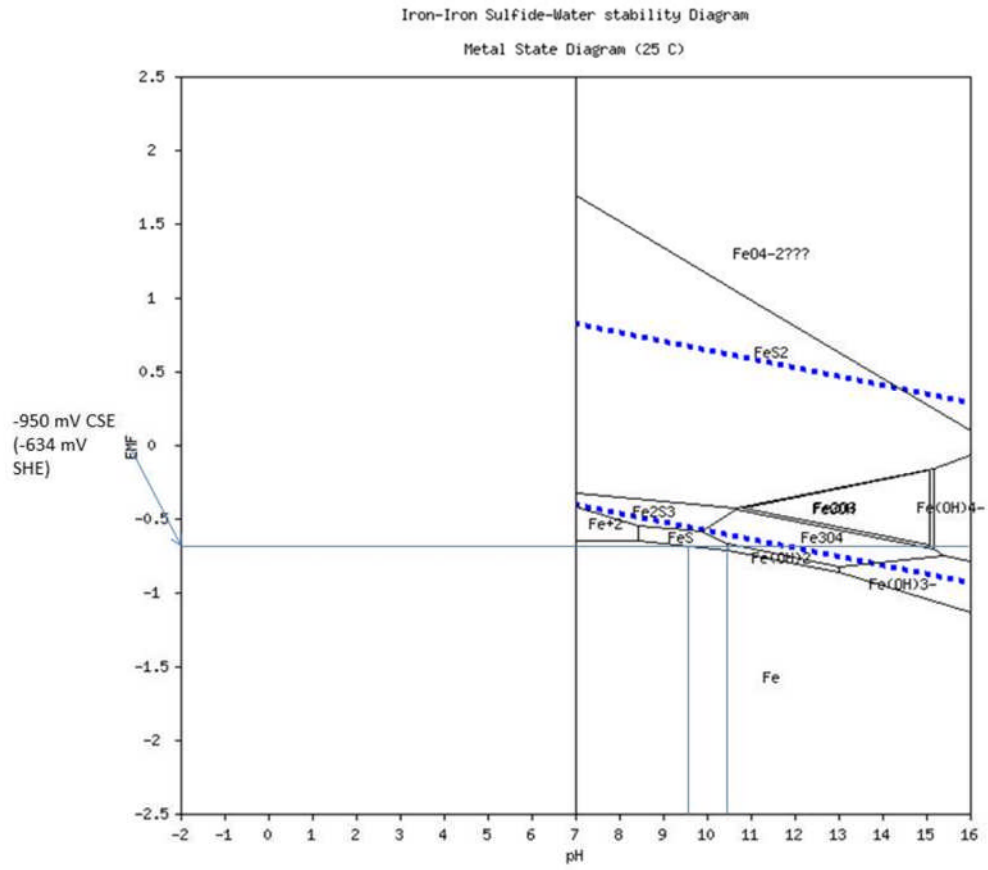

Figure 4-8: Iron-iron sulfide-water stability diagram [105]

The diagram above shows stability regions for iron sulfide (FeS), ferric sulfide (Fe_2S_3), pyrite (FeS_2). It can be observed that at potential -950 mV and below, iron sulfide is marginally stable at a small pH range of around 9.5 to 10.5. Below this potential, no sulfide compound is stable. And as can be seen from the diagram, above this potential, a wide range of sulfide compounds are stable. Thus, cathodic polarization below -950 mV has the effect imposing an environment where iron sulfides are not thermodynamically stable.

4.4 Effects of cathodic potentials on SRB viability on metal surface

The following table summarises the SRB cfu counts from the serial dilution results for all potentials, in accordance to Table 3-9.

Potential (mV)	1st dilution	2nd dilution	3rd dilution	MPN of 1st dilution (cfu/ml)	MPN of 1st vial (cfu/ml)	Total cfu	Cfu/unit area (cfu/mm^2)
-800	3	2	1	15	1500	15,000	47,000
-850	3	3	1	45	4500	45,000	141,000
-900	3	2	1	15	1500	15,000	47,000
-950	3	2	1	15	1500	15,000	47,000

Table 4-1: SRB MPN count for the range of potentials studied

MPN is based on the application of the theory of probability. Generally, MPN are done in triplicate (the case in this experimental work), 5 or 10 tube MPN series. 5 and 10 tube MPN series represents higher accuracy and narrows down the confidence limits. The following assumptions were made during the count procedure:

1. The SRB were evenly distributed in the vials after ultrasonication.
2. The organisms exist as single entities.

The following table shows the MPN counts and the corresponding 95% confidence limits [106].

Potential (mV)	Cfu/unit area (cfu/mm^2)	95% confidence limits	
		Lower	Upper
-800	47,000	12,000	131,000
-850	141,000	28,000	625,000
-900	47,000	12,000	131,000
-950	47,000	12,000	131,000

Table 4-2: MPN count 95% confidence limits

From Table 4-1, all potentials resulted in the same number of SRB MPN count except for potential polarized at -850 mV. The SRB count for sample polarized at -850 mV showed SRB count one order higher than the other potentials. However, this is not thought to be significant enough to conclude that this cathodic potential has significant effect compared to other potentials studied.

The counts obtained from this procedure reflect the viable sessile SRB on the metal surfaces. In order to become sessile, bacteria must attach themselves to metal surfaces. Although cathodic polarization encourages the generation of negatively charged hydroxyl ions which should repel the usually negatively charged bacteria, the observation in this experiment showed that the cathodic polarization did not have significant effect on bacterial attachment and viability on the metal surfaces in the range of potentials studied . This may be due to surfaces in aqueous surrounding absorbing organic molecules and forming a conditioning film that assisted bacterial attachment [21]. The works of Edyvean et al. showed that the higher current density on metal surfaces reduces bacterial attachment to metal surfaces with increasing cathodic protection level applied [73]. However, cathodic oxygen consumption resulting from cathodic polarization has been demonstrated favourable to aerobic bacteria [80], as is the fact that hydrogen generated at more negative potentials may be supportive of anaerobic bacteria that grow by utilizing hydrogen such as SRB.

4.5 General Discussion

From the results, it can be observed that the current demand increased for potentials above -950 mV, where no calcareous deposit formed on the samples. The potentials increased (ennobled) when held at a constant current. However, current demand decreased for samples showing presence of calcareous deposit. Through the potential range studied, the attachment and viability of SRB on cathodically protected steel surface were not affected. Iron sulfide was formed on samples polarized at potentials more noble than -950 mV. The increase in current demand and potentials could be accounted as loss of cathodic protection capability. Calcareous deposit were formed at -950 mV, however this did not affect attachment and viability of SRB on the metal surface. It also helped to reduce current demand to cathodically protect steel surfaces.

Iron sulfide was formed on samples polarized at -800 to -900 mV, but it was absent on metal polarized at -950 mV.

Increase in alkalinity at the metal surface due to cathodic protection potential causes formation of calcareous film, and could also affect SRB viability. High pH values can harm or destroy bacteria due to lysis of lipids and proteins in the cell membrane by alkali. Chemical reactions related with pH increase have further restraining effects on bacterial attachment [88]. However, down to -950 mV, the increase in alkalinity on the metal surfaces did not have effect on SRB viability.

Two factors that contributed to the increase in current demand and potentials, which are consumption of molecular hydrogen by SRB and deposition of iron sulfide were discussed. However, a more direct factor thought to influence this phenomenon is the effect of iron sulfide deposition that caused increase in effective cathode area. This is because viable SRB were still detected at -950 mV, but the current demand decreased. A previous work by Characklis et al [107] suggested that attachment and viability of SRB on metal surfaces can be affected by calcareous deposit formation. However, in the current study, the more aggressive generation of hydrogen at more negative potentials that is favourable to the SRB may help explaining the viability of SRB at -950 mV, although calcareous deposit was formed on the samples.

The cathodic protection criterion of -950 mV (or more negative) for metals exposed MIC risk appeared to have effect on reducing the probability of deposition of iron sulfide, presumably due to the fact that sulfide compounds are not thermodynamically stable below this potential. Above this potential, iron sulfide compounds are fairly stable on metal surfaces.

From the results and discussion throughout, it can be summarized that biofilm and bacterial metabolism within the biofilm can affect polarization processes. The generation of hydrogen may be favourable to SRB respiration and growth. The subsequent iron sulfide formation caused an increase in cathodic current demand. However, the factors affecting SRB attachment and viability on the metal surface could be influenced by any one of the following; calcareous deposit formation, the cathodic potentials, the presence of nutrient available to SRB; or any combination among these three factors. This area of the research work warrants further investigation as to

determine which factor really influence SRB attachment and viability on polarized metal surfaces.

5 CONCLUSION

The following conclusions can be drawn from the discussion and observation from the experimental works.

5.1 Galvanostatic experiment

1. Biofilm and the activities of the constituent microorganisms in this experiment may have contributed to ennoblement of cathodic potentials observed for samples where visible calcareous deposit was not formed.
2. The stagnant medium and lack of nutrient in this experiment was thought to be the reason for the absence of SRB in the higher current densities (36.6 $\mu A/cm^2$ and 59.5 $\mu A/cm^2$). pH changes on the metal surface are another explanation.
3. This experiment also provided an estimate that the range of cathodic potentials that have effects on MIC is between -800 mV and -1000 mV (CSE).
4. Calcareous deposit was shown to form at -950 mV and -1000 mV and may have effects on the attachment process of bacteria to metal surfaces.

5.2 Potentiostatic experiment

1. The use of a multipotentiostat in this experiment proved to be able to provide a stable potential over a long period of time.
2. SRB activity on metal surfaces polarized at -800 mV to -900 mV causes increase in current demand to protect a metal at a fixed potential.
3. At cathodic potential of -950 mV and below, FeS is not thermodynamically stable. Calcareous deposit formed at this potential but little, if any, FeS was detected.
4. In the range of potentials studied, cathodic polarization did not have effect on bacterial attachment and viability on metal surfaces.

5.3 Suggestion for further work

1. It is recommended to perform the potentiostatic study on a more negative potential of -1000 mV.
2. Since calcareous deposit is a significant feature of cathodic protection at more negative potentials, it is proposed to study the mechanism of calcareous deposition under cathodic protection and effects of biofilms on this mechanism and vice-versa.

6 APPENDIX

6.1 Triplicate picture for SRB presence test described in Section 3.4.7.2 (In addition to Figure 3-22).

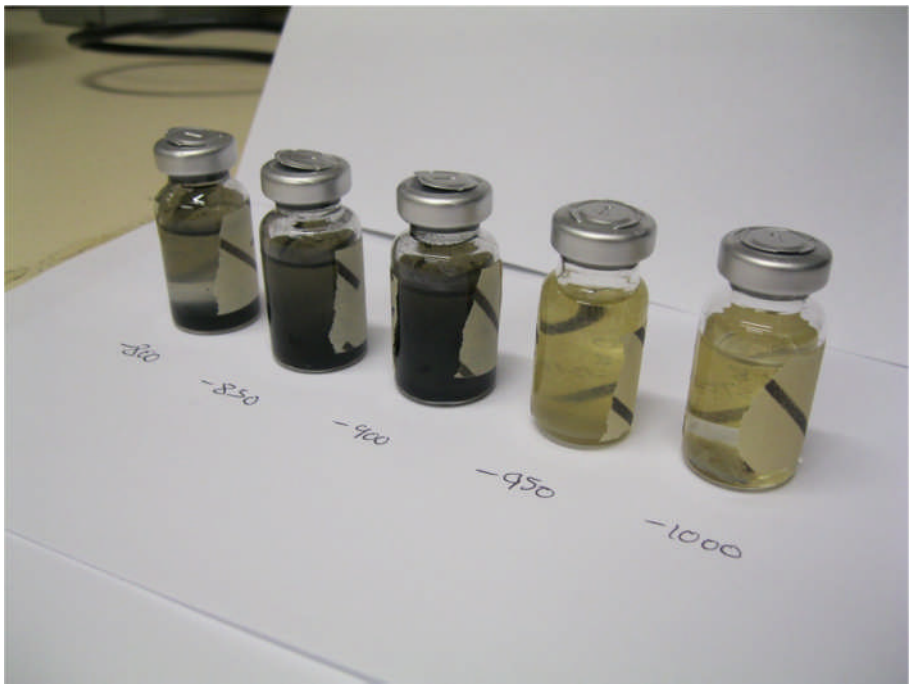

Figure 6-1: SRB presence test (Sample 2)

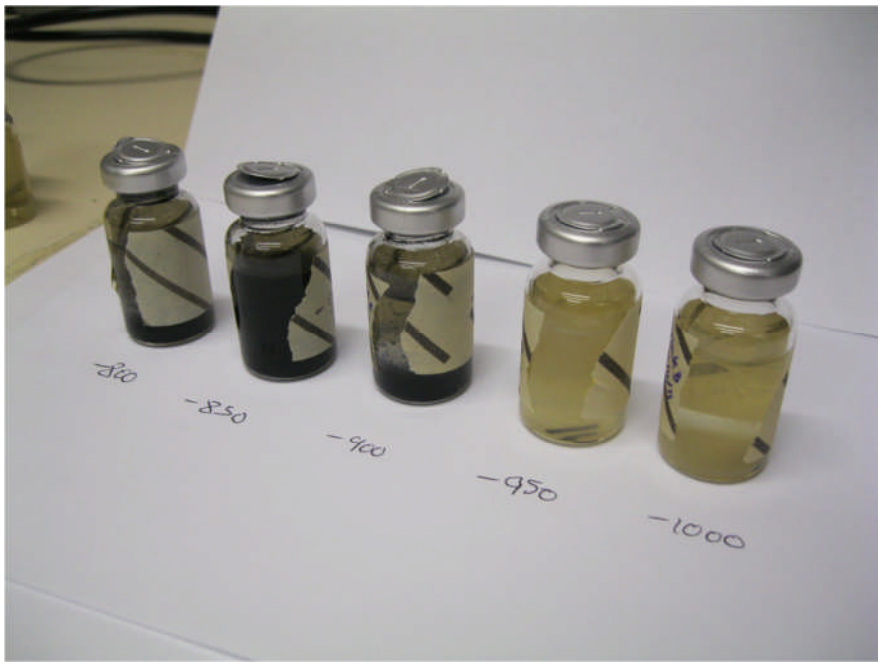

Figure 6-2: SRB presence test (Sample 3)

6.2 *Pictures of SRB MPN count results*

Figure 6-3: MPN results for samples polarized at -800 mV

Figure 6-4: MPN results for samples polarized at -850 mV

Figure 6-5: MPN results for samples polarized at -900 mV

Figure 6-6: MPN results for samples polarized at -950 mV

7 REFERENCES

1. M.D. Romero, A. Quintero, G. Romero, O.D. Rinc, J. Parra, M. Bracho, R. Ruiz and L. Ocando, *Cathodic Polarization Effect on Sessile SRB Growth and Iron Protection*, in *CORROSION/2006*. 2006, NACE International Paper no. 06526: San Diego, California.
2. G.C. Wells, *The Importance Of Controlled Humidity In Long Time Preservation.* Journal of the American Society for Naval Engineers, 1948. **60**(2): p. 127-138.
3. P.A. Schweitzer, *Fundamentals of metallic corrosion: atmospheric and media corrosion of metals*. 2006: Taylor & Francis.
4. W.G. Characklis, B.J. Little and M.S. McCauley, *Biofilms and their effects on local electrochemistry*, in *Microbial Corrosion: 1988 Workshop Proceedings*. 1989, EPRI: Palo Alto, California.
5. B.J. Little, J.S. Lee and R.I. Ray, *The influence of marine biofilms on corrosion: A concise review.* Electrochimica Acta, 2008. **54**(1): p. 2-7.
6. M.J. Franklin, D.C. White and H.S. Isaacs, *Pitting corrosion by bacteria on carbon steel, determined by the scanning vibrating electrode technique.* Corrosion Science, 1991. **32**(9): p. 945-952.
7. R. Sandoval-Jabalera, G.V. Nevarez-Moorillon, J.G. Chacon-Nava, J.M. Malo-Tomayo and A. Martinez-Villafane, *Electrochemical Behaviour Of Uns S17700 And Uns N08800 Alloys In Synthetic Wastewater.* Journal of Mexican Chemical Society, 2006. **50**(1): p. 14-18.
8. M.F.D. Romero and S. Urdaneta, *Correlation Between Desulfovibrio Sessile Growth and OCP, Hydrogen Permeation, Corrosion Products and Morphological Attack on Iron*, in *CORROSION/2004 Paper no. 04576*. 2004, NACE International: New Orleans. p. 27.
9. B.Little and P. Wagner, *Myths related to microbiologically influenced corrosion.* 1997. **36**(6): p. 40-44.
10. R. Javaherdashti, *A review of some characteristics of MIC caused by sulfate-reducing bacteria: Past, present and future.* Anti-Corrosion Methods and Materials, 1999. **46**(3): p. 173-180.
11. A. Patterson and C. Argent, *FFS assessment report for PL 333 (16 inch) 13 km Crude Oil Pipeline (Bakau-A to WL-A)*. 2008.
12. S.Y. Li, Y.G. Kim, and Y.T. Kho, *Corrosion behavior of carbon steel influenced by sulfate reducing bacteria in soil environments*, in *CORROSION/2003*. 2003, NACE International Paper no. 03549.
13. P.S.Guiamet , S.G.G.D. Saravia and H.A. Videla, *An innovative method for preventing biocorrosion through microbial adhesion inhibition.* International Biodeterioration and Biodegradation, 1999. **43**(1-2): p. 31-35.
14. K. Xu, *Voltammetric Microelectrodes for Biocorrosion Studies.* Corrosion, 1998. **54**(10): p. 814.
15. H.A. Videla, *An overview of mechanisms by which sulphate-reducing bacteria influence corrosion of steel in marine environments.* Biofouling, 2000. **15**(1-3): p. 37.
16. R.A. King, *Microbiologically induced corrosion and biofilm interactions*, in *MIC – An International Perspective Symposium*. 2007, Curtin University: Perth, Australia.
17. H. Videla, *Manual of Biocorrosion*. 1996: CRC Press.
18. B. Little, P. Wagner and F. Mansfeld, *An overview of microbiologically influenced corrosion.* Electrochimica Acta, 1992. **37**(12): p. 2185-2194.
19. E. Heitz, H.C. Flemming and W. Sand, *Microbially influenced corrosion of materials : scientific and engineering aspects*. 1996, Berlin: Springer-Verlag.
20. E. Heitz, *A Working Party Report on Microbiological Degradation of Materials and Methods of Protection*. 1992, European Federation of of Corrosion Publication.
21. W.A. Hamilton, *Sulphate-reducing bacteria and anaerobic corrosion.* Annual Review Microbiology, 1985. **39**: p. 195-217.

22. Chamritski, I.G., et al., *Effect of iron-oxidizing bacteria on pitting of stainless steel.* 2004. **60**(7): p. 658-69.
23. Sand, W., *Microbial mechanisms of deterioration of inorganic substrates - A general mechanistic overview.* International Biodeterioration & Biodegradation, 1997. **40**(2-4): p. 183-190.
24. Little, B. and P. Wagner, *Myths related to microbiologically influenced corrosion.* Materials Performance, 1997. **36**(6): p. 40-44.
25. G.H. Booth, *Microbiological Corrosion*. Vol. CE/1. 1971: M&B Monographs.
26. S.S. Mohanty, T. Das, S.P. Mishra, G. Roy and G.R. Chaudhury, *Kinetics of sulfate reduction under different growth media by sulfate reducing bacteria.* Biomedical and Life Sciences, 2003. **13**(1).
27. J.A. Costello, *Cathodic Depolarization By Sulfate-Reducing Bacteria.* South African Journal of Science, 1974. **70**(7): p. 202.
28. B.L. Hilton and J.A. Oleszkiewicz, *Sulfide-Induced Inhibition Of Anaerobic-Digestion - Closure.* Journal of Environmental Engineering-Asce, 1990. **116**(5): p. 1007-1008.
29. V.L. Rainha and I.T.E. Fonseca, *Kinetic studies on the SRB influenced corrosion of steel: A first approach.* Corrosion Science, 1997. **39**(4): p. 807-813.
30. W.G. Characklis and P. Wilderer, *Structure and function of biofilms / W. G. Characklis and P. A. Wilderer, editors*, ed.1989, Chichester: Wiley.
31. J.R. Kearns and B.J. Little, *Microbiologically Influenced Corrosion Testing (STP 1232)*. 1994: ASTM.
32. Z. Lewandowski, P. Stoodley and S. Altobelli, *Experimental and conceptual studies on mass transport in biofilms.* Water Science and Technology, 1995. **31**(1): p. 153-162.
33. D. Starosvetsky, R. Armon, J. Yahalom and J. Starosvetsky, *Pitting corrosion of carbon steel caused by iron bacteria.* International Biodeterioration & Biodegradation, 2001. **47**(2): p. 79-87.
34. N. Muthukumar, S. Mohanan, S. Marumuthu, P. Subrmanian, P. Palaniswamy and M. Raghavan, *The role of fungi on diesel degradation, and their influence on corrosion of API 5LX steel.* Corrosion Prevention & Control, 2005. **52**(4): p. 123.
35. F. Murdoch and P.G. Smith, *Formation of manganese micro-nodules on water pipeline materials.* Water Research, 1999. **33**(12): p. 2893-2895.
36. T. Zhang, H.H.P. Fang and B.C.B. Ko, *Methanogen population in a marine biofilm corrosive to mild steel.* Applied microbiology and biotechnology, 2003. **63**(1): p. 101.
37. R.W. Lutey and R. Saito, *The occurrence and influence of anaerobic bacteria in cooling water systems.* International Biodeterioration & Biodegradation, 1996. **37**(1-2): p. 127-128.
38. D. Nica, J. L. Davis, L. Kirby, G. Zuo and D. J. Roberts, *Isolation and characterization of microorganisms involved in the biodeterioration of concrete in sewers.* International Biodeterioration & Biodegradation, 2000. **46**(1): p. 61-68.
39. J. Overmann and H. van Gemerden, *Microbial interactions involving sulfur bacteria: implications for the ecology and evolution of bacterial communities.* FEMS Microbiology Reviews, 2000. **24**(5): p. 591-599.
40. J.W. Costerton, G.G. Geesey and K.J. Cheng, *How Bacteria Stick.* Scientific American, 1978. **238**(1): p. 86-95.
41. T. Ford and R. Mitchell, *The Ecology Of Microbial Corrosion.* Advances in Microbial Ecology, 1990. **11**: p. 231-262.
42. E. Otero, J.M. Bastidas and V. López, *Analysis of a premature failure of welded AISI 316L stainless steel pipes originated by Microbial induced corrosion.* Materials and Corrosion/Werkstoffe und Korrosion, 1997. **48**(7): p. 447-454.
43. S.J. Yuan and S.O. Pehkonen, *AFM study of microbial colonization and its deleterious effect on 304 stainless steel by Pseudomonas NCIMB 2021 and Desulfovibrio desulfuricans in simulated seawater.* Corrosion Science, 2009. **51**(6): p. 1372-1385.

44. H. Liu, *Role of corrosion products in biofilms in microbiologically induced corrosion of carbon steel.* British Corrosion Journal, 2000. **35**(2).
45. *Petronas profit falls on lower sales, oil price*. December 2009 [cited 2010 20 January]; Available from: http://carigalipetronas.blogspot.com/2009/12/petronas-profit-falls-on-lower-sales.html.
46. S.M. El-Raghy, H.M. Abou El-Leil and H.H. Ghazal, *Microbial-induced corrosion of subsea pipeline in the Gulf of Suez.* Spe Production & Facilities, 2000. **15**(2): p. 126-129.
47. *ASM Metals Handbook - Corrosion*. Vol. 13. 1987.
48. Von Beckmann, W., W. Schwenk, and W. Prinz, *Cathodic Corrosion Protection*. 1998, Houston: Gulf Publishing Company.
49. N. Perez, *Electrochemistry and Corrosion Science*. 2004.
50. E. Bardal, *Corrosion and Protection*, ed. B. Derby. 2004: Springer.
51. PETRONAS, *PRINCIPLES OF MATERIALS ENGINEERING & CORROSION CONTROL IN E&P OPERATIONS*. 1987. p. 104-105.
52. M.O. Durham and R.A. Durham, *Cathodic protection.* Industry Applications Magazine, IEEE, 2005. **11**(1): p. 41-47.
53. K. Zakowski and K. Darowicki, *Evaluation and characterisation of the condition of individual components of cathodic protection systems.* Anti-Corrosion Methods and Materials, 2004. **5**(4): p. 253-258.
54. L.L. Shreir and P.C.S. Hayfield, *Impressed Current Anodes*, ed. V. Ashworth and C.J.L. Booker. 1986, Chichester, UK: Ellis Horwood.
55. W.V. Baeckmann, W. Schwenk and W.Prinz, *Handbook of cathodic corrosion protection - Theory and practice of electrochemical protection processes*. 1997, Houston, Tex.: Gulf Pub. Co.
56. *NACE RP0169-2002: Control of External Corrosion on Underground or Submerged Metallic Piping Systems*. 2002, National Association of Corrosion Engineers (NACE).
57. R.H. Brown and R.B. Mears, *Cathodic Protection.* Transactions of The Electrochemical Society, 1942. **81**(1): p. 455-483.
58. H.H. Uhlig and R.R. Winston, *Corrosion and corrosion control: An introduction to corrosion science and engineering*. Vol. Third Edition. 1985: Wiley.
59. J. Didas, *Cathodic protection and its application to mature pipelines.* Materials Performance, April 2000.
60. J.D. Cox, *How does the " Spike" affect 'instant-off' readings?* Materials Performance, January 1992.
61. T.J. Barlo, *Origin and Validation of the 100 mV Polarization Criterion*, in *CORROSION/2001*. 2001, NACE International Paper no. 01581: Houston, Texas.
62. J. Horváth and M. Novák, *Potential/pH equilibrium diagrams of some Me---S---H2O ternary systems and their interpretation from the point of view of metallic corrosion.* Corrosion Science, 1964. **4**(1-4): p. 159-178.
63. D.L. Piron, *The electrochemistry of corrosion*. 1991, Houston, TX: NACE.
64. *BS EN 13174:2001: Cathodic protection for harbour installations*. 2001.
65. DNV, *Recommended Practice DNV-RP-B401*. 2005.
66. V. Ashworth, *The Theory of Cathodic Protection and Its Relation to the Electrochemical Theory of Corrosion*. Ellis Horwood, Cathodic Protection: Theory and Practice. 1986. 13-30.
67. O. Moos and P. Gümpel, *Comparison of the microbiological influence on the electro-chemical potential of stainless steel between macro- and micro-areas of specimens.* Special Issue BIOCORROSION OF MATERIALS Selection of papers from the International Conference (BIOCORYS 2007) 14-17 June 2007, Paris, France, 2008. **54**(1): p. 53-59.
68. J.G. Guezennec, *Cathodic protection and microbially induced corrosion.* Special Issue Marine Biofouling and Corrosion, 1994. **34**(3-4): p. 275-288.

69. F. Kajiyama and K. Okamura, *Evaluating cathodic protection reliability on steel pipe in microbially active soils.* CORROSION, 1999. **55**(1): p. 74-80.
70. B. Little, P. Wagner and D. Duquette, *Microbiologically Induced Increase In Corrosion Current Density Of Stainless Steel Under Cathodic Protection.* CORROSION, 1988. **44**(5): p. 270-274.
71. C. Barchiche, *Characterisation of calcareous deposits by electrochemical methods: role of sulphates, calcium concentration and temperature.* Electrochimica Acta. **49**(17-18): p. 2833-2839.
72. K. Miyanaga, *Biocidal effect of cathodic protection on bacterial viability in biofilm attached to carbon steel.* Biotechnology and Bioengineering, 2007. **97**(4): p. 850.
73. R.G.J. Edyvean, A. D. Maines, C. J. Hutchinson, N. J. Silk and L. V. Evans, *Interactions between cathodic protection and bacterial settlement on steel in seawater.* Special Issue Microbially Influenced Corrosion, 1992. **29**(3-4): p. 251-271.
74. S.H. Flint, P.J. Bremer and J.D. Brooks, *Biofilms in dairy manufacturing plant-description, current concerns and methods of control.* Biofouling: The Journal of Bioadhesion and Biofilm Research, 1997. **11**(1): p. 81-97.
75. J. Lee, *Bacterial biofilms less likely on electropolished steel.* Agricultural Research, 1998. **46**(2): p. 10-11.
76. M.C.M. Loosdrecht, W. Norde, J. Lyklema and J. B. Z. Alexander, *Hydrophobic and electrostatic parameters in bacterial adhesion.* Aquatic Sciences - Research Across Boundaries, 1990. **52**(1): p. 103-114.
77. K.R. Sreekumari , K. Nandakumar and Y. Kikuchi, *Bacterial attachment to stainless steel welds: Significance of substratum microstructure.* Biofouling, 2001. **17**(4): p. 303-316.
78. S. Maxwell, *Effect of cathodic protection on the activity of microbial biofilms.* Materials Performance, 1986. **25**(11): p. 53-56.
79. M.D. Romero, A. Quintero, G. Romero, O.D. Rinc, J. Parra, M. Bracho, R. Ruiz and L. Ocando, *Cathodic Polarization Effect on Sessile SRB Growth and Iron Protection.* Corrosion 2006, 2006(06526): p. 22.
80. J. Guezennec, *Influence of cathodic protection of mild steel on the growth of sulphate-reducing bacteria at 35°C in marine sediments.* Biofouling: The Journal of Bioadhesion and Biofilm Research, 1991. **3**(4): p. 339 - 348.
81. H.P. Dahr, D.W. Howell and J.O.M. Bockris, *The use of in situ chemical reduction of oxygen in the diminution of adsorbed bacteria on metals in seawater.* J. Electrochem. Soc, (129): p. 2178-82.
82. A.S. Gordon, S.M. Gerchakov and L.R. Udey, *The effect of polarization on the attachment of marine bacteria to copper and platinum surfaces.* Canadian Journal of Microbiology, 1981. **27**(7): p. 698-703.
83. E. Littauer and D.M. Jennings, *The prevention of marine fouling by electrical currents*, in *Proc. 2nd Int. Congress on Marine Corrosion and Fouling*. 1968: Athens, Greece. p. 527-536.
84. S.C. Dexter and S.-H. Lin, *Effect of marine biofilms on cathodic protection.* Special Issue Microbially Influenced Corrosion, 1992. **29**(3-4): p. 231-249.
85. R. Johnsen and E. Bardal, *Cathodic properties of different stainless steels in natural seawater.* CORROSION, 1985. **41**(5): p. 296-302.
86. S. Pathmanaban and B.S. Phull, *Calcareous Deposits on Cathodically Protected Structures in Sea Water*, in *UK National Corrosion Conference 1982*. 1982: London. p. 165-168.
87. M.A. Guillen and S. Feliu, *Contribution To The Study Of Several Variables Which Affect The Cathodic Protection Of Steel*, in *Naval Scientific And Technical Information Centre*. 1968. p. 32.

88. A. Katerina and F.F. Joseph, *Removal of Pseudomonas putida Biofilm and Associated Extracellular Polymeric Substances from Stainless Steel by Alkali Cleaning.* Journal of Food Protection, 2005. **68**: p. 277-281.
89. *Potentiostat*. [cited 2011 May 21]; Available from: http://en.wikipedia.org/wiki/Potentiostat.
90. *ISO 12473:2006 (E) - General Principles of Cathodic Protection in seawater*. 2006. p. 15.
91. *Seawater*. [cited 2011 Feb 15]; Available from: http://en.wikipedia.org/wiki/Seawater.
92. *UV Disinfection for Enhanced Oil Recovery and Other Oilfield Applications*. 2011 [cited 2011 April 12]; Available from: http://www.atguv.com/news/45/uv_disinfection_for_enhanced_oil_recovery_and_other_oilfield_applications.
93. P.N. Levett, *Anaerobic Microbiology - A Practical Approach*. 1991: IRL Press at Oxford University Press.
94. R.A. Cottis, Personal Communication with A.B. Masli, 2010.
95. *The MPN Method*. [cited 2011 30 March]; Available from: http://www.jlindquist.net/generalmicro/102dil3.html.
96. *NACE TMO194-94: Field monitoring of bacterial growth in oilfield systems*. 1994, NACE: Houston.
97. *Colony-forming unit*. 2011 [cited 2011 22 Sept]; Available from: http://en.wikipedia.org/wiki/Colony-forming_unit.
98. G.H. Booth and A.K. Tiller, *Polarization studies of mild steel in cultures of sulphate-reducing bacteria.* Transactions of the Faraday Society, 1960. **56**: p. 1689-1696.
99. G.G. Geesey, Z. Lewandowski and H.C. Flemming, *Biofouling and biocorrosion in industrial water systems*, ed. G.G. Geesey, Z. Lewandowski, and H.-C. Flemming. 1994, Boca Raton: Lewis Publishers.
100. J.F.D. Stott, *What Progress In The Understanding Of Microbially Induced Corrosion Has Been Made In The Last 25 Years - A Personal Viewpoint.* Corrosion science, 1993. **35**(1-4): p. 667.
101. C.G. Munger, *Sulfides: Their effect on coatings and substrates.* Materials Performance, 1978. **17**(1): p. 20-23.
102. S.W. Borenstein, *Microbiologically Influenced corrosion handbook*. 1994, Cambridge, England: Woodhead Publishing Limited. 288.
103. W. Lee, Z. Lewandowski, P. H. Nielsen and W. A. Hamilton, , *Role of sulfate reducing bacteria in corrosion of mild steel: A review.* Biofouling, 1995. **8**(3): p. 165-194.
104. R.G.J. Edyvean, *Interactions Between Microfouling and the Calcareous Deposit Formed on Cathodically Protected Steel in Sea Water*, in *Marine Biology, Sixth International Congress*. 1984, Marine Corrosion and Fouling: Athens, Greece.
105. *Fe-S-water equilibrium diagram*. [cited 2011 10 August]; Available from: http://www.argentumsolutions.com/cgi-bin/thermexpert?nonmetalsel=0&phlow=&phhigh=&temperature=25&metal=2&nonmetal1=3&sessionID=11083008052266&firstname=&middleinitial=&lastname=&affiliation=&email=&run=0&firsttime=1&graph_title=Fe-S-water+equilibrium+diagram.
106. *Most Probable Number Procedure and Table*. 2008, United States Department of Agriculture (USDA).
107. Characklis, W.G., K.E. Cooksey, and I.L. Allen, *Biofilms and Microbial Fouling*. 1983, Academic Press. p. 93-138.